Dynamic *In Vitro* Models for Reproductive and Developmental Toxicology

Susanna Holley Wegner

A dissertation
submitted in partial fulfillment of the
requirements for the degree of

Doctor of Philosophy

University of Washington
2014

Dissertation Committee:
Dr. Elaine M. Faustman, Chair
Dr. Terry Kavanagh
Dr. Ed Kelly
Dr. Lucio Costa
Dr. William Griffith

Program Authorized to Offer Degree:
Environmental and Occupational Health Sciences
School of Public Health

University of Washington

Abstract

Dynamic *in vitro* models for reproductive and developmental toxicology

Susanna H. Wegner

Chair of Supervisory Committee:

Professor Elaine M. Faustman

Department of Environmental and Occupational Health Sciences

As *in vitro* models play an increasingly important role in evaluation of potential developmental and reproductive toxicants, it is essential that we define how well these models can capture developmental stages and processes that are vulnerable to toxicant perturbation. In this research we evaluate two dynamic *in vitro* models: a primary co-culture of neonatal rat testis and a human progenitor cell model of neuronal differentiation. Longterm viability, morphological characteristics, and expression of cell type- and stage-specific proteins in *in vitro* cultures were characterized by live/dead cell staining, immunofluorescent imaging, and western blotting. We then defined a framework for quantifying dynamic changes in pathways through time in normal development *in vivo*. Gene expression and pathway dynamics distilled from microarray data were used to anchor the *in vitro* models to *in vivo* developmental processes. Striking similarities were found between *in vivo* and *in vitro* models in gene expression for key pathways associated with each developmental process. Basic characterization revealed that testicular co-cultures survive up to 21 days in culture and contain spermatogonial germ cells, Sertoli cells and Leydig cells, form tube-like structures *in vitro* and actively produce testosterone through the first week in culture. Pathway analysis of gene expression data through time reveals that the testicular co-culture captures key developmental processes that can be targeted by male reproductive toxicants, including Sertoli cell and Leydig cell differentiation, testosterone production, immune activity, signal transduction, tube formation, and tight junction formation. Basic characterization of differentiating neural progenitor cells indicates that the cells survive and differentiate through 21 days in culture, increasingly expressing protein associated with differentiated neurons, adopting neuronal morphology and forming complex neural networks. Pathway analysis reveals that differentiating neural progenitor cells successfully capture differentiation towards a forebrain identity, expressing receptors associated with specific neuronal subtypes. In addition to identifying processes that are clearly captured *in vitro*, we also define the limits of these models by identifying gene expression dynamics found only *in vitro* or only *in vivo*. By further defining the domain of applicability for each of these *in vitro* models, we can help to ensure that these models are used effectively and appropriately for identification of potential chemical hazards.

Table of Contents

List of Figures

List of Tables

List of Abbreviations

3βHSD	3β hydroxysteroid dehydrogenase
AOP	Adverse Outcome Pathway
Cox2	Cyclooxygenase 2
DPP	Dipentyl phthalate
hNPC	human neural progenitor cell
FSH	follicle stimulating hormone
GD	Gestational day
GO	Gene Onotology
LDH	Lactate Dehydrogenase
NRC	National Research Council
PCNA	Proliferating Cell Nuclear Antigen
PND	Postnatal Day
REACH	Registration, Evaluation, Authorization and Restriction of Chemicals
Scp3	Synaptonemal Complex 3
Star	Steroidogenic acute regulatory protein
Stra8	Stimulated by Retinoic Acid Gene 8

Acknowledgements

I am grateful to my advisor, Dr. Elaine M. Faustman for her guidance and patience, to the other members of my dissertation committee, Terry Kavanagh, Ed Kelly, Lucio Costa and Bill Griffith for their thoughtful comments on my research. I am especially grateful to Bill for his help and advice on biostatistical approaches. Thank you also, to Xiaozhong Yu, for his early guidance and advice as my project took shape. I am particularly grateful to my fellow graduate students in the lab, especially, Sean Harris, Julie Park, and Hee Yeon Kim who all spent many hours preparing cell cultures and running assays. Ian Stanaway provided invaluable help with coding for microarray data analysis and figure generation. Sungwoo Hong provided excellent support in the lab along with an army of undergraduate work study students. Collin White in the cytometry core offered valuable technical expertise and patience as I learned to use the fluorescent microscope and attempted to sort our complex cultures by flow cytometry. Everyone in IRARC, including Eric Vigoren, Kethanh Doung, Alison Laing, Marissa Smith, Tomomi Workman, Sara Pacheco, Sanne Hermsen, Carly Strecker, Jim Wallace, Sean Brachvogel, and Nicole Cederblom has been helpful throughout the last six years. Finally this work would not have been possible without funding from the NIEHS EPT training grant that funded my education, as well as the Food and Drug Administration, and Child Health Center grants that funded my research.

CHAPTER 1: Introduction

Public Health Impact of Developmental Toxicity

The developing organism can be profoundly sensitive to environmental exposures. Because of tragic population-level exposures to methylmercury, alcohol, and thalidomide we now know that *in utero* exposures with no lasting effect on maternal health can result in severe lifelong disability (Fabro et al. 1967; de Sanctis et al. 2011; Grandjean and Herz 2011). In addition to demonstrating such direct effects on development, epidemiological studies provide evidence for the Barker hypothesis, which proposes that fetal exposures can influence susceptibility to adult disease later in life (Barker 2004; Barker 2007). The importance of the timing of exposure and difficulty in connecting *in utero* exposures to health outcomes later in life makes identification of environmental risk factors a particularly challenging task. In the face of these logistical challenges, such significant epidemiological findings highlight the need to identify potential reproductive and developmental toxicants before populations are exposed. Furthermore, there is compelling evidence that environmental factors contribute to several prevalent, developmentally based disorders, such as testicular dysgenesis syndrome (Skakkebaek et al. 2001; Sharpe and Skakkebaek 2008) and neurodevelopmental disorders (Landrigan et al. 2012; Grandjean and Landrigan 2014). Better understanding of environmental contributions to disease would inform public health measures to reduce hazardous exposures and prevent debilitating and costly conditions.

Shifting Towards *In vitro* Testing

Despite concern over environmental contributions to developmental disorders, the vast majority of the estimated 75,000-85,000 chemicals currently in commerce remain untested for reproductive and developmental toxicity (Goldman and Koduru 2000; Judson et al. 2009). There is therefore an urgent need to screen a large number of untested chemicals for reproductive and

developmental toxicity so the health risks can be understood and prevented. Current testing paradigms require multigenerational animal models (http://www.oecd-ilibrary.org/environment/oecd-guidelines-for-the-testing-of-chemicals-section-4-health-effects_20745788) that are resource intensive and time consuming and raise ethical considerations. In light of the wide range of compounds yet to be tested, these animal models are not well suited to rapidly address the lack of data on reproductive and developmental toxicity. This has led to great demand for development and validation of *in vitro* models that capture complex and dynamic biological processes that occur during development. The regulatory mandate of REACH legislation in Europe (EU 2006) as well as a range of chemical legislation passed in numerous US states and proposed in the US Congress (Belliveau 2011) has heightened the demand for rapid *in vitro* screening that can inform chemical regulation.

The National Research Council (NRC 2007) articulated the research agenda required to achieve these policy goals with a vision for "toxicity testing in the 21st century" that urges a shift towards a pathway-based approach to evaluation of toxicity using *in vitro* models. This approach takes advantage of highly conserved signaling pathways that are known to regulate complex developmental processes and maintain homeostasis in a diverse range of tissues. Measuring perturbation of these conserved pathways *in vitro* has therefore been proposed as an efficient way of predicting a range of developmental endpoints (NRC 2000). Pathway perturbation identified *in vitro* could then be incorporated into computational models and translated for population level risk assessments (Rusyn and Daston 2010; Judson et al. 2011; Krewski et al. 2011).

However, the dynamic complexity of development poses special challenges for creation of robust models for high throughput screening in toxicology. Developmental context can dramatically alter the type and intensity of response to toxicant perturbation (Knudsen et al. 2011). As development progresses, differentiating tissues and organs go through critical windows of susceptibility to environmental perturbation, often corresponding to the period when that tissue is most dramatically changing and most responsive to endogenous developmental

signaling. In brain development, for example, subtle differences in cell migration patterns or differentiation processes can profoundly alter development and result in neurodevelopmental disabilities (Rice and Barone 2000). The concept of the developmental origins of adult disease adds further complexity to developmental toxicity testing. By influencing epigenetic programs, toxicant exposures during critical periods of development can influence susceptibility to disease throughout life (Barouki et al. 2012). Predicting these effects will require measuring subtle perturbations of the developmental program. Because of the special complexity of development, transitioning reproductive and developmental toxicology testing away from resource intensive animal models will require an array of *in vitro* models that capture a range of developmental stages and tissue types sensitive to environmental perturbation.

The initial *in vitro* screens being tested and applied in Tox21 (the inter-agency collaboration to make the NRC vision for toxicity testing in the 21st century a reality) do not represent the complexity of dynamic developmental processes or reflect developmental context (Judson et al. 2010; Reif et al. 2010; Sipes et al. 2013) though it is precisely this context that can determine toxicity. Optimization of *in vitro* models that reflect *in vivo* developmental dynamics and allow us to capture developmental context is a key challenge in truly moving toxicology testing to the 21st century.

Emerging *In vitro* Models to Capture Developmental Processes

A host of dynamic primary cell culture and *ex vivo* tissue culture models can capture vulnerable developmental stages and processes and are already used in toxicology. For example whole embryo cultures allow *ex vivo* evaluation of toxicity during early embryonic development (Gregotti et al. 1994; Adler et al. 2011; Robinson et al. 2011). High density 'micromass' cultures of limb bud or neuronal cells isolated midway through organogenesis provide a model of cellular differentiation *in vitro* (Flint 1983; Flint et al. 1984; Whittaker and Faustman 1992; Gregotti et al. 1994). Stem cells are also emerging as an important *in vitro* model of cellular differentiation (Cho

and Li 2007; Stummann and Bremer 2008; Robinson et al. 2011; van Dartel and Piersma 2011). For example, the embryonic stem cell test uses mouse, and more recently, human stem cells as a toxicological model for early stages of embryonic development and differentiation into a range of specific tissues (Seiler et al. 2004; zur Nieden et al. 2004; Pal et al. 2011; Hayess et al. 2013).

In vitro models of surfaces and other materials can facilitate three-dimensional growth for differentiating cells in culture (Yu et al. 2005; Boyd et al. 2007; Buzanska et al. 2010; Pierret et al. 2010). Complex *in vivo* like niches can also be created by taking advantage of self-organization of cells in culture. For example, differentiating neurons can self-organize to recapitulate the complex inside-out development of cortical layers and even to generate 'cerebral organoids" *in vitro* (Eiraku et al. 2008; Gaspard et al. 2008; Lancaster et al. 2013).

Many of these emerging *in vitro* models of developmental processes are currently being optimized for high-throughput testing of reproductive and developmental toxicity endpoints like cytotoxicity, progression through differentiation, maturation, and cell morphology (Breier et al. 2008; Radio and Mundy 2008; Stummann et al. 2009; Fritsche et al. 2011). However, before emerging *in vitro* approaches for reproductive and developmental toxicity testing can be embraced, the models and methods used must be thoughtfully designed and carefully validated (Hartung 2010; Adler et al. 2011; Hartung et al. 2011). As these promising developmental models are increasingly considered for toxicity screening, a major challenge is to identify the endpoints within these models that are most predictive of *in vivo* developmental perturbation.

Quantifying Pathway Perturbation to Evaluate Developmental Toxicity

Throughout development, regionally specific signaling guides cell fate. The precise coordination of key signaling pathways that are tailored to each region is therefore crucial to development. Amazingly, all the complexity of development seems to be orchestrated by the coordinated signaling of 17 conserved signaling pathways (Gerhart 1999; NRC 2000; Knudsen et al. 2011). These signaling pathways are highly dynamic, varying in expression and degree of

importance across tissues and time. The complex dynamics of developmental signaling pathways means that reproductive and developmental toxicity is highly dependent on context. The biological effects of perturbation of a particular signaling pathway will depend on the role of that pathway in the development of a given tissue at a particular developmental stage. Because developmental signaling pathways and hormonal signaling are so crucial to regulation of development, perturbation of these pathways is often an underlying mechanism of developmental toxicity. Pathway-based assays in *in vitro* models are therefore emerging as a valuable tool to predict perturbation of pathway dynamics by toxicants, simultaneously anticipating toxicity as well as mechanism of action (NRC 2007; Judson et al. 2010; Knudsen et al. 2011). Pathway perturbation can be detected through apical endpoint assays that reflect pathway function or by toxicogenomic profiling to measure expression of genes. For example, several systems-based analyses of transcriptomic and epigenomic data have been used to characterize murine neural stem cell differentiation processes and to begin to apply a systems-based approach for identification of neurotoxicants in *in vitro* systems (Theunissen et al. 2011; Zimmer et al. 2011; Theunissen et al. 2012).

However, pathway perturbation measured *in vitro* is only informative to the extent that the *in vitro* model successfully captures pathways that are important to *in vivo* development; A model that fails to reflect vulnerable developmental processes may also fail to detect perturbation of these vulnerable processes. Furthermore, though some developmental pathway responses are universal, tissue and context-specific responses are also important contributors to developmental toxicity. It is therefore essential to define normal developmental dynamics across a range of tissue types *in vitro* and anchor these *in vitro* models to *in vivo* processes before *in vitro* results can be interpreted for risk assessment.

Using Pathways to Anchor *In vitro* to *In vivo*

In order to determine the relevance of *in vitro* data for *in vivo* development, it is essential to identify conserved processes that can serve to anchor responses across systems. Changes in well-defined pathways *in vitro* can be linked to known phenotypic responses to changes in these same pathways *in vivo* (States et al. 2011). Several recent studies offer a framework for defining these anchors. A seminal toxicogenomics paper demonstrates a strong correlation between a phenotypic response to formaldehyde exposure in rat nasal epithelium and a more sensitive genomic 'fingerprint' also associated with exposure (Andersen et al. 2008; Daston 2008). This concept has also been demonstrated in zebrafish which allow rapid generation and assessment of altered developmental phenotypes (Tilton and Tanguay 2008; Bugiak and Weber 2010). This framework of 'phenotypic anchoring' provides a model for translation between *in vivo* and *in vitro* models. Anchoring toxicogenomics data from dynamic *in vitro* models to data from corresponding *in vivo* systems helps to define the domain of applicability of these inherently reductive models. Several informative comparisons of toxicogenomic responses measured *in vivo* and *in vitro* illustrate the importance of clearly characterizing the strengths and limitations of each *in vitro* model (Dere et al. 2006; Robinson et al. 2011; Doktorova et al. 2012). For example a comparison of toxicogenomic responses to retinoic acid in whole embryo culture and *in vivo* rat embryonic development demonstrates similarities in the pathways affected in both models, but also key differences in the timing of the response *in vivo* and *ex vivo* (Robinson et al. 2012).

In *in vitro* models that may capture dynamic developmental processes, it is also important to compare 'normal' gene expression dynamics *in vivo* and *in vitro* in the absence of exposures (Robinson et al. 2012). Thus far, few *in vitro* models for development have been assessed in this way. Moving forward, however, this type of characterization will be important in crafting assays that ask appropriate questions of *in vitro* models and clearly defining the appropriate applications of these models so that *in vitro* data can be translated appropriately for risk assessment.

Creating a Framework for Anchoring *In vitro* to *In vivo*

In the current research, I address the need to anchor *in vitro* models for developmental toxicology to *in vivo* developmental processes by demonstrating this type of comparison for two model systems. Specifically, I compare gene expression dynamics of *in vitro* models of rat neonatal testis and human neuronal differentiation to gene expression dynamics through time *in vivo.*

Dissertation Outline

The overarching goal of this dissertation is to define a framework for characterizing 'normal' developmental processes captured in *in vitro* models and anchoring the processes captured *in vitro* to sensitive phases of *in vivo* development. I use this framework to identify the strengths and limitations of two *in vitro* models of sensitive developmental stages in order to define the "domain of applicability" of each model.

I begin in **Chapter 2**, by describing a method for quantifying pathway dynamics through time to define a baseline for normal *in vivo* development and provide a framework for quantification of perturbation of pathway dynamics in response to toxicant exposure. This framework for quantitatively defining normal development *in vivo* sets the stage for anchoring *in vitro* models to key stages and processes of *in vivo* development. Subsequent chapters use this framework to evaluate two *in vitro* models of sensitive developmental processes.

In **Chapter 3** I characterize a primary testicular co-culture that captures key aspects of a sensitive phase of testicular development. Applying the framework defined in Chapter 2, I quantify temporal pathway dynamics *in vitro*, and compare gene expression *in vitro* with gene expression at corresponding timepoints *in vivo* in order to define the relevance of the model for *in vivo* biology.

In **Chapter 4** I further employ the *in vitro* testicular co-culture defined in Chapter 3 to explore the role of inflammation in mediating dipentyl phthalate toxicity. In addition to shedding

light on specific mechanisms of phthalate reproductive toxicity, this work demonstrates the potential toxicological screening applications for a well-defined *in vitro* model.

In **Chapter 5** I mirror the *in vivo/in vitro* comparison performed in Chapter 3 to evaluate a second *in vitro* model. I characterize *in vitro* neuronal differentiation processes captured using a commercially available human neural progenitor cells. In order to define the relevance of the model for *in vivo* biology, I compare gene expression dynamics *in vitro* with gene expression dynamics in early human brain development.

In **Chapter 6** I summarize the key finding of this research and identify future research questions to explore.

Specific Aims and Hypotheses

Chapter 2

Specific Aim: Apply a quantitative pathway-based approach to offer a baseline for future characterization of perturbation of normal development.

Hypothesis: The quantitative pathway based approach will reflect known developmental dynamics of male reproductive development described in the literature, offering a quantitative baseline for future evaluation of Adverse Outcome Pathways deviating from normal development.

Chapter 3

Specific Aim: Characterize an *in vitro* testicular co-culture in its ability to capture processes of male reproductive development sensitive to perturbation.

Hypothesis: The *in vitro* testicular co-culture will capture pathways important for testicular development.

Chapter 4.

Specific Aim: Apply the *in vitro* testicular co-culture defined in Chapter 3 to evaluate the role of inflammation, specifically cyclooxygenase II in mediating the testicular toxicity of dipentyl phthalate

Hypothesis: Cyclooxygenase II plays a role in mediating the response to dipentyl phthalate in our testicular co-culture and inhibition of cyclooxygenase II will prevent dipentyl phthalate-induced toxicity.

Chapter 5

Specific Aim: Characterize an *in vitro* model of neural differentiation in its ability to capture processes of early brain development that are sensitive to perturbation.

Hypothesis: The *in vitro* human neural progenitor cell model will capture pathways important for *in vivo* forebrain development.

CHAPTER 2: Stage-specific signaling pathways during murine testis development and spermatogenesis: a pathway-based analysis to quantify developmental dynamics

This chapter is in preparation for submission to Reproductive Toxicology. The authors of the manuscript are:

Susanna H. Wegner, Xiaozhong Yu*, Sara Pacheco Shubin, William C. Griffith, and Elaine M. Faustman

Dept. of Environmental and Occupational Health Sciences, University of Washington

*Current Address: College of Public Health, University of Georgia

Abstract

Shifting the field of developmental toxicology towards evaluation of pathway perturbation requires defining normal developmental dynamics. The dynamics captured in *in vivo* and *in vitro* models for toxicology must reflect the full spectrum of sensitive developmental processes that may be impacted by environmental chemicals. Existing gene expression datasets contain much of the data necessary to accomplish this. This project examined a publicly available dataset to quantify pathway dynamics during the sensitive processes of testicular development and spermatogenesis and to anchor critical pathways perturbed by toxicants within the context of normal developmental dynamics. Genes significantly changed throughout testis development and the first wave of spermatogenesis in mice were identified and clustered by their direction of change throughout development using *K*-means clustering. We used MAPPfinder to identify Gene Ontology terms enriched among each cluster of significantly changed genes. Temporal pathway dynamics were quantified based on the average expression intensity for all genes associated with a given pathway at each timepoint. This analysis captured critical processes defining testis development and spermatogenesis. The peak in steroidogenesis known to occur

around gestational day 16.5was quantitatively identified, as was the dramatic increase in meiosis and spermatogenesis related pathways that correspond to progression through the first wave of spermatogenesis. Our analysis provides a quantitative description of functional changes in pathways that occur throughout key processes of reproductive development which can be vulnerable to perturbation by toxicants during critical periods of susceptibility. By quantitatively defining normal pathway dynamics of testis development, we establish a framework for quantifying the effects of environmental exposures or genetic variants on developmental dynamics. This framework provides a basis for anchoring adverse outcome pathways analysis within tissue and time-specific developmental contexts.

Introduction

Increasing rates of reproductive disorders that have origins in early reproductive development demonstrate the need for methods to characterize and quantify perturbations of developmental processes in gonadal development and spermatogenesis. For example, there is mounting evidence for a consistent decline in semen quality in recent decades, accompanied by an increasing prevalence of male reproductive disorders, including hypospadias, undescended testes, and testicular cancer (Carlsen et al. 1992; Swan et al. 1997; Andersen et al. 2000; Skakkebaek et al. 2001; Jensen et al. 2002; Rolland et al. 2013). All of these adverse reproductive health outcomes are manifestations of testicular dysgenesis syndrome (TDS), a set of conditions believed to have common origins during early gonadal development (Sharpe and Skakkebaek 2008). Early testicular development and spermatogenesis are very sensitive processes that depend on a series of precisely timed steps regulated by hormonal cues and germ cell microenvironments (Berruti 1998; Western 2009). These processes in male reproductive development are therefore particularly vulnerable to perturbation by genetic and environmental factors (Gray et al. 2000; Parks et al. 2000). Indeed, the recent increase in TDS related conditions has been hypothesized to be a result of environmental factors that can influence early male reproductive development, such as exposure to endocrine disrupting chemicals (Sharpe and Skakkebaek 2008).

Exploration of the complex interaction of environmental and genetic factors underlying reproductive disorders requires a systems-based framework for characterizing normal and perturbed pathway dynamics during critical windows of male reproductive development. The field of toxicology is increasingly shifting towards characterization of pathway perturbation as a sensitive indicator of toxicity (NRC 2000). A quantitative framework for measuring shifts from normal pathway dynamics would facilitate quantification of pathway perturbation by toxicants. Furthermore, incorporation of *in vitro* models into chemical screening, underscores the need to anchor pathway dynamics captured in these *in vitro* models to pathway dynamics driving *in vivo* development. The first step in being able place pathway perturbation measured *in vivo* and *in*

vitro within the context of normal development is to define normal pathway dynamics *in vivo* in an easily translatable, quantitative framework.

Fortunately, much of the data needed to provide this baseline characterization of normal developmental dynamics is available in publicly available datasets. Microarray-based high-throughput gene expression analysis has proven to be an effective method for studying the changes in gene expression associated with the growth and development of mammalian tissues (Armit 2007; Marjani et al. 2009). Many of the genetic drivers of male reproductive development have been characterized through mouse knockout models (Escalier 2001; Verhoeven et al. 2010) and global gene expression analysis (Shima et al. 2004; Small et al. 2005; Clemente et al. 2006; Houmard et al. 2009; Bouma et al. 2010). The Griswold lab at Washington State University has employed microarray-based gene expression analysis to characterize dynamic changes in global gene expression patterns over the course of several particularly sensitive processes of male reproductive development in mice (Shima et al. 2004; Small et al. 2005). The group identified genes with changing expression patterns throughout gonadal differentiation and development and the first wave of spermatogenesis (Shima et al. 2004; Small et al. 2005). The gene expression profiles observed by Small *et al* reiterated the known functional activities of each cell type, and suggested the involvement of novel genes in the maturation of the testis and differentiation of germ cells. Their temporal microarray study provides a valuable resource for evaluating biological factors that influence testis maturation and spermatogenesis. However, as with all microarray data, the functional interpretation of such a vast set of genomic data presents a major challenge. In order to elucidate the biological consequences of these expression changes in single genes, gene expression data must be integrated with quantitative information on functional changes in whole gene networks and developmental signaling pathways over time.

Gene ontology (GO) analysis is a powerful tool for translating a vast amount of genomic data into a description of functional changes in gene networks and signaling pathways. The GO approach has been successfully combined with pathway analysis to generate an unbiased

determination of the statistical significance of changes observed in pathways of interest (Dennis et al. 2003; Doniger et al. 2003; Al-Shahrour et al. 2004; Beissbarth and Speed 2004). For example, previous GO analysis of testicular gene expression has successfully identified pathways that are significantly changed throughout murine spermatogenesis (Laiho et al. 2013). However, standard GO analysis results in a list of enriched pathways with no quantitative description of how these pathways are changed. In addition these approaches did not retain quantitative information on the expression of individual genes and are limited to the evaluation of only two experimental dimensions.

In order to address the need to quantify changes in pathway dynamics through time or in response to an environmental exposure, our lab developed the GO-Quant approach (Yu et al. 2006). GO-Quant incorporates gene expression data with Gene Ontology analysis in MAPPfinder (Doniger et al. 2003) to calculate the average intensity of expression of all significantly altered genes associated with a given GO term. This allows the quantitative evaluation of the dynamics of entire gene pathways along a third dimension, such as developmental stage or toxicant dose. We first applied this quantitative pathway-based approach in a published dose- and time-dependent genomic dataset (Dillman et al. 2005) and found that our systematic approach quantitatively described the degree to which functional gene systems changed across dose or time course (Cunnigham 2006; Yu et al. 2006). We have subsequently used our quantitative pathway analysis for a genome-wide assessment of phthalate toxicity in an *in vitro* rat testis co-culture model (Yu et al. 2009) and for an assessment of time- and dose-dependent methylmercury toxicity in developing mouse embryos undergoing neurulation (Robinson et al. 2010).

In the current study, we applied our established quantitative pathway-based approach to a publicly available dataset of murine male reproductive development (Shima et al. 2004) to quantify the dynamic functional changes in biological processes that characterize normal testicular development and the first wave of spermatogenesis *in vivo*. Through this analysis we demonstrate that our approach can quantitatively illustrate pathway dynamics throughout a

complex developmental process *in vivo,* successfully capturing well characterized developmental milestones. The result provides a framework for quantifying perturbation of normal developmental pathways *in vivo* as well as anchoring emerging *in vitro* models of male reproductive development to *in vivo* pathway dynamics.

Materials and Methods

Gene Expression Data Set

For this analysis we obtained publically available temporal mouse genomic data during early testis development **(**gestational days (GD) 11.5, 12.5, 14.5, 16.5, and 18.5) and the first wave of spermatogenesis (postnatal days (PND) 0, 3, 6, 8, 10, 14, 18, 20, 30, 35, and 56). Gene expression intensity in testicular tissue at each timepoint was quantified using Affymetrix MGU74Av2, Bv2, and Cv2 arrays. Detailed methods of sample collection and microarray processing are available in the original papers (Shima et al. 2004; Small et al. 2005). NCBI's gene expression omnibus (GEO, http://www.ncbi.nlm.nih.gov/geo/) was used to retrieve the raw dataset.

Identification and Clustering of Significantly Changed Genes

Microarray analysis was conducted based on our established quantitative pathway-based approach as shown in Figure 1 (Yu et al. 2006). Significantly changed probes were identified using BRB ArrayTools, developed by Dr. Richard Simon and the BRB ArrayTools Development Team. Data were normalized by gcRMA normalization and log2 transformed. In order to identify significantly changed probes, we conducted an ANOVA class comparison across timepoints. Genes that were significantly altered ($p \leq 0.001$) across time were selected and *K*-means cluster analysis was used to group genes based on the similarity of their patterns of mean expression though time. Since there are generally two directions of gene expression changes at a certain time (either up-regulation or down-regulation within a specific gene category), the average of these

two different directions of gene expression alteration would mask the degree of absolute change in a pathway. For pathway analysis, we therefore separated significantly changed genes into two groups with patterns of expression tending towards consistent up- or down-regulation across time based on *K*-means cluster analysis (Soukas et al. 2000).

Identification of Enriched GO terms

We applied MAPPfinder to identify enriched Gene Ontology (GO) terms at $p \leq 0.001$ (Dahlquist et al. 2002) in up- and down-regulated probes at each timepoint. Enriched GO terms were ranked by Z-score and permutation p-value (Dahlquist et al. 2002). As previously described, the Z-score, a statistical measure of significance for gene expression in a given group, was calculated by subtracting the number of genes expected to be randomly changed in a GO term from the observed number of changed genes in that GO term. This value was then divided by the standard deviation of the observed number of genes under a hypergeometric distribution. The equation is written out as

$$\text{Z score}=(r-n*(R/N))/((n*(R/N))(1-(R/N))(1-((n-1)/(N-1)))^{\wedge 1/2} \quad (1)$$

where *N* is the total number of genes measured, *R* is the total number of genes meeting the criterion that the gene be significantly changed based on an *F* test at significant $p <= 0.001$ value, *n* is the total number of genes in each specific GO term, and *r* is the number of genes meeting the criterion in this specific GO term. Complete lists of GO terms enriched among significantly up- or down-regulated genes are available as supplemental data (Supplemental Tables 1 and 2).

Quantification of Pathway Dynamics Throughout Development

To quantify the dynamic changes in GO terms through time, we used GO-Quant to link enriched GO terms to the expression values of all the significantly up- or down-regulated genes contained within the pathway. By incorporating gene expression data into the pathway analysis, we could compute the average intensity of expression among genes in each enriched GO term at each

timepoint. These values at individual timepoints were then normalized to 'average' expression across time by subtracting the average expression intensity of genes in the GO term across all the timepoints. This yielded a log2 ratio of mean expression at each timepoint relative to the average mean expression across all timepoints. Plotting the log2 ratio for each GO term through time illustrates temporal pathway dynamics throughout development. GO terms included in the figures and tables presented here are the ten biological processes with the highest Z-scores that are relevant to each of the dominant categories selected.

Results

Our quantitative pathway analysis (summarized in Figure 1A) translates a vast amount of information on expression of single genes into a quantitative summary of temporal changes in activity across entire gene networks and biological processes described by GO terms (Figure 1B). Of the approximately 36,000 probes on the array, 9,599 probes were significantly changed through time. Significant genes were clustered into two groups based on their general expression trends using K-means clustering. This resulted in segregation of significantly changed genes into two sets: one set with overall upward trends in expression and another set with overall downward trends in expression. We then used MAPPFinder to identify GO terms describing biological processes that were enriched among each of these two gene clusters. We found 308 GO terms enriched among genes with downwards trends in expression and 112 GO terms enriched among genes with upward trends in expression. For each of these enriched GO terms, GO-Quant facilitated generation of a quantitative temporal summary of average gene expression dynamics at each timepoint among genes significantly changed in the pathway through time.

GO Terms Significantly Enriched Among Genes with Upward Trends in Expression

The GO terms most overwhelmingly overrepresented among genes with significantly increased expression are dominated by terms associated with spermatogenesis and meiosis (Table 1). Indeed, 12 of the top 20 (60%) of significantly enriched GO terms ranked by Z-score are

directly relevant to spermatogenesis or meiosis (Supplemental Table 1). Quantitative pathway analysis reveals that average gene expression in GO terms related to meiosis (Figure 2B) begins increasing around PND 3, slightly preceding the spermatogenesis and spermatid maturation signal. We see a dramatic increase in the average expression of genes in GO terms relating to spermatogenesis and spermatid development throughout testis development, capturing gene expression dynamics that are closely aligned in time with known developmental outcomes (Figure 2A). Average expression of genes involved in a host of GO terms relating to spermatid development and differentiation begin a gradual increase on PND 10 with the emergence of spermatocytes, increase around PND 20 when spermatids appear, and remain high through PND 56 as the first wave of spermatogenesis is completed and spermatozoa are produced. Simultaneously, average expression in GO terms associated with a panel of pathways related to ubiquitin mediated processes (Figure 2C) and epigenetic processes (Figure 2D) increases in parallel, with over a quarter of the genes associated with chromatin remodeling and ubiquitin cycle changing significantly through spermatogenesis.

GO Terms Significantly Enriched Among Genes with Downward Trends in Expression

The dominant themes in GO terms enriched among genes with decreasing expression through time include developmental processes, metabolic processes, developmental signaling pathways, mitosis, and steroid regulation (Table 2). Quantitative pathway analysis illustrates dynamic changes in GO terms related to steroid regulation throughout testis development. For example, average gene expression in sterol metabolic and biosynthetic processes peak at GD 16.5, decrease before birth, and decrease further after spermatid development commences (Figure 3A). Several other catabolic and metabolic pathways, including lipid metabolism, follow a similar pattern of expression (Figure 3B).

Our analysis also reveals dynamic changes of signal transduction pathways throughout spermatogenesis (Figure 3C). Average gene expression of many developmental signaling pathways, including BMP, Notch, and MAPK signaling, are elevated towards the end of gestation

and during the earliest stages of spermatogenesis, peaking between GD 16.5 and PND 3. Average expression in these developmental signaling pathways decreases dramatically between PND 14 and PND 18, as testicular formation and development give way to functional adult tissue.

GO terms for developmental processes (Figure 3D) and mitosis (Figure 3E) display a similar pattern of dramatic upregulation during peak testicular development, dropping off as testes mature and spermatogenesis progresses. For example, pathways involved in cell growth and differentiation, mitosis, and cellular morphogenesis and development, are generally elevated during gestation and the first week of life. Then, around PND 8, expression of genes in these pathways begins a gradual decrease. This decrease corresponds to the end stages of testis development and maturation and the beginning of spermatogenesis.

Discussion

Our systematic pathway-based approach distills complex genomic data into a quantitative description of pathway dynamics over the course of gonadal development and spermatogenesis. This analysis successfully captures well characterized developmental processes, offering a quantitative framework for assessing normal temporal dynamics of reproductive development and measuring any perturbation of these dynamics that could lead to pathology. Finally, by defining *in vivo* pathway dynamics, this analysis facilitates evaluation of the ability of emerging *in vitro* systems to capture important developmental pathways.

Pathway analysis captures dynamics of key events known to drive testicular development and spermatogenesis

The trends highlighted by our analysis are consistent with well characterized developmental processes described in the literature. For example, the notable peak in expression of pathways related to steroidogenesis and hormonal regulation observed in our analysis at GD 16.5 corresponds to the well characterized peak in testosterone known to drive male reproductive development (Verhoeven et al. 2010; O'Shaughnessy and Fowler 2011). The significant increase

in steroidogenesis during this phase has previously been identified as a critical initiator of testis development and masculinization of the fetus (Verhoeven et al. 2010; O'Shaughnessy and Fowler 2011). Expression of a host of genes in the mouse reproductive tract has been shown to be modulated by estrogen and testosterone (Snyder et al. 2009).

Meiosis in the testis does not begin until around PND5, with the initiation of the first wave of spermatogenesis (Bowles and Koopman 2010). This is clearly illustrated at the pathway level in our pathway analysis. Conversely, the dramatic proliferation of somatic cells that occurs early in testis development plays a role in promoting the male fate by increasing the number of SRY-producing cells and marks a key difference between male and female development (Piprek 2010). Accordingly, in this analysis, we see pathways that promote proliferation and mitosis are expressed in developing testes and then downregulated as functionally mature testes begin spermatogenesis.

During spermatogenesis, chromatin restructuring facilitates sperm compaction and regulation of DNA methylation (Groudine and Conkin 1985; Jenkins and Carrell 2012). Precise regulation of these epigenetic processes is essential for sperm development as well as for appropriate expression of the paternal genome in the developing embryo(Jenkins and Carrell 2012). The ubiquitin system plays an important role in performing the histone modifications that underlie this chromatin restructuring (Baarends et al. 2000). The prominent increase in expression of genes associated with ubiquitin mediated processes and epigenetic processes that is observed concurrently with spermatogenesis in our analysis illustrates the temporal dynamics of these well-described regulatory processes.

Our analysis also successfully captures the important role of signal transduction pathways in regulating development. At least 17 highly conserved signaling pathways a re now recognized for their central role in guiding developmental processes (Gerhart 1999; NRC 2000). Many of these signaling pathways are specifically implicated in guiding the processes of gonadal differentiation and testicular development (Brennan and Capel 2004) and germ cell differentiation

(Zhao and Garbers 2002). In the current analysis, we capture the increased expression of genes involved in these signal transduction pathways throughout gestation and testicular maturation. These signaling pathways are then downregulated as testis tissue achieves maturation and begins the process of meiosis and spermatogenesis.

Pathway analysis can facilitate discovery of new roles for pathways dynamically changed in testicular development

In addition to accurately illustrating these well characterized developmental processes, quantitative pathway analysis is also a powerful tool for providing new insight into the stage-specific regulation of signaling pathways involved in the unique and complex processes of gonadal differentiation and spermatogenesis. The precise balance of these signaling pathways is hypothesized to play a key role in male development by initiating the differentiation of the fetal Leydig cells that produce masculinizing hormones (Barsoum and Yao 2010). The current analysis shows a wide range of signal transduction pathways that go through dramatic changes in expression in testicular tissue over the course of the first wave of spermatogenesis. Further investigation of the fluctuations in these signaling pathways over time could provide insight into their roles in the regulation and maintenance of spermatogenesis.

We also find that pathways related to cellular metabolism of lipids and proteins follow the same pattern of expression as steroidogenesis pathways during spermatogenesis. If these pathways are in fact linked, this is consistent with the hypothesis that cellular metabolism pathways are a target of androgen action, allowing androgens to modulate the testis environment to promote spermatogenesis (Verhoeven et al. 2010). These observations illustrate that our pathway-based approach can provide quantitative information on the dynamic changes seen in a range of signaling pathways over the course of development. Deeper exploration of this pathway analysis may reveal additional novel pathways that are important in the reproductive development.

Benefits and drawbacks of the quantitative pathway-based approach

There are many benefits to applying a pathway based approach to analyze temporal gene expression data. For example, we reduce the potential for overlooking key pathways whose subtle changes have large effects by considering the pathway as a whole as opposed to individual genes. We also reduce the amount of statistical noise, as entire gene networks are far less likely than individual genes to be significantly increased simply by chance. It is important to note that while average pathway expression provides an informative summary of pathway dynamics driving developmental processes, this method is not ideal for identification and characterization of single genes that serve as key developmental regulators. In addition, the quality of a pathway-based analysis is limited by the quality of the curation of each pathway. Indeed, there are several pathways enriched in our analysis (e.g. heart development and neural tube development) that are likely to be an artifact of genes that have simultaneous roles in multiple pathways or signal transduction that is highly conserved across a diverse range of developmental processes.

Applications for developmental toxicology: defining sensitive phases of development and generating complex, context dependent Adverse Outcome Pathways

In addition to providing insight into normal gonadal development and spermatogenesis, this quantitative gene ontology analysis offers a new lens through which to evaluate developmental pathology. This will be a particularly valuable tool for our field of developmental toxicology. Understanding the dynamics of signaling pathways can further define key phases of susceptibility to environmental factors. For example quantitative characterization of the pathway dynamics that drive steroid regulation can shed light on key windows of susceptibility of this process to endocrine disrupting chemicals (Sanderson 2006; Sharpe and Skakkebaek 2008).

The challenge of regulatory chemical testing requirements and the vast number of chemicals yet to be tested will require innovative computational toxicology methods (NRC 2007; Rusyn and Daston 2010). Toxicity-related alterations in gene transcription and biological pathway dynamics have been proposed as valuable metrics for chemical risk assessment that

could be generated by high-throughput methods (Judson et al. 2011; Thomas et al. 2011). To that end, a quantitative pathway-based approach can be applied to predict and measure the effects of chemical exposure on signaling pathway dynamics. This approach is a powerful way to quantify changes in the developmental dynamics of signaling pathways in response to genetic mutations and environmental factors. Changes in the peaks, slopes and duration of the dynamic expression patterns of signaling pathways in response to toxicant exposure will provide a sensitive measure of reproductive developmental toxicity and offer insight into mechanisms of toxicity. Quantitative pathway-based characterization of signaling pathway dynamics could also inform mathematical models for *in silico* simulation of the specific impacts of gene changes or environmental exposures on developmental outcomes. Furthermore, quantifying the perturbation of developmental pathway dynamics in response to toxicant exposures could facilitate articulation of "Adverse Outcome Pathways", which are emerging as an increasingly valuable tool for translating toxicological data for risk assessment (Ankley et al. 2010). Therefore, in addition to shedding light on normal developmental dynamics, this quantitative pathway- based approach provides a framework for quantifying deviation from normal developmental processes.

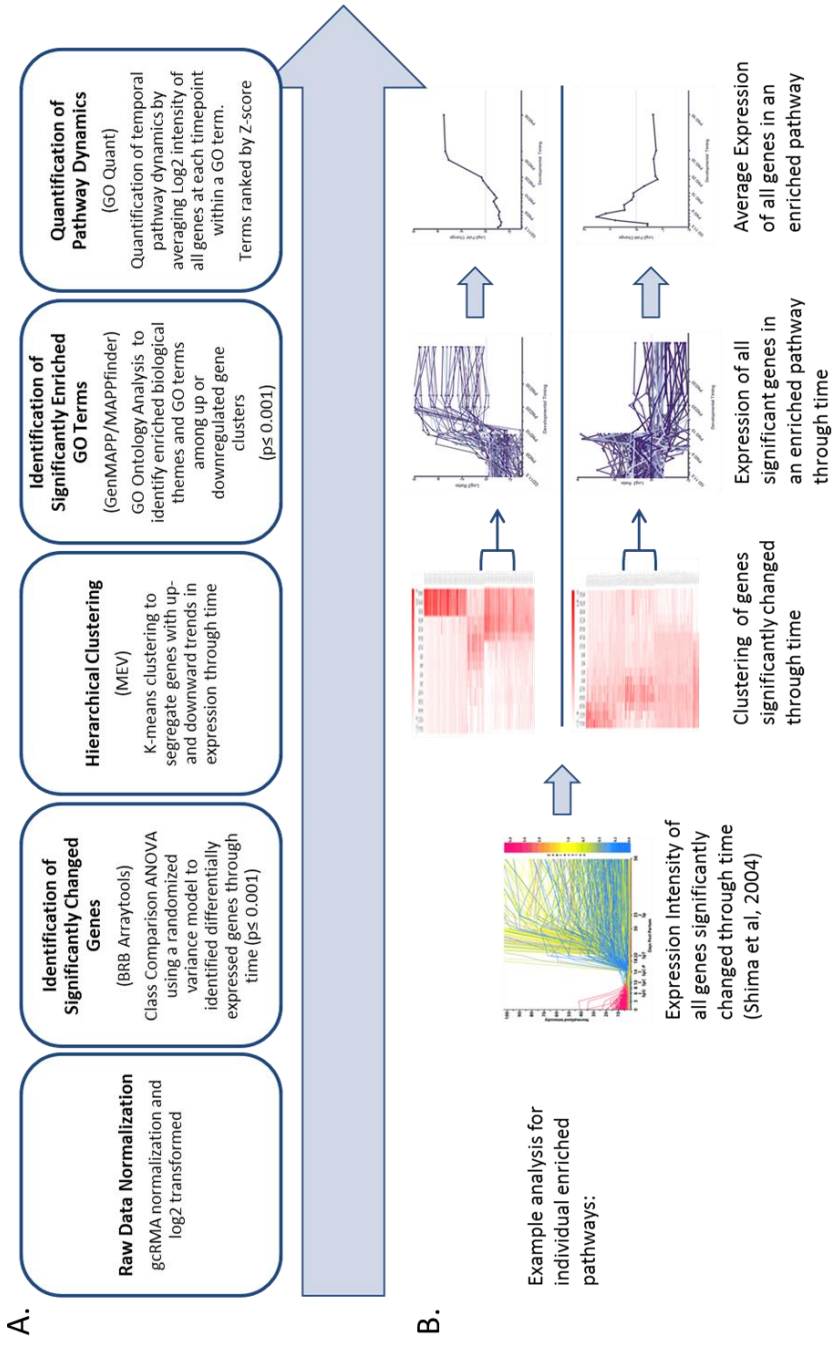

Figure 1. Microarray Analysis Pipeline for Quantification of Pathway Dynamics. A) Summary of analysis pipeline B) Illustration of data analysis process. Starting with single gene expression in testis through time (Shima et al, 2004) we normalized data and identified significantly changed genes using BRB Arraytools software, clustered genes with significantly increasing or decreasing expression through time using Multiple Experiment Viewer software (MEV), then used GO Quant software to identify GO terms enriched among these clusters and average the expression of all significantly changed genes in that pathway to produce a quantitative summary of gene expression dynamics in each GO term through time.

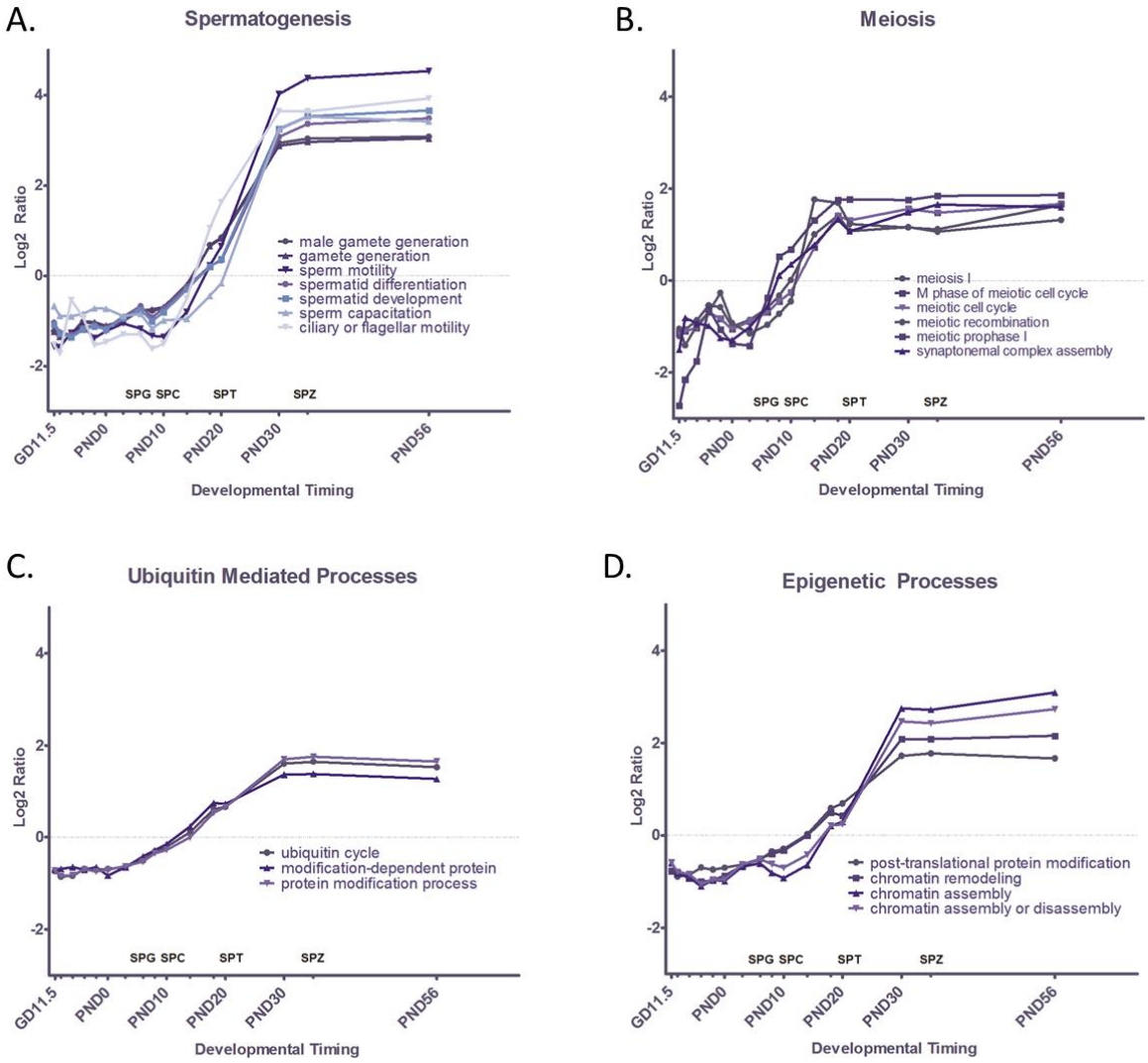

Figure 2. Quantified Pathway Dynamics of GO Terms that Significantly Increase Through Time. GO terms enriched among genes with significantly increasing expression ($p<0.001$) through time were identified through MAPPfinder. Significantly enriched GO terms ($p<0.001$) were ranked by Z-score and dominant themes among these terms were identified as A) Spermatogenesis, B) Meiosis, C) Ubiquitin Mediated Processes, and D) Epigenetic Processes. Dynamic change in GO terms related to each dominant theme are plotted here as the ratio of average Log2 intensity of expression of all significantly changed genes at each timepoint in a GO term over Average Log2 intensity across all timepoints for that GO term. Corresponding stages of spermatogenesis, including spermatogonia (SPG), spermatocyte (SPC), spermatid (SPT), and spermatozoa (SPZ) are indicated along the X axis.

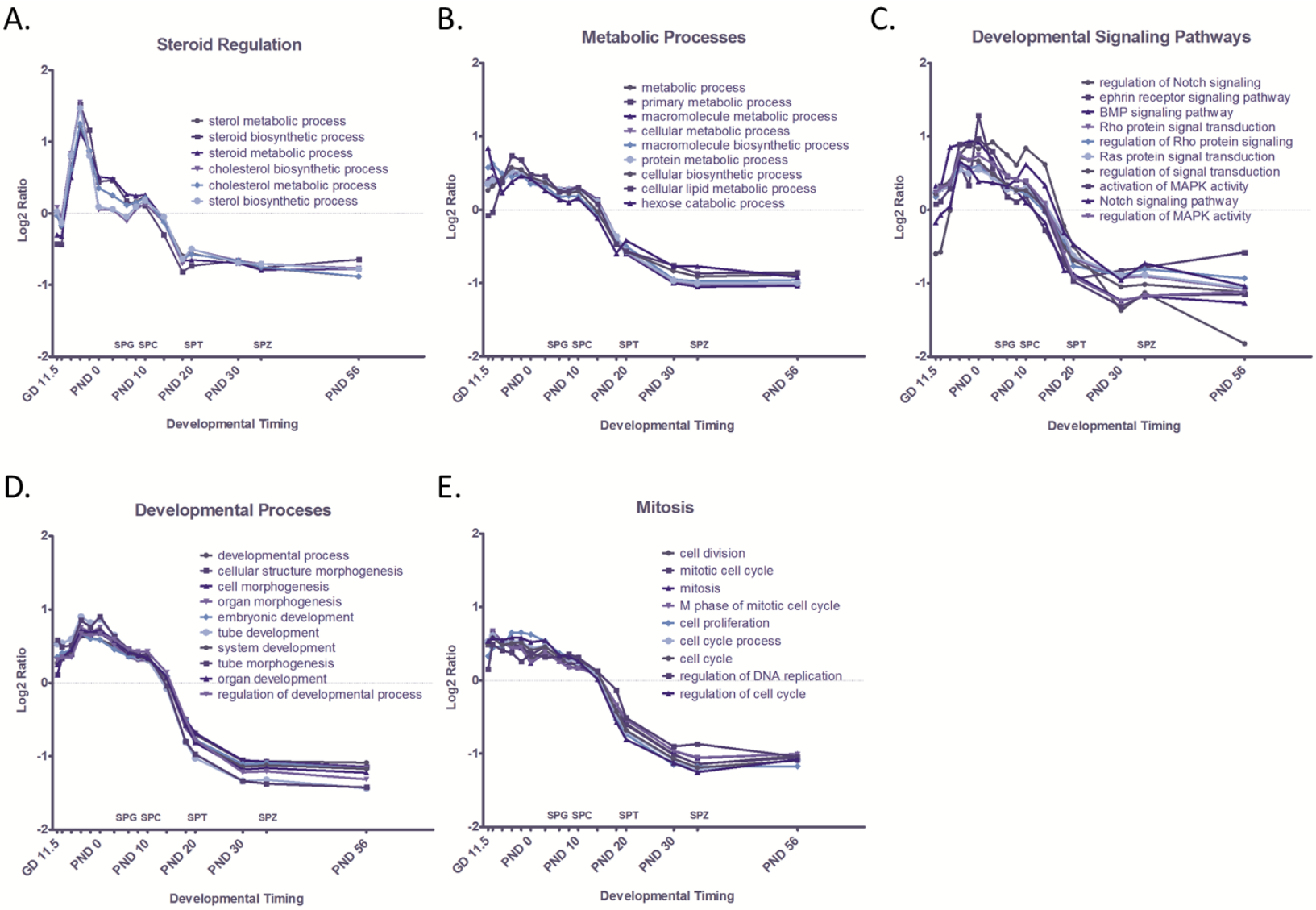
A.
Steroid Regulation
sterol metabolic process
steroid biosynthetic process
steroid metabolic process
cholesterol biosynthetic process
cholesterol metabolic process
sterol biosynthetic process
B.
Metabolic Processes
metabolic process
primary metabolic process
macromolecule metabolic process
cellular metabolic process
macromolecule biosynthetic process
protein metabolic process
cellular biosynthetic process
cellular lipid metabolic process
hexose catabolic process
C.
Developmental Signaling Pathways
regulation of Notch signaling
ephrin receptor signaling pathway
BMP signaling pathway
Rho protein signal transduction
regulation of Rho protein signaling
Ras protein signal transduction
regulation of signal transduction
activation of MAPK activity
Notch signaling pathway
regulation of MAPK activity
D.
Developmental Proceses
developmental process
cellular structure morphogenesis
cell morphogenesis
organ morphogenesis
embryonic development
tube development
system development
tube morphogenesis
organ development
regulation of developmental process
E.
Mitosis
cell division
mitotic cell cycle
mitosis
M phase of mitotic cell cycle
cell proliferation
cell cycle process
cell cycle
regulation of DNA replication
regulation of cell cycle
Log2 Ratio
SPG SPC SPT SPZ
GD 11.5 PND 0 PND 10 PND 20 PND 30 PND 56
Developmental Timing

Figure 3. Quantified Pathway Dynamics of GO terms that Significantly Decrease Through Time. GO terms enriched among genes with significantly decreasing expression ($p<0.001$) through time were identified through MAPPfinder. Significantly enriched GO terms ($p<0.001$) were ranked by Z-score and dominant themes among these terms were identified as A) Steroid Regulation B) Cellular Metabolism C) Developmental Signaling Pathways, D) Developmental Processes, and E) Meiosis. Dynamic change in GO terms related to each dominant theme are plotted here as the ratio of average Log2 intensity of expression of all significantly changed genes at each timepoint in a GO term over Average Log2 intensity across all timepoints for that GO term. Corresponding stages of spermatogenesis, including spermatogonia (SPG), spermatocyte (SPC), spermatid (SPT), and spermatozoa (SPZ) are indicated along the X axis.

Table 2.1. GO Terms Enriched Among Genes With Significantly Increased Expression Through Time

GOID	GO Name	# Genes in GO	% of Present Genes Changed	% of Genes Present on Array	Z-Score	Parametric p-value
Spermatogenesis and Sperm Maturation						
48232	male gamete generation	194	53.3	70.6	11.935	4.0E-05
7283	spermatogenesis	194	53.3	70.6	11.935	4.0E-05
7276	gamete generation	278	41.8	66.2	9.601	5.1E-05
30317	sperm motility	15	75	106.7	6.427	3.7E-05
48515	spermatid differentiation	36	56.2	88.9	6.202	7.7E-05
7286	spermatid development	34	56.7	88.2	6.067	3.3E-05
1539	ciliary or flagellar motility	6	100	66.7	4.574	1.7E-06
48240	sperm capacitation	5	100	60	3.961	3.3E-05
Meiotic Cell Cycle						
7127	meiosis I	32	63.2	59.4	5.597	1.9E-04
51327	M phase of meiotic cell cycle	76	37.7	69.7	4.309	1.5E-04
7126	meiosis	76	37.7	69.7	4.309	1.5E-04
51321	meiotic cell cycle	77	37	70.1	4.21	1.5E-04
7131	meiotic recombination	17	75	23.5	3.212	6.4E-06
7128	meiotic prophase I	4	60	125	2.677	1.0E-07
7130	synaptonemal complex assembly	6	60	83.3	2.677	1.1E-04
Ubiquitin Mediated Processes						
6512	ubiquitin cycle	433	25.3	83.1	4.837	7.7E-05
6511	ubiquitin-dependent protein catabolic process	165	28.9	69.1	3.767	6.9E-05
19941	modification-dependent protein catabolic process	167	28.4	69.5	3.654	6.9E-05
43632	modification-dependent macromolecule catabolic process	167	28.4	69.5	3.654	6.9E-05
6464	protein modification process	1609	19.5	78.3	3.535	8.7E-05
Epigenetic Regulation						
43687	post-translational protein modification	1375	19.1	79.1	2.895	8.5E-05
6338	chromatin remodeling	52	28.9	73.1	2.169	8.6E-05
31497	chromatin assembly	142	25.4	44.4	2.026	3.6E-05
6333	chromatin assembly or disassembly	180	23.6	49.4	1.945	7.0E-05

Table 2.2. GO Terms Enriched Among Genes With Significantly Decreased Expression Through Time

GOID	GO Name	# Genes in GO	% of Present Genes Changed	% of Genes Present on Array	Z-Score	Parametric p-value
Steroid Regulation						
16125	sterol metabolic process	73	44.1	80.8	2.997	7.3E-05
6694	steroid biosynthetic process	75	46.3	72	3.237	5.7E-05
6695	cholesterol biosynthetic process	25	55	80	2.846	4.1E-05
8203	cholesterol metabolic process	67	43.4	79.1	2.729	6.0E-05
16126	sterol biosynthetic process	31	50	83.9	2.67	7.4E-05
8202	steroid metabolic process	145	36.5	79.3	2.358	9.8E-05
Cellular Metabolism						
8152	metabolic process	8113	28.8	76.1	4.835	1.3E-04
44238	primary metabolic process	7338	29	75.1	4.83	1.3E-04
43170	macromolecule metabolic process	6411	28.8	74.7	3.91	1.3E-04
44237	cellular metabolic process	7311	28.9	75.4	4.651	1.3E-04
9059	macromolecule biosynthetic process	899	34.8	65.5	4.476	1.5E-04
19538	protein metabolic process	3404	29.4	74	3.263	1.3E-04
44249	cellular biosynthetic process	646	33.1	74.9	3.156	1.4E-04
44255	cellular lipid metabolic process	542	33.2	81.2	3.063	1.4E-04
19320	hexose catabolic process	91	44.2	57.1	2.839	1.3E-04
46365	monosaccharide catabolic process	91	44.2	57.1	2.839	1.3E-04
Developmental Processes						
32502	developmental process	3292	31.8	75.6	6.268	1.2E-04
32989	cellular structure morphogenesis	485	39.4	77.9	5.61	7.9E-05
902	cell morphogenesis	485	39.4	77.9	5.61	7.9E-05
9887	organ morphogenesis	457	39.2	82.1	5.49	8.6E-05
9790	embryonic development	362	39.2	94.5	5.229	6.1E-05
35295	tube development	128	46.9	100	5.146	5.3E-05
48731	system development	1704	32.5	74.9	4.824	1.0E-04
35239	tube morphogenesis	83	48.9	106	4.683	6.2E-05
48513	organ development	1345	32.2	76.4	4.077	1.0E-04
50793	regulation of developmental process	256	38.8	85.5	4.039	7.9E-05
Developmental Signaling Pathways						
8593	regulation of Notch signaling pathway	5	100	80	3.304	2.0E-05
48013	ephrin receptor signaling pathway	3	100	133.3	3.304	4.2E-05
30509	BMP signaling pathway	26	57.1	80.8	3.139	1.5E-04
7266	Rho protein signal transduction	102	41.5	80.4	3.002	1.6E-04
43405	regulation of MAPK activity	77	44.4	70.1	2.929	9.7E-05
35023	regulation of Rho protein signal transduction	72	42.2	88.9	2.781	1.8E-04
7265	Ras protein signal transduction	172	37.4	71.5	2.66	1.7E-04
9966	regulation of signal transduction	411	32.1	78.8	2.171	1.6E-04
187	activation of MAPK activity	48	43.8	66.7	2.164	9.9E-05
7219	Notch signaling pathway	51	40.9	86.3	2.113	5.6E-05
Mitotic Cell Cycle						

51301	cell division	218	42.9	90.8	5.155	1.7E-04
278	mitotic cell cycle	249	39.6	81.1	4.133	1.3E-04
7067	mitosis	168	41.7	85.7	4.043	1.4E-04
87	M phase of mitotic cell cycle	170	41.5	86.5	4.039	1.4E-04
8283	cell proliferation	648	35.3	63	3.925	9.8E-05
22402	cell cycle process	646	34.9	69.2	3.923	1.4E-04
7049	cell cycle	762	33.7	74.4	3.773	1.3E-04
6275	regulation of DNA replication	19	70	52.6	3.083	1.5E-04
51726	regulation of cell cycle	461	33.5	60.3	2.523	1.3E-04
74	regulation of progression through cell cycle	459	33.5	59.9	2.509	1.3E-04

Table 2.3. Full list of GO Terms Enriched Among Genes With Significantly Increased Expression Through Time

GOID	GO Name	# Genes in GO	%Genes Changed	%Genes Present	Z-Score	Parametric p-value
48232	male gamete generation	194	53.3	70.6	11.94	4.0E-05
7283	Spermatogenesis	194	53.3	70.6	11.94	4.0E-05
19953	sexual reproduction	327	45	67.9	11.87	4.6E-05
3	Reproduction	492	35.5	65.2	9.62	5.2E-05
7276	gamete generation	278	41.8	66.2	9.60	5.1E-05
9566	Fertilization	48	62.9	72.9	7.55	2.0E-05
7338	single fertilization	48	61.8	70.8	7.27	2.1E-05
30317	sperm motility	15	75	106.7	6.43	3.7E-05
48515	spermatid differentiation	36	56.2	88.9	6.20	7.7E-05
7286	spermatid development	34	56.7	88.2	6.07	3.3E-05
7127	meiosis I	32	63.2	59.4	5.60	1.9E-04
6457	protein folding	238	29.5	72.7	4.84	1.2E-04
6512	ubiquitin cycle	433	25.3	83.1	4.84	7.7E-05
35036	sperm-egg recognition	12	66.7	100	4.78	1.5E-07
1539	ciliary or flagellar motility	6	100	66.7	4.57	1.7E-06
7129	Synapsis	9	75	88.9	4.54	2.2E-04
9988	cell-cell recognition	13	61.5	100	4.47	1.5E-07
51327	M phase of meiotic cell cycle	76	37.7	69.7	4.31	1.5E-04
7126	Meiosis	76	37.7	69.7	4.31	1.5E-04
7339	binding of sperm to zona pellucida	11	63.6	100	4.30	1.6E-07
51321	meiotic cell cycle	77	37	70.1	4.21	1.5E-04
48240	sperm capacitation	5	100	60	3.96	3.3E-05
6644	phospholipid metabolic process	127	30.1	81.1	3.90	9.7E-05
2483	antigen processing and presentation of endogenous peptide antigen	8	80	62.5	3.90	4.8E-05
19885	antigen processing and presentation of endogenous peptide antigen via MHC class I	8	80	62.5	3.90	4.8E-05
30163	protein catabolic process	220	27.2	71.8	3.85	9.4E-05
6643	membrane lipid metabolic process	173	28	76.3	3.77	9.0E-05
6511	ubiquitin-dependent protein catabolic process	165	28.9	69.1	3.77	6.9E-05
19941	modification-dependent protein catabolic process	167	28.4	69.5	3.65	6.9E-05
43632	modification-dependent macromolecule catabolic process	167	28.4	69.5	3.65	6.9E-05
8654	phospholipid biosynthetic process	67	33.9	83.6	3.65	3.7E-05
6352	transcription initiation	45	37.8	82.2	3.62	5.1E-05
44265	cellular macromolecule catabolic process	319	25.1	64.9	3.58	5.9E-05
6516	glycoprotein catabolic process	16	62.5	50	3.58	1.4E-04
6913	nucleocytoplasmic transport	127	29.7	71.7	3.55	1.2E-04

51603	proteolysis involved in cellular protein catabolic process	170	28	69.4	3.54	6.9E-05
6464	protein modification process	1609	19.5	78.3	3.54	8.7E-05
6508	proteolysis	806	21.3	70.5	3.49	8.2E-05
6611	protein export from nucleus	16	50	87.5	3.46	1.3E-04
9057	macromolecule catabolic process	387	23.8	67.2	3.46	7.8E-05
22414	reproductive process	248	26.1	63.3	3.46	5.4E-05
44257	cellular protein catabolic process	172	27.5	69.8	3.43	6.9E-05
46467	membrane lipid biosynthetic process	85	31.3	78.8	3.42	3.4E-05
65004	protein-DNA complex assembly	172	29.2	51.7	3.39	5.0E-05
7342	fusion of sperm to egg plasma membrane	9	66.7	66.7	3.38	8.0E-07
51169	nuclear transport	115	29.6	70.4	3.34	1.3E-04
43412	biopolymer modification	1677	19.2	78.1	3.31	8.6E-05
7017	microtubule-based process	216	25.6	72.2	3.28	9.2E-05
44267	cellular protein metabolic process	3258	18.2	74	3.26	9.3E-05
45862	positive regulation of proteolysis	5	75	80	3.21	3.1E-05
7131	meiotic recombination	17	75	23.5	3.21	6.4E-06
6003	fructose 2\,6-bisphosphate metabolic process	4	75	100	3.21	2.5E-04
9894	regulation of catabolic process	19	50	63.2	3.21	2.1E-05
44260	cellular macromolecule metabolic process	3301	18.1	74.1	3.14	9.3E-05
19538	protein metabolic process	3404	18.1	74	3.12	9.2E-05
6986	response to unfolded protein	62	38.5	41.9	3.12	3.9E-05
51789	response to protein stimulus	62	38.5	41.9	3.12	3.9E-05
19318	hexose metabolic process	174	26.5	67.2	3.09	7.0E-05
22403	cell cycle phase	289	23.5	78.2	3.06	1.2E-04
9056	catabolic process	639	21	72.1	2.97	7.2E-05
279	M phase	232	23.9	81	2.97	1.3E-04
7340	acrosome reaction	12	57.1	58.3	2.96	4.5E-07
45026	plasma membrane fusion	10	57.1	70	2.96	8.0E-07
19883	antigen processing and presentation of endogenous antigen	11	57.1	63.6	2.96	4.8E-05
5996	monosaccharide metabolic process	178	25.8	67.4	2.93	7.0E-05
42176	regulation of protein catabolic process	14	50	71.4	2.93	2.5E-05
6515	misfolded or incompletely synthesized protein catabolic process	19	50	52.6	2.93	1.9E-04
30433	ER-associated protein catabolic process	18	50	55.6	2.93	1.9E-04
6493	protein amino acid O-linked glycosylation	16	50	62.5	2.93	1.7E-04
6367	transcription initiation from RNA polymerase II promoter	25	40	80	2.92	7.1E-05
43687	post-translational protein modification	1375	19.1	79.1	2.90	8.5E-05
51170	nuclear import	80	29.5	76.2	2.87	1.2E-04
43285	biopolymer catabolic process	285	23.2	71.2	2.78	9.5E-05

30503	regulation of cell redox homeostasis	7	60	71.4	2.68	1.8E-05
7128	meiotic prophase I	4	60	125	2.68	1.0E-07
7130	synaptonemal complex assembly	6	60	83.3	2.68	1.1E-04
51324	prophase	4	60	125	2.68	1.0E-07
6000	fructose metabolic process	13	60	38.5	2.68	2.5E-04
6072	glycerol-3-phosphate metabolic process	7	60	71.4	2.68	4.7E-05
42787	protein ubiquitination during ubiquitin-dependent protein catabolic process	5	60	100	2.68	1.2E-04
9191	ribonucleoside diphosphate catabolic process	5	60	100	2.68	1.2E-05
46470	phosphatidylcholine metabolic process	7	60	71.4	2.68	3.4E-04
31365	N-terminal protein amino acid modification	6	60	83.3	2.68	3.6E-04
6606	protein import into nucleus	79	28.8	74.7	2.68	1.2E-04
7001	chromosome organization and biogenesis (sensu Eukaryota)	390	22.1	64.9	2.66	1.1E-04
45582	positive regulation of T cell differentiation	11	45.5	100	2.66	1.4E-04
51168	nuclear export	40	34.6	65	2.58	2.1E-04
6096	glycolysis	76	30.2	56.6	2.54	1.8E-05
6006	glucose metabolic process	133	25.8	66.9	2.53	4.8E-05
51276	chromosome organization and biogenesis	399	21.5	66.4	2.45	1.1E-04
7018	microtubule-based movement	115	26.3	66.1	2.45	6.6E-05
18342	protein prenylation	17	41.7	70.6	2.42	1.2E-04
16311	dephosphorylation	146	24	82.9	2.38	1.4E-04
48002	antigen processing and presentation of peptide antigen	37	30.6	97.3	2.37	1.1E-04
46164	alcohol catabolic process	93	27.8	58.1	2.35	2.7E-05
8037	cell recognition	41	31.2	78	2.35	3.8E-07
6944	membrane fusion	31	37.5	51.6	2.34	8.7E-05
18346	protein amino acid prenylation	13	44.4	69.2	2.32	1.5E-04
46165	alcohol biosynthetic process	27	35	74.1	2.31	7.4E-05
46364	monosaccharide biosynthetic process	27	35	74.1	2.31	7.4E-05
19319	hexose biosynthetic process	27	35	74.1	2.31	7.4E-05
6066	alcohol metabolic process	300	21.6	72.7	2.23	7.1E-05
7049	cell cycle	762	19.4	74.4	2.22	1.1E-04
6007	glucose catabolic process	86	27.5	59.3	2.22	2.5E-05
51252	regulation of RNA metabolic process	17	38.5	76.5	2.20	3.5E-04
44248	cellular catabolic process	510	20.2	69.8	2.18	6.4E-05
32446	protein modification by small protein conjugation	75	26.2	81.3	2.17	6.3E-05
6338	chromatin remodeling	52	28.9	73.1	2.17	8.6E-05
46365	monosaccharide catabolic process	91	26.9	57.1	2.14	2.5E-05
19320	hexose catabolic process	91	26.9	57.1	2.14	2.5E-05
46916	transition metal ion homeostasis	49	30	61.2	2.08	6.1E-05
31497	chromatin assembly	142	25.4	44.4	2.03	3.6E-05

6333	chromatin assembly or disassembly	180	23.6	49.4	1.95	7.0E-05

Table 2.4. Full list of GO Terms Enriched Among Genes With Significantly Decreased Expression Through Time

GOID	GO Name	# Genes in GO	% Genes Changed	% Genes Present	Z-Score	Parametric p-value
9653	anatomical structure morphogenesis	1089	37.5	80.2	7.35	8.8E-05
9987	cellular process	12349	28.7	67	6.42	1.3E-04
32502	developmental process	3292	31.8	75.6	6.27	1.2E-04
48856	anatomical structure development	2002	33.4	74.8	6.16	9.9E-05
9058	biosynthetic process	1471	34.6	70	5.87	1.4E-04
902	cell morphogenesis	485	39.4	77.9	5.61	7.9E-05
32989	cellular structure morphogenesis	485	39.4	77.9	5.61	7.9E-05
9887	organ morphogenesis	457	39.2	82.1	5.49	8.6E-05
7167	enzyme linked receptor protein signaling pathway	278	43.7	71.6	5.42	9.7E-05
30036	actin cytoskeleton organization and biogenesis	196	46.6	74.5	5.42	7.1E-05
1525	angiogenesis	132	48.3	89.4	5.29	6.2E-05
9790	embryonic development	362	39.2	94.5	5.23	6.1E-05
30029	actin filament-based process	207	45.2	74.9	5.18	7.0E-05
7507	heart development	133	45.8	108.3	5.18	5.3E-05
51301	cell division	218	42.9	90.8	5.15	1.7E-04
35295	tube development	128	46.9	100	5.15	5.3E-05
7275	multicellular organismal development	2140	31.9	77.5	5.05	1.1E-04
48646	anatomical structure formation	173	44.4	92.5	5.04	7.4E-05
1944	vasculature development	190	42.9	93.2	4.87	7.2E-05
16043	cellular component organization and biogenesis	2656	31.4	70.2	4.86	1.2E-04
8152	metabolic process	8113	28.8	76.1	4.83	1.3E-04
44238	primary metabolic process	7338	29	75.1	4.83	1.3E-04
48731	system development	1704	32.5	74.9	4.82	1.0E-04
48514	blood vessel morphogenesis	162	44	92.6	4.78	7.5E-05
1568	blood vessel development	187	42.5	93	4.71	7.3E-05
35239	tube morphogenesis	83	48.9	106	4.68	6.2E-05
55008	cardiac muscle morphogensis	4	100	200	4.67	5.5E-05
44237	cellular metabolic process	7311	28.9	75.4	4.65	1.3E-04
1763	morphogenesis of a branching structure	49	54.7	108.2	4.59	6.3E-05
9059	macromolecule biosynthetic process	899	34.8	65.5	4.48	1.5E-04
48754	branching morphogenesis of a tube	46	55.1	106.5	4.48	5.1E-05
55010	ventricular cardiac muscle morphogenesis	4	100	175	4.37	5.0E-05
7399	nervous system development	658	35.2	74.3	4.25	1.0E-04
65007	biological regulation	4497	29.6	74.5	4.21	1.2E-04
22610	biological adhesion	645	35.4	70.5	4.20	8.5E-05
7155	cell adhesion	645	35.4	70.5	4.20	8.5E-05
278	mitotic cell cycle	249	39.6	81.1	4.13	1.3E-04
7178	transmembrane receptor protein serine/threonine kinase signaling pathway	87	50	71.3	4.13	1.2E-04

15669	gas transport	17	81.8	64.7	4.12	8.7E-05
50789	regulation of biological process	4133	29.7	75.1	4.11	1.3E-04
6996	organelle organization and biogenesis	1201	33.1	65.9	4.10	1.1E-04
30865	cortical cytoskeleton organization and biogenesis	14	76.9	92.9	4.08	1.5E-04
48513	organ development	1345	32.2	76.4	4.08	1.0E-04
7067	mitosis	168	41.7	85.7	4.04	1.4E-04
87	M phase of mitotic cell cycle	170	41.5	86.5	4.04	1.4E-04
50793	regulation of developmental process	256	38.8	85.5	4.04	7.9E-05
7169	transmembrane receptor protein tyrosine kinase signaling pathway	177	42.1	75.1	4.00	8.3E-05
9880	embryonic pattern specification	41	55.3	92.7	3.96	7.9E-05
8283	cell proliferation	648	35.3	63	3.93	9.8E-05
22402	cell cycle process	646	34.9	69.2	3.92	1.4E-04
43170	macromolecule metabolic process	6411	28.8	74.7	3.91	1.3E-04
22603	regulation of anatomical structure morphogenesis	46	53.7	89.1	3.89	3.8E-05
8360	regulation of cell shape	46	53.7	89.1	3.88	3.8E-05
22604	regulation of cell morphogenesis	46	53.7	89.1	3.88	3.8E-05
6412	translation	656	35.2	61.4	3.87	1.4E-04
48644	muscle morphogenesis	6	80	166.7	3.80	5.5E-05
7049	cell cycle	762	33.7	74.4	3.77	1.3E-04
8150	biological_process	14509	27.6	67.7	3.77	1.3E-04
30323	respiratory tube development	54	51.1	87	3.76	3.3E-05
22403	cell cycle phase	289	37.6	78.2	3.69	1.2E-04
7010	cytoskeleton organization and biogenesis	504	35.5	68.3	3.67	9.3E-05
30900	forebrain development	65	46.3	103.1	3.60	8.3E-05
31032	actomyosin structure organization and biogenesis	25	63.2	76	3.58	8.3E-05
30324	lung development	53	50	86.8	3.55	3.5E-05
9792	embryonic development ending in birth or egg hatching	149	39.2	102.7	3.48	4.8E-05
15671	oxygen transport	16	77.8	56.2	3.45	1.1E-04
43009	chordate embryonic development	147	39.1	102.7	3.42	4.9E-05
279	M phase	232	37.8	81	3.41	1.3E-04
51128	regulation of cellular component organization and biogenesis	68	46.6	85.3	3.40	9.8E-05
50794	regulation of cellular process	3752	29.3	74.9	3.39	1.2E-04
45765	regulation of angiogenesis	34	55.6	79.4	3.37	1.5E-04
8593	regulation of Notch signaling pathway	5	100	80	3.30	2.0E-05
48013	ephrin receptor signaling pathway	3	100	133.3	3.30	4.2E-05
48468	cell development	1610	30.8	74.2	3.27	1.3E-04
19538	protein metabolic process	3404	29.4	74	3.26	1.3E-04
6817	phosphate transport	84	44.6	77.4	3.25	1.2E-04
6694	steroid biosynthetic process	75	46.3	72	3.24	5.7E-05
6270	DNA replication initiation	26	64.3	53.8	3.17	1.4E-04
44249	cellular biosynthetic process	646	33.1	74.9	3.16	1.4E-04
30509	BMP signaling pathway	26	57.1	80.8	3.14	1.5E-04
6729	tetrahydrobiopterin biosynthetic process	6	83.3	100	3.13	1.8E-04

45995	regulation of embryonic development	7	83.3	85.7	3.13	2.1E-06
46146	tetrahydrobiopterin metabolic process	6	83.3	100	3.13	1.8E-04
51291	protein heterooligomerization	10	83.3	60	3.13	2.8E-05
8064	regulation of actin polymerization and/or depolymerization	41	51.6	75.6	3.12	9.1E-05
30832	regulation of actin filament length	42	51.6	73.8	3.12	9.1E-05
48546	digestive tract morphogenesis	10	66.7	120	3.12	7.8E-06
51169	nuclear transport	115	42	70.4	3.09	9.8E-05
9220	pyrimidine ribonucleotide biosynthetic process	16	70	62.5	3.08	6.8E-05
6275	regulation of DNA replication	19	70	52.6	3.08	1.5E-04
30866	cortical actin cytoskeleton organization and biogenesis	11	70	90.9	3.08	1.9E-04
8088	axon cargo transport	14	70	71.4	3.08	8.9E-05
7439	ectodermal gut development	8	75	100	3.08	1.0E-05
48567	ectodermal gut morphogenesis	8	75	100	3.08	1.0E-05
44255	cellular lipid metabolic process	542	33.2	81.2	3.06	1.4E-04
32990	cell part morphogenesis	249	36.3	80.7	3.06	1.0E-04
48858	cell projection morphogenesis	249	36.3	80.7	3.06	1.0E-04
30030	cell projection organization and biogenesis	249	36.3	80.7	3.06	1.0E-04
6403	RNA localization	49	50	69.4	3.05	1.7E-04
6790	sulfur metabolic process	78	45.3	67.9	3.04	1.0E-04
7266	Rho protein signal transduction	102	41.5	80.4	3.00	1.6E-04
16125	sterol metabolic process	73	44.1	80.8	3.00	7.3E-05
1501	skeletal development	205	37.6	72.7	2.98	1.2E-04
6221	pyrimidine nucleotide biosynthetic process	22	58.8	77.3	2.98	9.7E-05
30154	cell differentiation	2098	29.9	78.6	2.97	1.2E-04
48869	cellular developmental process	2098	29.9	78.6	2.97	1.2E-04
904	cellular morphogenesis during differentiation	182	37.8	78.6	2.97	1.1E-04
48332	mesoderm morphogenesis	24	51.9	112.5	2.94	8.7E-05
43405	regulation of MAPK activity	77	44.4	70.1	2.93	9.7E-05
46164	alcohol catabolic process	93	44.4	58.1	2.93	1.3E-04
59	protein import into nucleus\, docking	15	60	100	2.90	1.6E-04
51261	protein depolymerization	34	50	88.2	2.87	9.3E-05
7015	actin filament organization	50	47.4	76	2.86	3.9E-05
7179	transforming growth factor beta receptor signaling pathway	57	47.4	66.7	2.86	1.1E-04
15931	nucleobase\, nucleoside\, nucleotide and nucleic acid transport	54	47.4	70.4	2.86	2.4E-04
35112	genitalia morphogenesis	1	100	300	2.86	2.3E-07
7213	acetylcholine receptor signaling\, muscarinic pathway	6	100	50	2.86	1.8E-05
48010	vascular endothelial growth factor receptor signaling pathway	2	100	150	2.86	2.0E-05
30513	positive regulation of BMP signaling pathway	3	100	100	2.86	2.5E-04

31529	ruffle organization and biogenesis	3	100	100	2.86	3.4E-04
6290	pyrimidine dimer repair	4	100	75	2.86	3.1E-05
6435	threonyl-tRNA aminoacylation	3	100	100	2.86	9.7E-05
7043	intercellular junction assembly	9	100	33.3	2.86	1.4E-06
6598	polyamine catabolic process	3	100	100	2.86	1.7E-04
30538	embryonic genitalia morphogenesis	1	100	300	2.86	2.3E-07
6695	cholesterol biosynthetic process	25	55	80	2.85	4.1E-05
46365	monosaccharide catabolic process	91	44.2	57.1	2.84	1.3E-04
19320	hexose catabolic process	91	44.2	57.1	2.84	1.3E-04
8154	actin polymerization and/or depolymerization	54	46.3	75.9	2.83	8.3E-05
50658	RNA transport	47	48.5	70.2	2.81	1.8E-04
51236	establishment of RNA localization	47	48.5	70.2	2.81	1.8E-04
50657	nucleic acid transport	47	48.5	70.2	2.81	1.8E-04
32787	monocarboxylic acid metabolic process	225	35.8	84.4	2.81	1.3E-04
46907	intracellular transport	737	32	73.7	2.81	1.4E-04
6629	lipid metabolic process	650	32.2	78.3	2.80	1.5E-04
51170	nuclear import	80	42.6	76.2	2.79	8.2E-05
35023	regulation of Rho protein signal transduction	72	42.2	88.9	2.78	1.8E-04
42127	regulation of cell proliferation	425	34	67.1	2.78	9.4E-05
51028	mRNA transport	43	50	65.1	2.77	2.0E-04
48568	embryonic organ development	29	50	96.6	2.77	2.8E-05
44260	cellular macromolecule metabolic process	3301	29.1	74.1	2.77	1.3E-04
44267	cellular protein metabolic process	3258	29.1	74	2.77	1.3E-04
45454	cell redox homeostasis	58	44.7	81	2.77	8.9E-05
32501	multicellular organismal process	4035	29.2	52.9	2.76	1.1E-04
9218	pyrimidine ribonucleotide metabolic process	17	63.6	64.7	2.76	6.8E-05
1676	long-chain fatty acid metabolic process	16	63.6	68.8	2.76	3.0E-04
48628	myoblast maturation	29	55.6	62.1	2.75	5.1E-05
6913	nucleocytoplasmic transport	127	39.6	71.7	2.75	9.3E-05
7163	establishment and/or maintenance of cell polarity	33	52.2	69.7	2.75	1.5E-05
7369	gastrulation	51	43.4	103.9	2.73	6.4E-05
8203	cholesterol metabolic process	67	43.4	79.1	2.73	6.0E-05
51129	negative regulation of cell organization and biogenesis	34	48.4	91.2	2.71	9.3E-05
6606	protein import into nucleus	79	42.4	74.7	2.70	8.5E-05
48557	embryonic digestive tract morphogenesis	6	66.7	150	2.70	1.4E-06
48547	gut morphogenesis	9	66.7	100	2.70	1.0E-05
30510	regulation of BMP signaling pathway	13	66.7	69.2	2.70	1.6E-04
21915	neural tube development	37	45.2	113.5	2.70	6.9E-05
43549	regulation of kinase activity	193	37	69.9	2.69	1.2E-04
48699	generation of neurons	307	34.3	81.8	2.69	9.8E-05
16050	vesicle organization and biogenesis	9	80	55.6	2.68	2.2E-04
40016	embryonic cleavage	5	80	100	2.68	9.3E-05
8215	spermine metabolic process	6	80	83.3	2.68	6.2E-06

15012	heparan sulfate proteoglycan biosynthetic process	8	80	62.5	2.68	2.5E-04
46128	purine ribonucleoside metabolic process	6	80	83.3	2.68	7.4E-05
48488	synaptic vesicle endocytosis	11	80	45.5	2.68	1.5E-04
6400	tRNA modification	7	80	71.4	2.68	1.8E-04
30325	adrenal gland development	6	80	83.3	2.68	2.2E-04
7440	foregut morphogenesis	4	80	125	2.68	1.5E-05
1704	formation of primary germ layer	25	50	104	2.67	9.4E-05
16126	sterol biosynthetic process	31	50	83.9	2.67	7.4E-05
43406	positive regulation of MAPK activity	52	47.1	65.4	2.67	9.9E-05
47496	vesicle transport along microtubule	5	71.4	140	2.66	5.4E-05
9396	folic acid and derivative biosynthetic process	6	71.4	116.7	2.66	1.3E-04
30838	positive regulation of actin filament polymerization	7	71.4	100	2.66	2.0E-04
43525	positive regulation of neuron apoptosis	5	71.4	140	2.66	2.9E-04
7265	Ras protein signal transduction	172	37.4	71.5	2.66	1.7E-04
7409	axonogenesis	158	37.4	77.8	2.66	1.2E-04
50673	epithelial cell proliferation	23	52.4	91.3	2.65	8.4E-05
51338	regulation of transferase activity	198	36.7	70.2	2.64	1.2E-04
6007	glucose catabolic process	86	43.1	59.3	2.63	1.2E-04
22008	neurogenesis	330	33.8	82.4	2.63	1.1E-04
6461	protein complex assembly	203	36.8	65.5	2.62	1.3E-04
45859	regulation of protein kinase activity	186	36.9	69.9	2.61	1.3E-04
6631	fatty acid metabolic process	166	36.4	86.1	2.59	1.6E-04
1707	mesoderm formation	23	50	104.3	2.57	1.0E-04
96	sulfur amino acid metabolic process	21	57.1	66.7	2.56	1.1E-04
55001	muscle cell development	20	57.1	70	2.56	6.3E-05
6261	DNA-dependent DNA replication	73	43.5	63	2.55	1.2E-04
48667	neuron morphogenesis during differentiation	166	36.6	78.9	2.55	1.2E-04
48812	neurite morphogenesis	166	36.6	78.9	2.55	1.2E-04
1569	patterning of blood vessels	18	52.6	105.6	2.54	5.6E-05
51098	regulation of binding	23	52.6	82.6	2.54	1.8E-04
48627	myoblast development	30	52.6	63.3	2.54	5.1E-05
51052	regulation of DNA metabolic process	37	52.6	51.4	2.54	1.3E-04
8610	lipid biosynthetic process	256	34.7	78.9	2.53	1.1E-04
51726	regulation of cell cycle	461	33.5	60.3	2.52	1.3E-04
74	regulation of progression through cell cycle	459	33.5	59.9	2.51	1.3E-04
6082	organic acid metabolic process	521	32.2	79.3	2.51	1.3E-04
19752	carboxylic acid metabolic process	520	32.2	79.4	2.51	1.3E-04
8285	negative regulation of cell proliferation	189	37.3	58.2	2.48	9.9E-05
7417	central nervous system development	224	35.1	77.7	2.47	8.2E-05
16525	negative regulation of angiogenesis	15	58.3	80	2.47	1.2E-04
48565	gut development	15	58.3	80	2.47	8.9E-06
30833	regulation of actin filament polymerization	17	58.3	70.6	2.46	1.5E-04
40007	growth	252	34.5	78.2	2.46	9.9E-05

48519	negative regulation of biological process	1018	30.6	76.1	2.44	1.2E-04
10003	gastrulation (sensu Mammalia)	18	52.9	94.4	2.43	2.7E-05
46849	bone remodeling	99	38.4	86.9	2.43	1.4E-04
51216	cartilage development	37	45.5	89.2	2.42	9.3E-05
16331	morphogenesis of embryonic epithelium	52	41.5	101.9	2.42	7.3E-05
22607	cellular component assembly	536	32.6	61.8	2.41	1.4E-04
1503	ossification	89	39	86.5	2.41	1.5E-04
15980	energy derivation by oxidation of organic compounds	81	40.7	72.8	2.41	1.2E-04
2009	morphogenesis of an epithelium	106	37	101.9	2.41	1.1E-04
44272	sulfur compound biosynthetic process	35	48	71.4	2.39	1.6E-04
48523	negative regulation of cellular process	967	30.7	74.6	2.39	1.2E-04
31175	neurite development	192	35.3	79.7	2.38	1.1E-04
35088	establishment and/or maintenance of apical/basal cell polarity	12	60	83.3	2.37	2.5E-05
50818	regulation of coagulation	11	60	90.9	2.37	5.1E-05
8202	steroid metabolic process	145	36.5	79.3	2.36	9.8E-05
31214	biomineral formation	90	38.5	86.7	2.33	1.5E-04
31110	regulation of microtubule polymerization or depolymerization	14	53.3	107.1	2.32	1.2E-04
50678	regulation of epithelial cell proliferation	18	53.3	83.3	2.32	9.4E-05
8637	apoptotic mitochondrial changes	18	53.3	83.3	2.32	8.0E-05
17038	protein import	93	39.1	74.2	2.31	1.0E-04
51270	regulation of cell motility	67	40.4	85.1	2.31	6.3E-05
44275	cellular carbohydrate catabolic process	110	39.7	57.3	2.31	1.3E-04
48469	cell maturation	83	40	72.3	2.31	4.6E-05
14031	mesenchymal cell development	28	45.2	110.7	2.31	4.7E-05
6241	CTP biosynthetic process	13	62.5	61.5	2.28	6.6E-06
9209	pyrimidine ribonucleoside triphosphate biosynthetic process	13	62.5	61.5	2.28	6.6E-06
6098	pentose-phosphate shunt	9	62.5	88.9	2.28	2.4E-04
97	sulfur amino acid biosynthetic process	12	62.5	66.7	2.28	9.6E-05
1836	release of cytochrome c from mitochondria	10	62.5	80	2.28	1.3E-04
6465	signal peptide processing	8	62.5	100	2.28	3.1E-06
6740	NADPH regeneration	9	62.5	88.9	2.28	2.4E-04
10165	response to X-ray	5	62.5	160	2.28	2.1E-04
43648	dicarboxylic acid metabolic process	12	62.5	66.7	2.28	1.4E-04
50920	regulation of chemotaxis	10	62.5	80	2.28	1.8E-04
50921	positive regulation of chemotaxis	9	62.5	88.9	2.28	1.8E-04
1837	epithelial to mesenchymal transition	6	62.5	133.3	2.28	3.7E-05
9208	pyrimidine ribonucleoside triphosphate metabolic process	13	62.5	61.5	2.28	6.6E-06
46036	CTP metabolic process	13	62.5	61.5	2.28	6.6E-06
51347	positive regulation of transferase activity	118	37.5	74.6	2.27	1.2E-04
1839	neural plate morphogenesis	35	43.2	105.7	2.26	9.1E-05
7420	brain development	152	35.3	89.5	2.24	8.8E-05
6066	alcohol metabolic process	300	33.5	72.7	2.24	1.0E-04
16049	cell growth	139	36.6	72.7	2.23	6.3E-05

6096	glycolysis	76	41.9	56.6	2.23	9.1E-05
7498	mesoderm development	51	41.9	84.3	2.23	6.8E-05
75	cell cycle checkpoint	47	46.2	55.3	2.23	1.2E-04
45333	cellular respiration	36	46.2	72.2	2.23	1.4E-04
51168	nuclear export	40	46.2	65	2.23	1.0E-04
1843	neural tube closure	22	46.2	118.2	2.23	1.0E-04
16337	cell-cell adhesion	250	34.6	63.6	2.23	6.4E-05
30182	neuron differentiation	273	33.5	78.8	2.22	1.1E-04
48562	embryonic organ morphogenesis	15	50	120	2.22	1.6E-06
30334	regulation of cell migration	58	40.8	84.5	2.22	7.2E-05
65009	regulation of a molecular function	365	32.8	71.8	2.22	1.5E-04
40012	regulation of locomotion	70	39.3	87.1	2.21	6.9E-05
42541	hemoglobin biosynthetic process	4	66.7	150	2.20	2.5E-04
20027	hemoglobin metabolic process	4	66.7	150	2.20	2.5E-04
6108	malate metabolic process	6	66.7	100	2.20	1.7E-04
48558	embryonic gut morphogenesis	5	66.7	120	2.20	2.1E-06
8156	negative regulation of DNA replication	12	66.7	50	2.20	2.5E-04
7028	cytoplasm organization and biogenesis	23	53.8	56.5	2.20	1.4E-04
15698	inorganic anion transport	153	36	72.5	2.20	1.6E-04
30239	myofibril assembly	19	53.8	68.4	2.20	5.1E-05
31111	negative regulation of microtubule polymerization or depolymerization	12	53.8	108.3	2.20	1.4E-04
55002	striated muscle cell development	19	53.8	68.4	2.20	5.1E-05
9165	nucleotide biosynthetic process	149	36.1	72.5	2.19	1.3E-04
2027	cardiac chronotropy	2	75	200	2.18	4.1E-05
9966	regulation of signal transduction	411	32.1	78.8	2.17	1.6E-04
40008	regulation of growth	169	35.1	79.3	2.17	1.0E-04
48762	mesenchymal cell differentiation	29	43.8	110.3	2.16	4.7E-05
187	activation of MAPK activity	48	43.8	66.7	2.16	9.9E-05
51246	regulation of protein metabolic process	276	33.3	77.2	2.16	1.2E-04
6284	base-excision repair	24	47.6	87.5	2.15	1.0E-04
7281	germ cell development	34	47.6	61.8	2.15	1.9E-05
8645	hexose transport	30	47.6	70	2.15	2.6E-04
15749	monosaccharide transport	30	47.6	70	2.15	2.6E-04
9952	anterior/posterior pattern formation	83	37.7	92.8	2.15	1.1E-04
30041	actin filament polymerization	28	47.6	75	2.15	1.2E-04
30282	bone mineralization	26	47.6	80.8	2.15	1.8E-04
16477	cell migration	285	33	80.7	2.15	9.0E-05
21700	developmental maturation	99	37.8	74.7	2.15	6.9E-05
43623	cellular protein complex assembly	48	42.9	72.9	2.14	1.1E-04
6259	DNA metabolic process	733	31	68.8	2.13	1.2E-04
6357	regulation of transcription from RNA polymerase II promoter	431	32.1	70.8	2.12	1.1E-04
31589	cell-substrate adhesion	74	38.7	83.8	2.12	6.1E-05
7219	Notch signaling pathway	51	40.9	86.3	2.11	5.6E-05
40029	regulation of gene expression\, epigenetic	64	40.9	68.8	2.11	1.9E-04
48666	neuron development	213	33.9	80.3	2.11	1.2E-04
8361	regulation of cell size	142	35.8	74.6	2.11	6.2E-05

9798	axis specification	17	50	94.1	2.09	1.4E-04
31570	DNA integrity checkpoint	26	50	61.5	2.09	4.0E-06
31109	microtubule polymerization or depolymerization	15	50	106.7	2.09	1.2E-04
45860	positive regulation of protein kinase activity	110	37	73.6	2.08	1.3E-04
7026	negative regulation of microtubule depolymerization	10	54.5	110	2.08	1.6E-04
7019	microtubule depolymerization	11	54.5	100	2.08	1.6E-04
31114	regulation of microtubule depolymerization	10	54.5	110	2.08	1.6E-04
9117	nucleotide metabolic process	229	34	70.7	2.06	1.3E-04
48771	tissue remodeling	105	36.2	89.5	2.05	1.6E-04
16052	carbohydrate catabolic process	115	37.9	57.4	2.03	1.3E-04
6220	pyrimidine nucleotide metabolic process	41	45.5	53.7	1.97	9.7E-05
271	polysaccharide biosynthetic process	24	45.5	91.7	1.97	1.4E-04
6793	phosphorus metabolic process	912	29.9	76.6	1.89	1.2E-04
6796	phosphate metabolic process	912	29.9	76.6	1.89	0.0001225

CHAPTER 3: Evaluation of a Dynamic *In vitro* Model of Testis Development

This chapter is in preparation for submission. The authors of the manuscript are:

Susanna Wegner, Ian Stanaway, Sean Harris, Julie Park, Sungwoo Hong, Elaine M. Faustman

Institute for Risk Analysis and Risk Communication, University of Washington School of Public Health, Seattle WA.

Abstract

Our 3-dimensional testicular co-culture shows promise as a model of male reproductive development. To evaluate the ability of this *in vitro* model to capture dynamic developmental processes, we characterized longterm viability, protein expression, testosterone production and morphology. Testicular co-cultures were prepared from postnatal day 5 male rats and cultured with a Matrigel overlay. Following a 2 day acclimation period, protein expression, testosterone concentrations and global gene expression were evaluated at a range of timepoints from experimental days 0-21. Western blotting revealed consistent expression of cell type-specific protein markers of Sertoli cells, Leydig cells, and spermatogonial cells and an increase in the early meiotic marker SCP3 through time. Measurement of testosterone concentrations in cell culture media by ELISA assay demonstrates that testosterone is actively produced in co-cultures through experimental day 5. We next compared global gene expression signals in these *in vitro* conditions with existing publicly available *in vivo* datasets of postnatal rat testis at days 6, 8 and 10. Among all expressed genes, we observed a strong correlation between relative gene expression intensity *in vivo* and *in vitro* at the earliest timepoints ($r=0.71$, $p<0.05$). Pathway analysis of the genes in the top 95th percentile of expression intensity in both systems revealed enrichment for GO terms associated with general homeostasis as well as processes important for testicular development. Furthermore, GO terms enriched among genes significantly changing in expression through time in the same direction *in vivo* and *in vitro* were associated with a range of themes relevant to testicular development, including developmental processes, tube formation,

cell migration and adhesion, cell cycling, hormonal regulation, and immune response. Pathway analysis of genes significantly changing in only *in vivo* or only *in vitro* through time revealed pathways changing uniquely in each system. We further compared *in vivo* and *in vitro* expression dynamics of genes involved in key pathways of particular interest in testicular development identified *a priori*. These terms were associated with specific cell type functions, developmental processes, regulatory processes, and processes important for mediating response to toxicants. Our analysis sheds light on the applicability of our model, anchoring the model to *in vivo* development in order to facilitate interpretation of toxicant pathway perturbation *in vitro*.

Introduction

Male fertility trends

Commonly used synthetic compounds have been implicated as male reproductive toxicants in laboratory studies (Mathur and D'Cruz 2011). In several cases, epidemiological research offers further evidence linking exposure to these chemicals to adverse reproductive outcomes. For example, there is growing epidemiological evidence linking exposure to reproductively toxic phthalate esters to outcomes like degraded semen quality and reduced fertility in adult men (Swan et al. 2003; Hauser et al. 2006; Jurewicz et al. 2009; Jurewicz et al. 2013; Buck Louis et al. 2014) and decreased anogenital distance in male neonates (Swan et al. 2005).

At the same time, an overall decline in male reproductive health and fertility has been documented in populations around the world in recent decades. For example, a significant decrease in semen quality (Carlsen et al. 1992; Swan et al. 2000; Adiga. et al. 2008; Shine et al. 2008; Rolland et al. 2013) and increasing rates of testicular cancers (Chia et al. 2010; Povey and Stocks 2010) has been observed in several large cohorts. Testicular Dysgenesis Syndrome (TDS), proposed as a common underlying cause of male reproductive pathologies like hypospadias, chryptorchidism, germ cell cancer, and low sperm count, is believed to have it roots in early testicular development (Skakkebaek et al. 2001; Sharpe and Skakkebaek 2008). The critical phases of testicular development during which TDS emerges may be particularly vulnerable to environmental perturbation (Sharpe and Skakkebaek 2008).

Need for in vitro models of developmental pathways

Given the clear public health importance of fertility and reproductive health there is a pressing need to identify and control environmental risk factors that can perturb male reproductive development. With the large number of chemicals yet to be fully assessed for their reproductive toxicity (Judson et al. 2009), it is impractical to tackle this challenge with costly and

time consuming animal testing. There is therefore an urgent need for high throughput and high content *in vitro* screens that can capture vulnerable developmental processes throughout the reproductive cycle (Parks Saldutti et al. 2013). In response to this clear need, A 2007 NRC report presented a vision for toxicity testing in the 21st century that emphasizes a shift towards predictive *in vitro* models to evaluate pathway perturbation (NRC 2007). Proposed approaches to implement this vision through high throughput *in vitro* testing and translation of *in vitro* pathway perturbation for risk assessment are continually being refined (Judson et al. 2010; Rusyn and Daston 2010; Judson et al. 2011). Furthermore, increasing consensus around the need for "Evidence based toxicology" demands thorough characterization of emerging *in vitro* models (Hartung et al. 2011; Stephens et al. 2013).

While there have been great advances in the development of *in vitro* testicular models (Parks Saldutti et al. 2013), emerging *in vitro* models must be evaluated for their ability to actually capture critical processes of testicular development before they can be relied on to screen potential reproductive toxicants. These defining processes of testicular development include somatic cell differentiation (Sharpe et al. 2003; Hermo et al. 2010), testosterone production (Lee et al. 1975), creation of complex testicular architecture and germ cell microenvironments (Hermo et al. 2010; Oatley and Brinster 2012) and the emergence of a population of pre-meiotic/early meiotic germ cells (Bowles and Koopman 2007; Hogarth and Griswold 2010).

In vitro testicular co-culture

Our lab has developed a novel three-dimensional *in vitro* primary neonatal rat testis co-culture that captures many aspects of testis development (Yu et al. 2005; Yu et al. 2009; Wegner et al. 2013). These testicular co-cultures contain spermatogonial germ cells as well as Sertoli cells and testosterone producing Leydig cells. Addition of a Matrigel overlay to cultures provides a 3-dimensional niche, enhances attachment and cell signaling, reduces stress signaling and dramatically increases cell viability (Yu et al. 2005). The presence of these three cell types and

the extracellular matrix scaffolding provided by the Matrigel create an environment that is more reminiscent of the *in vivo* niche. We have previously employed this model to accurately distinguish between reproductively toxic and non-reproductively toxic phthalate esters based on toxicogenomic responses (Yu et al. 2009).

Current project

In order to more fully define the relevance of this co-culture to *in vivo* testicular development, in this paper we evaluated its ability to capture well characterized processes that are essential for postnatal testicular development and early spermatogenesis. We characterized viability, protein expression of cell type-specific markers, morphological characteristics, and testosterone production through time in culture. We then used a publicly available dataset of gene expression in rodent testes *in vivo* on postnatal days 6-10 (Liu et al. 2012) to compare temporal gene expression dynamics in our *in vitro* model with those observed *in vivo*. We compared the most highly expressed genes in each model as well as the most significantly changed through time. We performed pathway enrichment analysis to identify Gene Ontology (GO) terms enriched among genes commonly expressed and commonly changing through time as well as those uniquely expressed or uniquely changing only in one system or the other. We then compared *in vivo* and *in vitro* gene expression of genes associated with GO terms identified *a priori* as being particularly important in this phase of testicular development. This set of comparisons allowed us to identify developmental pathway dynamics that are faithfully replicated *in vitro* as well as those that deviate from normal *in vivo* development in an *in vitro* context.

Methods

Testicular co-culture preparation and maintenance. Male Sprague-Dawley rat pups were received on post-natal day 4 (Harlan) and allowed 24 hours to acclimate. Testicular tissue was isolated on postnatal day 5 and digested into a single cell suspension as previously described in

detail (Yu et al. 2005; Wegner et al. 2013). Briefly, testes were detunicated to isolate seminiferous tubules. Tubules were gently digested with a series of collagenase (Sigma), hyauluronidase (Sigma), and DNAse (Qiagen) enzyme cocktails and Eagle's Minimal Essential Medium (MEM) (Invitrogen) washes, followed by a Trypsin (Gibco) digestion. Dissociated testicular cells were suspended in serum-free MEM containing 0.1mM nonessential amino acids (Sigma), 1mM sodium pyruvate (Sigma), 3mM sodium lactate (Sigma), and 1% ITS culture supplement (BD Biosciences) at a density of 0.8 $x10^6$ cells/ml. Cells were plated in 35mm culture dishes (2ml cell suspension/dish) and 30µL ice-cold Matrigel (BD Biosciences) extracellular matrix overlay was immediately added to the center of each dish (for a final concentration of 200 µg/ml) and gently swirled with cell suspension to provide a 3-dimensional scaffold. Co-cultures were incubated at 37˚C, 5% CO2, allowed to acclimate for 48 hours, then maintained up to 21 days in culture, replacing half of the media (900µl removed and 1ml added) every two days. "Experimental Day 0" refers to Day 2 *In vitro* (following the acclimation period).

Live/dead cell imaging. Live co-cultures were incubated 15 minutes at 37˚C with Calcien AM (Life Technologies), propidium iodide (Life Technologies) and Hoechst 33342 (Sigma), fluorescent dyes selectively targeting live cells, dead cells, and total nuclei respectively. Cell staining and morphology was visualized with a fluorescent microscope at 20x and 40x magnification. Images presented are representative of at least 3 independent experiments.

Western blotting. On Experimental Days 0, 1, 3, 5, 7, 10, 14, and 21 cells were harvested in lysis buffer (Cell Signaling Technology) and protein was isolated by sonication followed by centrifugation. Protein concentration of supernatant was determined using a commercially available protein assay kit (Protein Assay kit, Bio-Rad Laboratories) and all samples were brought to equal concentrations with lysis buffer and prepared for western blotting with sample buffer and reducing agent (Novex, Life Technologies). Samples were loaded in 10% Bis-Tris NuPage precast minigels (Life Technologies) and separated by size by running gels at 200V for approximately 45 minutes in running buffer containing 500µL Antioxidant (Novex, Life

Technologies). Protein was transferred to polyvinylidene difluoride nylon membranes (Bio-Rad Laboratories) for immunoblotting. Commassie staining of the gel confirmed efficiency of the transfer. Membranes were rinsed in tris-buffered saline (TBS) pH 7.6 then blocked for one hour with 5% nonfat dry milk in TBS with 0.1% Tween 20 (TTBS). Membranes were then rinsed 3 times with TTBS and incubated overnight with primary antibody. The following day, membranes were washed 3 times in TTBS and incubated 2 hours with secondary antibody conjugated to horseradish peroxidase diluted in 5% milk in TTBS. Antibodies used include SCP3 (ab97672, mouse monoclonal), 3betaHSD (ab75710, mouse monoclonal), stra8 (ab4902, polyclonal rabbit), c-kit (sc-168, rabbit polyclonal), vimentin (sc-6260, mouse monoclonal), PCNA (MAb424, mouse monoclonal), Actin (Sigma, mouse monoclonal) anti-rabbit secondary antibody (Cell Signaling Technology Inc.), and anti-mouse secondary antibody (BD Pharminogen). After secondary antibody incubations, membranes were washed 5 times for 5 minutes with TTBS and incubated with enhanced chemiluminescence detection reagent (GE Lifescience), then incubated with film. Exposed films were developed and digitally scanned. Band intensity was quantified by densitometry using ImageJ software. Expression intensity of each probe was normalized to intensity of corresponding actin loading controls. Data presented here reflect at least 3 independent experiments. Statistical significance of change in expression through time was determined by ANOVA and results are presented as the mean +/- standard error.

Testosterone assay. Cells were allowed 48hours to attach and acclimate following plating. To measure accumulation of testosterone in culture media following a media change, media and cell lysate were collected 8, 24, and 72 hours following a full media change on Experimental Day 0 (2 days after plating) with no additional media changes in between. To measure consistency of testosterone concentrations through time in longterm culture, media and cell lysate were collected 24 hours following half media changes (on Experimental Days 1, 3, 5, 7, 10, and 14). Testosterone concentrations in each media sample were determined by an ELISA assay for total testosterone according to the kit protocol (Neogen Corporation #402510). Testosterone

concentrations measured in the media were normalized to the protein content of corresponding cell lysate (determined by BioRad Protein Assay as described above). Data are presented in terms of fold change in total ng testosterone/ g protein relative to control. Data presented here reflect at least 3 independent experiments. Statistical significance was determined by ANOVA and results are presented as the mean +/- standard error.

Immunofluorescent imaging. Co-cultures were fixed with 4% paraformaldehyde (Sigma) for 30 minutes, then washed in PBS and stored at 4˚C until ready for immunofluoresnce. Fixed cells were washed 3 times with PBS, then blocked 1 hour with PBS blocking buffer containing 5% goat serum (Gibco) and Triton-X 100 to permeablize cell membranes. Cells were then incubated at 4˚C overnight with primary antibodies (listed above for western blotting) in PBS antibody dilution buffer containing 5% BSA and triton X 100. Samples were washed 3 times in PBS and incubated in Alexa flour tagged goat anti-rabbit and goat anti-mouse secondary antibodies (Life Technologies) diluted 1:750 in antibody dilution buffer for 2 hours. Samples were then washed three times, with Hoechst 33342 dye in the final wash to stain nuceli. Labeled cells were visualized at 40x magnification and color channels were processed and combined using ImageJ software.

Microarray processing. RNA samples were harvested in Trizol and isolated using the *mir*Vana™ miRNA Isolation Kit (Ambion). DNA was removed using the Turbo DNAse kit (Ambion) and cleaned up with the MinElute clean up kit (Qiagen). Purified RNA was probed using GeneChip *Rat* Gene *1.0 ST* Affymetrix Arrays. Gene expression at each timepoint was evaluated in samples from three independent cell preparations.

Comparison of gene expression in vivo and in vitro. *In vivo* testicular gene expression data was obtained from a publicly available dataset (Liu et al. 2012) of rat testicular development postnatal days 6, 8 and 10 measured on Nimble-Gen microarrays (Roche). Gene expression data for both *in vivo* and *in vitro* datasets was normalized by RMA in R using the LIMMA package.

To compare baseline expression *in vivo* at PND6 and *in vitro* on Experimental Day 0, we calculated the Pearson's correlation of relative expression intensity *in vivo* and *in vitro* for all genes present on both arrays. We then ranked genes in order of their relative expression intensity in each system and compared the genes in the top 75^{th} and 95^{th} percentiles of expression *in vivo* and *in vitro*. Pathway enrichment analysis was performed with GO Elite software to identify Gene Ontology database terms for biological processes enriched ($Z>2.0$, $p<0.05$) among genes expressed in the top 75^{th} and 95^{th} percentiles in both systems or uniquely in only one system.

Comparison of genes significantly changed through time in vivo and in vitro. Genes significantly changed through time in each system were identified by a fold change cut off of 1.5. Specifically, any gene exceeding this 1.5 fold change relative to expression at the earliest timepoint (post-natal day 6 *in vivo*; experimental day 0 *in vitro*) at any subsequent timepoint was considered significantly changed. Significantly changed genes in each model were then clustered according to their expression dynamics though time using K-means clustering (Soukas et al. 2000). Both *in vivo* and *in vitro*, K-means clustering indicated two main clusters of significantly changed genes, with generally increasing or generally decreasing expression through time. Clustered gene lists *in vivo* and *in vitro* were compared to identify genes significantly changed in both systems and genes that are uniquely changed only *in vivo* or only *in vitro*. We used GO Elite to identify GO biological processes enriched ($Z>2.0$, $p<0.05$) among the genes commonly changed in both systems as well those enriched among genes changed only *in vivo* or only *in vitro*. Enriched GO terms were manually grouped by general theme. Average expression of all genes associated with each enriched theme (regardless of their change through time) was calculated for each timepoint.

Comparison of pathway dynamics in GO terms identified a priori. Rat-specific lists of genes associated with GO biological processes relevant to testicular development were generated from the Gene Ontology Database (May 2014). We generated heatmaps to compare *in vivo* and *in vitro* expression of all genes associated with each of these selected GO terms through time, excluding

genes that were not present on both arrays or that did not exceed background expression levels in at least one of our models. Background expression for each array was determined based on the threshold intensity that negative controls failed to reach. Genes were clustered based on expression *in vivo*.

Results

Longterm viability and maintenance of specific cell types

Fluorescent imaging of co-cultures stained with specific live and dead cell stains provides a qualitative indication that cells remain viable for up to 21 days in culture (Figure 1).

Measurements of total protein content and protein expression of the proliferation marker PCNA indicate that co-cultures are most actively proliferating in the first 72 hours. Cultures continue proliferating throughout time in culture, though PCNA expression decreases by day 3, drops significantly at day 10 then increases again by day 14 and 21. Protein content peaks at day 7 and subsequently declines (Figure 2).

Protein expression of cell type-specific markers provides information about the presence and function of cell types in culture through time. Quantification of Western blots revealed continuous protein expression of cell-type specific markers of Sertoli cells (vimentin), Leydig cells (3βHSD), and spermatogonial cells (c-kit) (Figure 3a-c) through time in culture. Immunofluorescent imaging further confirms protein expression and illustrates the three dimensional nature of the culture and its ability to capture aspects of *in vivo* testicular structures. For example, c-kit positive spermatogonial cells can be seen surrounded by vimentin-positive sertoli cells, creating an *in vivo*-like niche (Figure 3d).

Germ cells poised for entry into meiosis are indicated by expression of the pro-meiotic signal, stimulated by retinoic acid gene 8 (Stra8) and the meiosis-specific synaptonemal complex protein 3 (Scp3). In fact, a peak in Scp3 protein expression around day 7, indicates that germ cells

may be actively entering the early stages of meiosis in culture (Figure 4a and b). Morphological imaging on day 5 demonstrates stra8-positive germ cells poised for meiosis in a tube-like niche formed by vimentin-positive Sertoli cells (Figure 4c). Though cultures are viable for up to 21 days, the decrease in Scp3 protein expression seen after day 7 suggests that co-cultures fail to continue progressing towards germ cell meiosis in the absence of external stimulation with pro-meiotic signals.

Testosterone production in vitro

In order to demonstrate active testosterone production in culture, we used an ELISA assay to measure total testosterone concentrations in cell culture media.
Testosterone concentrations through time in culture (measured 24 hours following partial media changes) demonstrate that overall testosterone concentrations are consistently maintained around 0.2-0.4 ng/g protein through Day 5, then significantly depleted by Day 7, and dropped to below the limit of detection (<0.002ng/ml) by Day 14 in culture. (Figure 5). Such active testosterone production during the first several days in culture provides further evidence for the presence of functional Leydig cells in culture. Raw testosterone concentrations in cell culture media reached as high as 0.3 ng/ml between media changes (data not shown).

Comparison of most highly expressed genes in vivo and in vitro

We compared gene expression through time in the co-culture with a publicly available dataset of testicular gene expression in rats on postnatal days 6, 8 and 10 *in vivo* (Figure 6). In order to determine how closely gene expression *in vitro* resembles gene expression *in vivo*, we first compared all genes expressed in PND 6 *in vivo* with those expressed on experimental day 0 *in vitro* (Figure 7a and b). The Pearson's coefficient for correlation between *in vivo* and *in vitro* gene expression intensity for all expressed genes at the earliest timepoints indicates strong concordance across systems ($r=0.71$, $p<0.05$). A similar comparison of gene expression intensity

on PND 10 *in vivo* and experimental day 3 *in vitro* ($r=0.69$, $p<0.05$) indicated that this similarity in overall gene expression is maintained through experimental day 3 *in vitro* (Supplemental Figure S1).

The most highly expressed genes (those in the top 50^{th}, 75^{th} and 95^{th} percentiles) on experimental day 0 *in vitro* closely mirror the most highly expressed genes on PND 6 *in vivo* (Figure 7c). Among the 433 genes that were expressed in the top 95^{th} percentile of expression intensity in both systems, we found enrichment for 115 GO biological processes (Table 1). These GO terms were related to themes important for testicular function and development (including developmental processes, cell differentiation and development, androgen signaling, growth factor signaling, immune response, and signal transduction) as well as maintenance of general homeostasis (metabolism, transcription and translation, protein processing, and cell cycling). Among genes that were uniquely expressed in the top 95^{th} percentile *in vitro* only (Supplemental Table 1) or *in vivo* only (Supplemental Table 2), enriched GO terms represented many of these same general themes. Genes most highly expressed *in vivo* were uniquely enriched for germ cell development. Meanwhile, GO terms uniquely enriched among genes most highly expressed only *in vitro* included tube morphogenesis.

Identification of significantly changed genes in vivo and in vitro

We also explored dynamics of genes that were significantly changed through time *in vivo* and *in vitro*. Among genes present on both arrays, we identified 3143 genes that were significantly changed through time *in vitro* and 8985 genes significantly changed between postnatal day 6-10 *in vivo*. Of these, 1350 were significantly changed in both *in vivo* and *in vitro* models through time (Figure 8). *In vitro*, changes in gene expression relative to day 0 peak around day 7. For the remainder of this analysis, we limited our focus to the first 7 days *in vitro*, as the *in vivo* data is most comparable to the first three experimental days and the protein

expression, testosterone production, and preliminary genes expression data all indicate a turning point in the co-culture after day 7.

K-means clustering to group genes based on temporal expression dynamics revealed 2 dominant clusters in both systems. In both cases, these clusters reflect genes with generally increasing expression or decreasing expression through time (from PND6 to 10 *in vivo* or up to day 7 *in vitro*). These clusters included 342 genes increased in expression through time in both systems, and 199 genes decreased in expression in both systems (Figure 8a).

Identification of pathways enriched among genes commonly changed in both systems or uniquely changed only in vivo or only in vitro

In order to further explore the pathways captured both *in vivo* and *in vitro*, we identified GO biological processes enriched among genes that were changed through time in both systems. Among the 541 genes that were significantly changed in the same direction both *in vivo* and *in vitro*, key themes that emerged among enriched GO terms include development and morphogenesis, cellular adhesion and migration, tube formation, immune function, cell cycling, steroid regulation, signal transduction, and response to oxidative stress levels (Table 2).

In order to identify processes unique to the *in vitro* model, we also identified pathways enriched among genes changed only *in vitro* (Supplemental Table 3). This set of genes contributed to many of the same pathways enriched among the genes changed through time in both systems. In addition, pathways unique to the *in vitro* system also emerged, including several associated with response to chemical stimulus, cell stress, and apoptosis.

In order to identify important *in vivo* processes in this stage of development that are not captured by the *in vitro* model, we also performed pathway analysis on the set of genes changed only *in vivo* (Supplemental Table 4). As in the *in vitro*-specific analysis, we find that these *in vivo*-specific genes contribute to many of the same GO terms and broader themes that are enriched among the genes commonly changed in both systems. In addition to these pathways,

however, we observed enrichment of GO terms unique to the *in vivo* system. These terms reflect a response to a broader set of hormones and growth factors that are not reflected *in vitro*, including parathyroid hormone, follicle stimulating hormone, and transforming growth factor-β.

Exploration of pathway dynamics of specific pathways of interest identified a priori

In addition to the unsupervised pathway analysis described above, we compared *in vivo* and *in vitro* expression dynamics of all genes (regardless of temporal change in expression) associated with GO terms identified *a priori* for their particular importance for male reproductive development. These terms reflect cell type-specific functions, relevant developmental processes, regulatory processes, and processes important for response to toxicants. We see striking agreement between the *in vivo* and *in vitro* systems in the genes most highly expressed within many of these GO terms of interest (Figure 9). For example, among genes associated with Sertoli cell differentiation and tight junction formation (associated with maturing Sertoli cells) we observe that the genes associated with these processes that were most highly expressed *in vivo* were also among the most highly expressed in the GO term *in vitro*. However, the FSHR and Soc1 genes associated with Sertoli cell differentiation emerged as being highly expressed *in vitro* but not *in vivo*. Similar agreement in overall gene expression trends between models was seen for a range of other pathways of interest, including Leydig cell differentiation, response to Vitamin A, response to FSH, tight junction formation, and steroid metabolism and biosynthesis. In all of these pathways, general expression patterns are consistent while a few genes differ in relative intensity across models. Despite general consistency in relative expression of genes within each GO term across models, the temporal dynamics of expression among genes associated with these GO terms was variable between the two models.

Gene expression trends in other GO terms of interest were less consistent *in vivo* and *in vitro*. For example, *in vitro* gene expression trends generally indicate an upregulation of stress

response genes, with many more genes highly expressed *in vitro* among GO terms related to oxidative stress and apoptosis.

Discussion

This research begins to more clearly define the appropriate applications for this testicular co-culture. The ability of this model to capture several key processes of a sensitive phase of male reproductive development makes it a promising tool for screening potential reproductive toxicants. Throughout both unsupervised and targeted pathway analysis we see a consistent pattern emerging around the relevant pathways our *in vitro* model captures. Processes captured *in vitro* include context-specific processes unique to post-natal testis development (eg. Leydig cell differentiation, testosterone production and Sertoli cell tight junction formation) as well as general developmental processes associated with highly conserved signaling pathways and regulatory mechanisms that are seen in a range of tissue types and developmental contexts (eg. signal transduction, cell cycling, and morphological development).

What context-specific processes are captured?

Protein and gene expression data confirm the presence and maintenance of Leydig cells, Sertoli cells, and spermatogonial germ cells, three major cell types of the developing testis, through time in the co-culture. This data is supported by the pathway analysis. Among the most highly expressed genes (those in the 95^{th} percentile of expression intensity) as well as genes significantly changed both *in vivo* and *in vitro* we observed enrichment for GO terms associated with cell differentiation and development. Targeted pathway analysis further demonstrated high concordance between *in vivo* and *in vitro* expression of genes associated with Leydig and Sertoli cell differentiation.

We also observed evidence in both our unbiased pathway analysis and targeted pathway analysis for a range of specific cell-type functions. For example, in all steps of our pathway analysis, we see strong evidence that expression of genes associated with steroid signaling and

regulation *in vivo* are reflected *in vitro*, supporting our observation of active testosterone production through the first 5 days in culture. Longterm testosterone production by Leydig cells *in vitro* has previously been shown to be enhanced by presence of Sertoli cells (Verhoeven and Cailleau 1990; Lejeune et al. 1998). This suggests that the complexity of the co-culture contributes to the successful production of testosterone *in vitro*, enhancing the relevance of the model to *in vivo* systems. Indeed, the highest testosterone concentrations measured in cell culture media were within an order of magnitude of circulating testosterone concentrations previously measured in neonatal rats (Lee et al. 1975).

Morphological observations of the formation of tube-like structures *in vitro* are also supported by the pathway analysis. Among the genes significantly changed through time both *in vivo* and *in vitro*, we observed enrichment for several GO terms associated with cellular adhesion and migration and tube formation. We also see enrichment for terms associated with tight junction formation, a characteristic function of Sertoli cells that is essential for germ cell development (Oatley and Brinster 2012) and can be targeted by a range of reproductive toxicants (Fiorini et al. 2004).

The immune system is emerging as another important regulator of testicular developmental processes that may be an important target of reproductive toxicants. For example, fetal macrophages have recently been shown to play an important role in the vascular reorganization that facilitates testicular development (DeFalco et al. 2014). There is also evidence that immune system function in the developing testis can be perturbed by toxicant exposure (Murphy et al. 2014). It is therefore encouraging that this *in vitro* model is able to capture elements of immune response processes, as illustrated by GO terms related to cytokine production and other immune responses that are enriched among genes highly expressed and significantly changed both *in vivo* and *in vitro*.

The ability of this *in vitro* system to capture processes specific to this stage of testicular development that could be perturbed by toxicants suggests the model could be a powerful screening tool.

What general developmental processes are captured in vitro?

A small set of highly conserved signal transduction pathways play a crucial role in regulating a diverse range of development processes. For this reason, measuring perturbation of these conserved pathways has been proposed as a valuable approach for predicting a wide range of developmental toxicity endpoints (Gerhart 1999; NRC 2000; Knudsen et al. 2011).

In addition to testis-specific signals, pathway analysis reveals that our testicular co-culture captures many of the highly conserved signaling pathways that drive cellular differentiation, development and morphogenesis in a range of developmental contexts. Specifically, GO terms related to Wnt, smoothened, Notch, SMAD, and BMP signal transduction pathways are enriched among the genes significantly changing in the same direction through time in both systems.

Because these highly conserved processes are replicated in a diverse set of tissue types throughout development, we see enrichment for seemingly unrelated developmental processes like cochlear development. Enrichment for this wide range of developmentally related GO terms that are unrelated to the testis is likely due to the presence of signals that regulate processes of developmental and morphogenesis throughout the body. The ability of our co-culture to capture dynamic change in several of these highly conserved pathways makes this a promising model for detecting aspects of general developmental toxicity as well as testicular-specific toxicity.

What occurs in vitro that may not reflect in vivo processes?

In addition to capturing aspects of pathways that are important *to vivo* development, the *in vitro* model is active in several pathways that appear to deviate from normal *in vivo* dynamics.

Though we have previously found that the addition of Matrigel minimizes stress signaling in this *in vitro* testis model (Yu et al. 2005) our pathway analysis consistently demonstrates that general stress response pathways, oxidative stress, and apoptosis are still more active in *in vitro* cultures than in *in vivo* testis. Oxidative stress is an important signal in normal development (Dennery 2007; Wells et al. 2009) and our targeted pathway analysis demonstrates that a subset of genes associated with oxidative stress are upregulated in the *in vivo* dataset. Though many of these same genes are upregulated *in vitro*, a large number of additional oxidative stress response genes are also upregulated, suggesting stress signaling associated with *in vitro* conditions that exceed oxidative stress signaling associated with normal development during this phase. Similarly, apoptosis is an important developmental process that facilitates morphogenesis and patterning and is associated with caspase signaling hypothesized to promote differentiation (Li et al. 2010; Kuranaga 2012). Our targeted pathway analysis revealed that a subset of genes associated with apoptosis are expressed in developing testes *in vivo*. However, far more genes associated with the GO term are upregulated *in vitro*, further indicating additional stress response and apoptosis in the *in vitro* system.

What important processes are not captured in this co-culture?

Though the *in vitro* co-culture is able to capture many aspects of this sensitive phase of testicular development, there are elements of the complex morphology and hormonal regulation associated with *in vivo* testicular development that we do not capture *in vitro*. Because the *in vitro* system is not in the context of the body as a whole, it does not benefit from the complex regulation of systemic signaling from hormones and growth factors. This is reflected in the fact that genes uniquely changed through time *in vivo* are associated with GO terms related to response to signals like FSH, parathyroid hormone, and TGF-β. In addition, while the morphology captured *in vitro* appears to recapitulate elements of the *in vivo* niche, it is important to note that the co-culture does not establish true tubes and that the Leydig cells normally

excluded from the seminiferous tubules are in contact with the other cell types. With future refinement of the model to incorporate tightly regulated delivery of hormones and growth factors via microfluidics that facilitate complex morphological development, we may be able to overcome some of these challenges and create a co-culture that is even more reminiscent of *in vivo* conditions.

Relevance for reproductive and developmental toxicology

The phase captured in this *in vitro* model is a particularly interesting and dynamic phase of testicular development. On postnatal day 5, the day our co-cultures are initiated, several major cell types of the rat testis are in a proliferative, immature state and about to transition through differentiation and maturation. Leydig cells typically begin to differentiate around PND10 in rats (Mendis-Handagama and Ariyaratne 2001) while Sertoli cells remain proliferative throughout puberty and being to differentiate around the onset of puberty around PND 15 (Sharpe et al. 2003). Meanwhile, germ cells at this stage include partially differentiated spermatogonial cells in preparation for entry into the earliest stages of meiosis around PND13 (Malkov et al. 1998). These processes of differentiation and maturation are directed by signaling from hormones, growth factors, and paracrine signals, including FSH, LH, thyroid, AMH, TGFβ,and IGF-1 (Mendis-Handagama and Ariyaratne 2001; Sharpe et al. 2003). Many of these signals are apparent in the *in vivo* genomic data we explored here. In the future, carefully regulated supplementation with some of these key regulators could help drive further differentiation *in vitro*. A model in which cells are poised for differentiation is particularly important for toxicological screening because several studies have demonstrated differential sensitivity of cells at different stages of differentiation (Schmid 1961; Creasy and Foster 1984; Tamm et al. 2006; Theunissen et al. 2010).

While this co-culture may serve as an informative model for aspects of early testicular development and spermatogenesis and some general developmental processes, it cannot stand alone as a predictor of male reproductive toxicity. Because chemical hazard is highly dependent

on developmental context, a complete evaluation of reproductive hazard must incorporate hazards unique to each developmental process. For example additional models would be required to predict perturbation of spermatogenesis.

In addition, important species differences exist in male reproductive toxicity (Habert et al. 2014). Currently no human *in vitro* models successfully capture so many cell types in such a dynamic stage of testicular development. Eventually this rodent model could be used to inform construction of human stem cell based models that would overcome species differences (Chapin et al. 2013).

The current analysis establishes a baseline to anchor normal pathway dynamics *in vitro* to relevant developmental processes *in vivo*. This framework can be applied to quantify toxicant perturbation of these normal developmental pathway dynamics with an understanding of their relevance to *in vivo* testicular development. In this analysis, we've shown that the co-culture captures pathways with relevance for predicting perturbation of general developmental processes (like signal transduction) and context-specific processes (like Leydig cell differentiation). Ultimately, this analysis can inform future toxicity studies so that our co-culture is applied to ask appropriate questions and the results can be interpreted within the context of how the *in vitro* model relates to *in vivo* development.

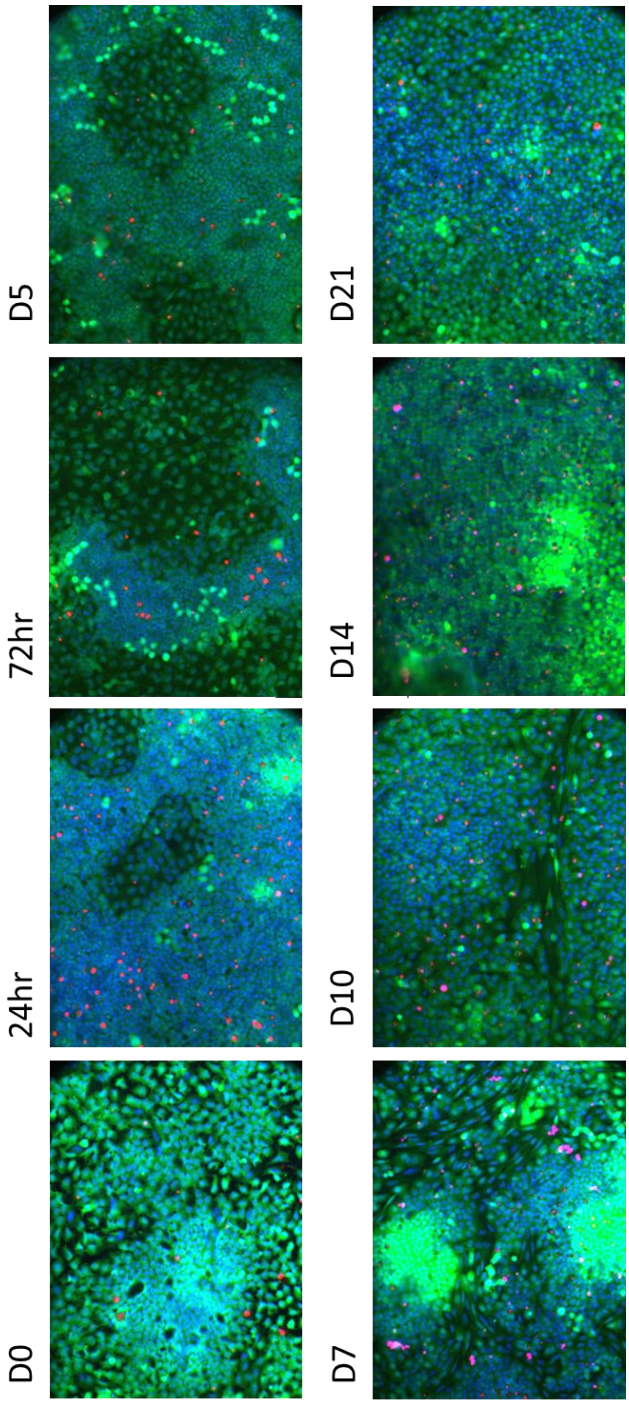

Figure 1. Cell Viability in testicular co-cultures through time. Fluorescent imaging (20x magnification) illustrates cell viability and cell death over time in culture. Green (Calcien AM) indicates live cells, red (Propidium Iodide) indicates dead cells and blue (Hoechst 33342) indicates total nuclei (both live and dead).

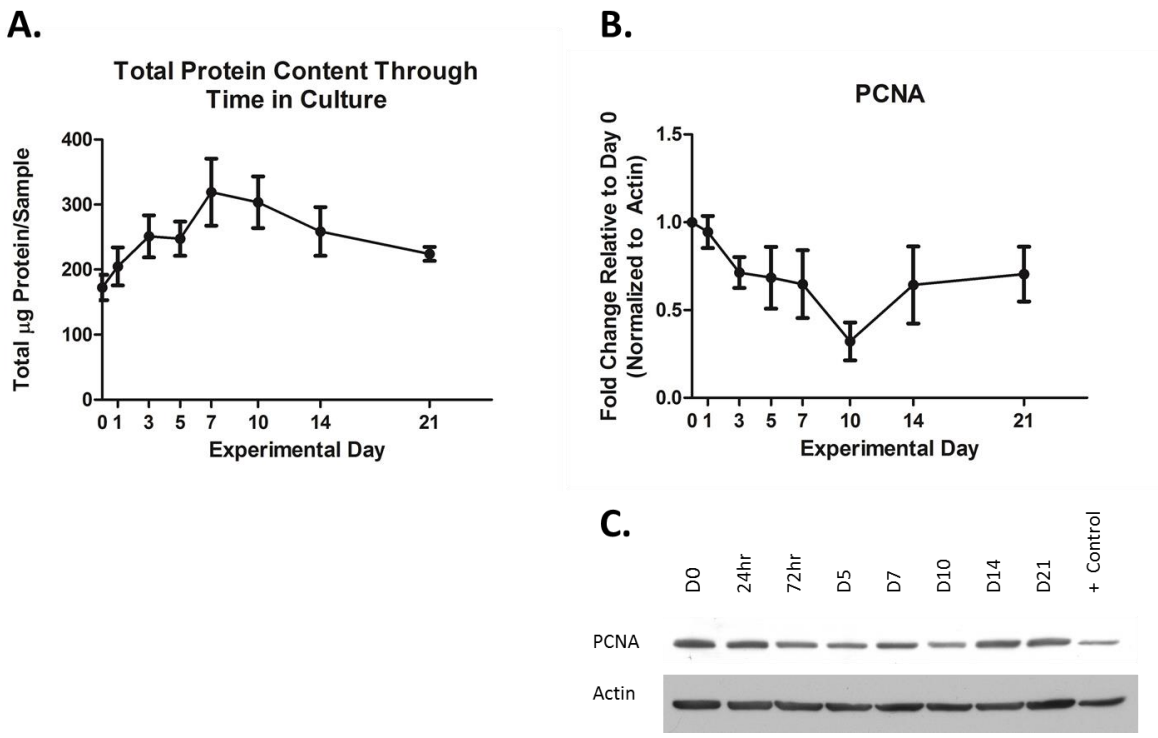

Figure 2. Cell proliferation through time in co-cultures. (A) Cell proliferation was assessed by changes in total protein content and by expression of PCNA protein. Total protein yield was quantified by BioRad protein assay. (B) Expression of PCNA was quantified by Western blotting. Western band intensity was quantified in ImageJ Software and normalized to β-actin loading controls. (C) Blots shown are representative of at least 3 independent blots; corresponding β-actin expression is shown to represent total protein loading. All data represent at least 3 independent replicates. Error bars represent standard error of the mean.

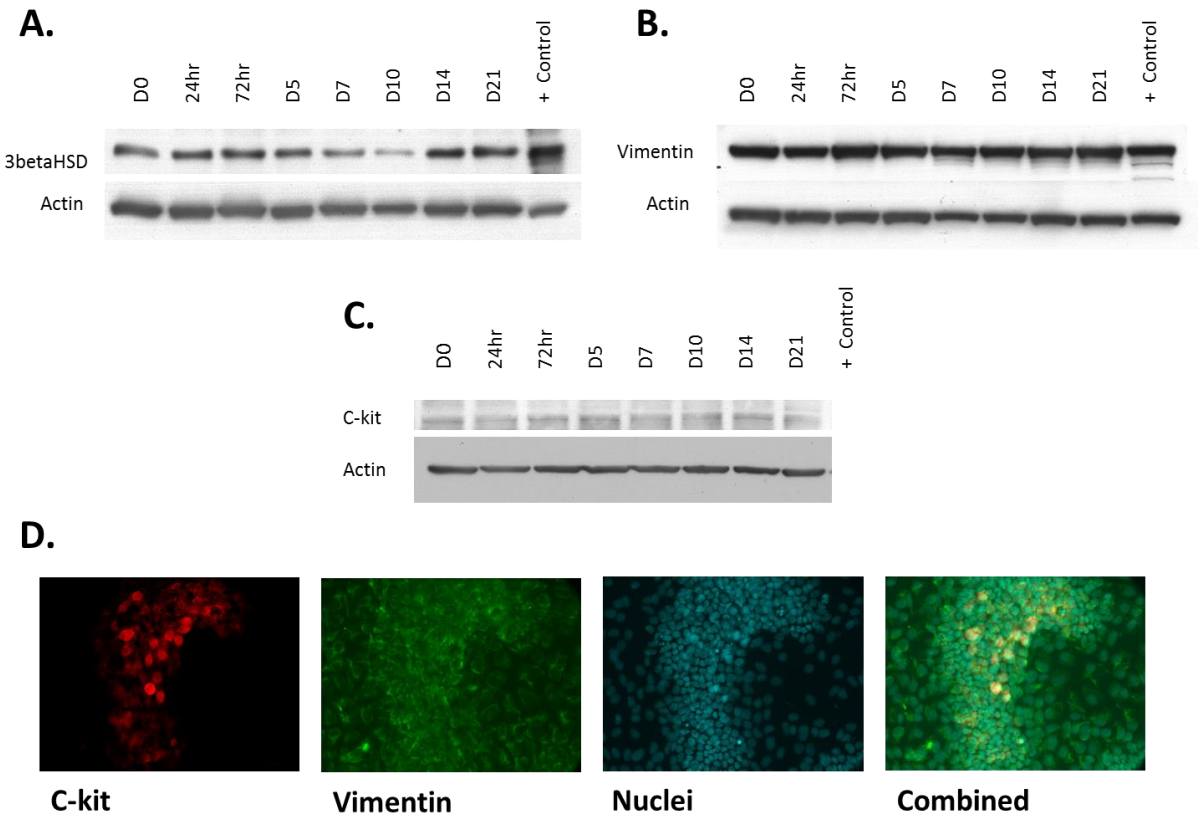

Figure 3. Consistent expression of cell type specific markers through time in culture. Western blotting for antibodies to cell-type specific proteins demonstrates the consistent presence of 3 major testicular cells types. Leydig cells are indicated by (A) 3betaHSD, (B) Sertoli cells are indicated by Vimentin, and (C) spermatogonial cells are indicated by c-kit. Blots shown are representative of at least 3 independent blots; Corresponding β-actin expression is shown to represent total protein loading. Western band intensity was quantified in ImageJ Software, but there was no significant change in any of these markers observed consistently across time. (D) Immunofluorescent images of co-cultures show c-kit positive spermatogonial cells surrounded by vimentin-positive sertoli cells in an *in vitro* niche. Pictures were taken at 40x magnification on experimental day 3 *in vitro*.

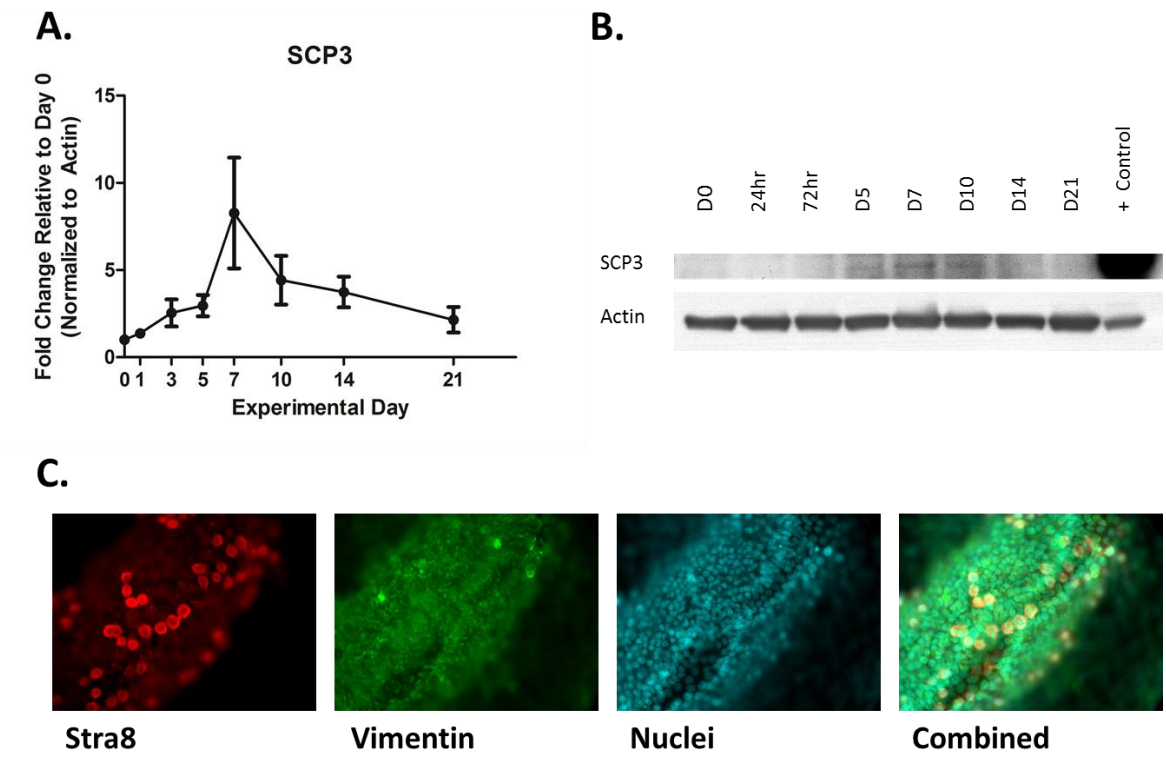

Figure 4. Evidence of pre-meiotic and early meiotic germ cells in co-culture. (A) Western blotting demonstrates increasing protein expression of the early meiosis marker scp3 through time. Western band intensity was quantified in ImageJ Software and normalized to β-actin loading control. Error bars indicate standard error of the mean. (B) Blots shown are representative of at least 3 independent blots; Corresponding β-actin expression is shown to represent total protein loading. (C) Immunofluorescent images of co-cultures show spermatogonial cells positive expressing the pre-meiotic marker stra8, surrounded by vimentin-positive sertoli cells in an *in vitro* niche. Pictures were taken at 40x magnification on experimental day 5 *in vitro*.

Figure 5. Testosterone production and maintenance in co-cultures through time. Total testosterone concentrations in media were measured by ELISA assays 24 hours following a partial media changes. Concentrations are normalized to corresponding total protein content from the same sample. Data represent at least 3 independent replicates Error bars indicate standard error of the mean.

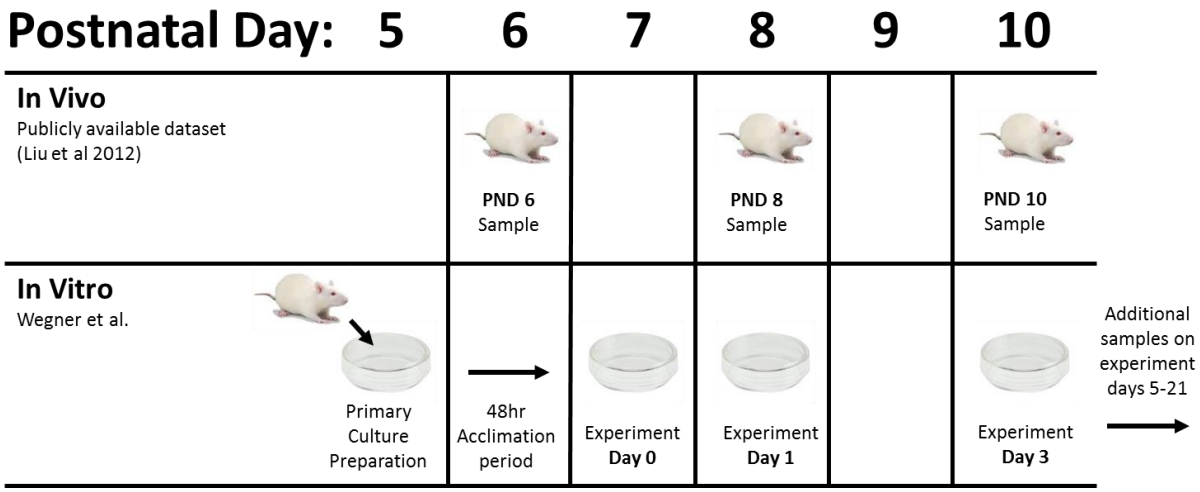

Figure 6. Overview of *in vivo / in vitro* comparison. Testicular co-cultures were prepared from male rats on postnatal day 5 and allowed to acclimate 48 hours prior to evaluation on experimental day 0. *In vitro* gene expression on experimental day 0-21 was compared to *in vivo* gene expression on postnatal days (PND) 6, 8, and 10.

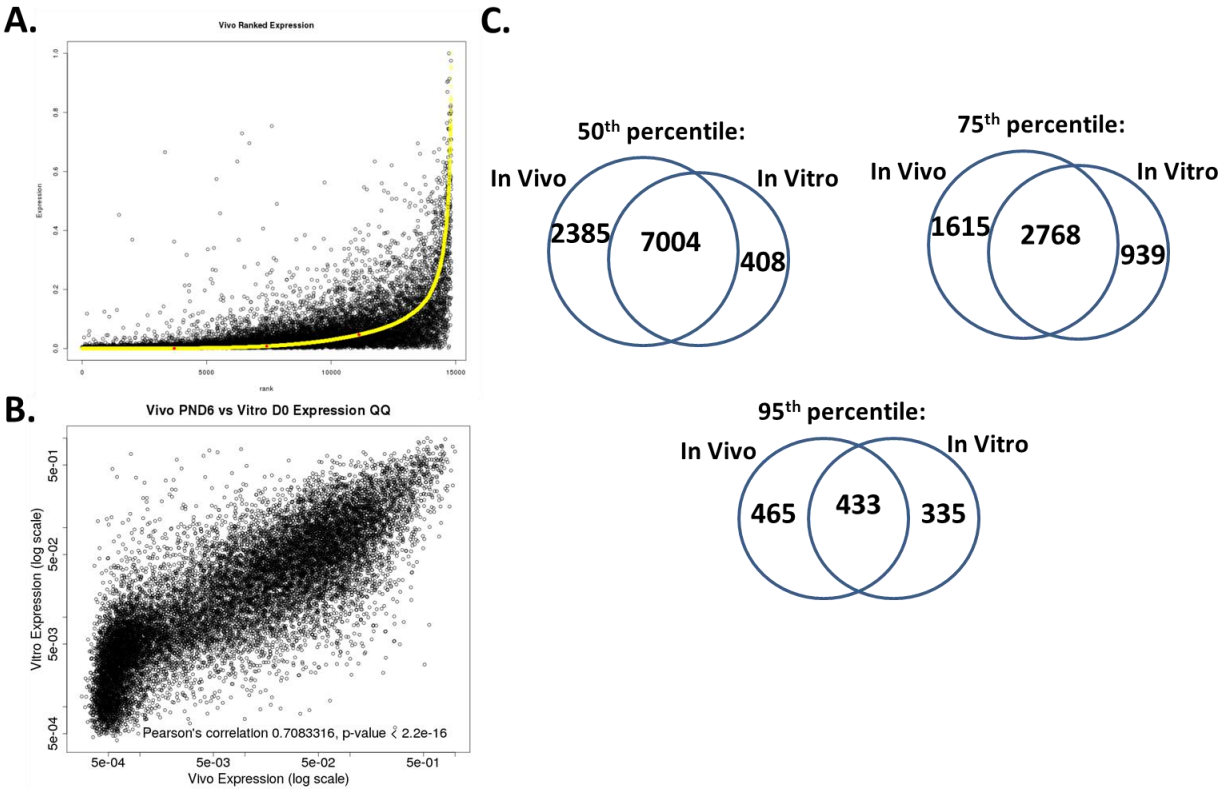

Figure 7. Comparison of gene expression on PND6 *in vivo* and experimental day 0 *in vitro*. (A) Genes ranked in order of expression intensity *in vivo* (along the yellow line) were compared to expression intensity of those same gene *in vitro* (plotted as black dots). (B) Correlation between expression intensity of a given gene *in vitro* with the expression intensity of those genes *in vivo*. Pearson's correlation = 0.71; $p<0.05$. (C) Summary of number of genes expressed in the highest 50th, 75th, and 95th percentiles *in vivo* and *in vitro* and the degree of overlap between the two systems.

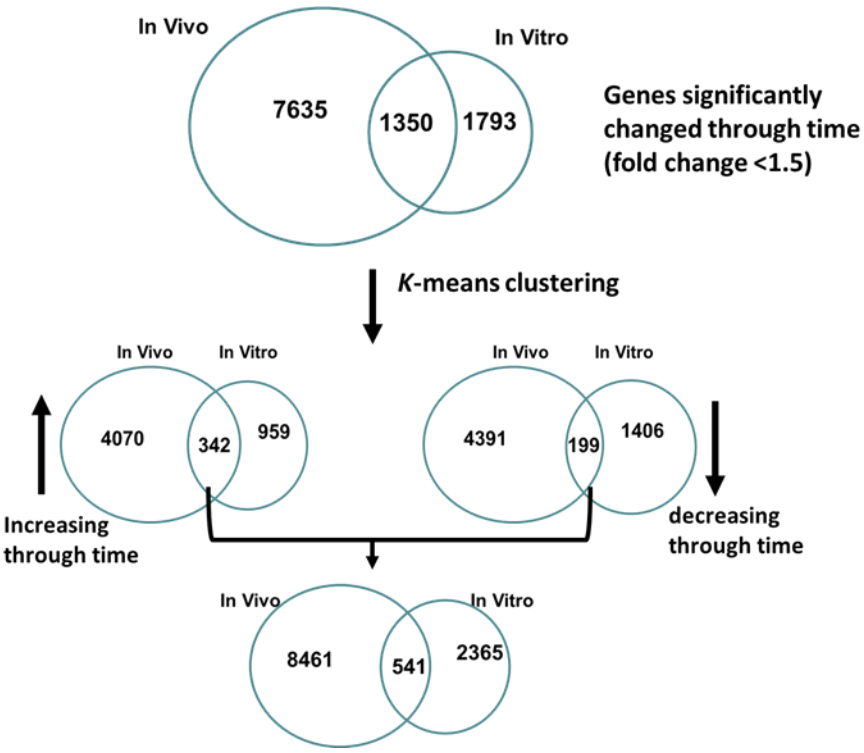

Figure 8. Comparison of genes significantly changed through time PND 6-10 *in vivo* And Experimental days 0-7 *in vitro*. (A) Venn diagrams of all genes significantly changed *in vivo* and *in vitro* and significantly changed genes segregated by *K*-means clustering into those that are generally increasing or generally decreasing through time. Those that were changing in the same direction in both systems were combined for pathway analysis. (B) Heatmap illustrating average gene expression through time for all genes associated with a selection of GO terms enriched among the 541 genes changing the same direction in both systems. These example GO terms were selected from the 159 enriched terms. Terms included are the three with the highest Z-scores within each of the general themes.

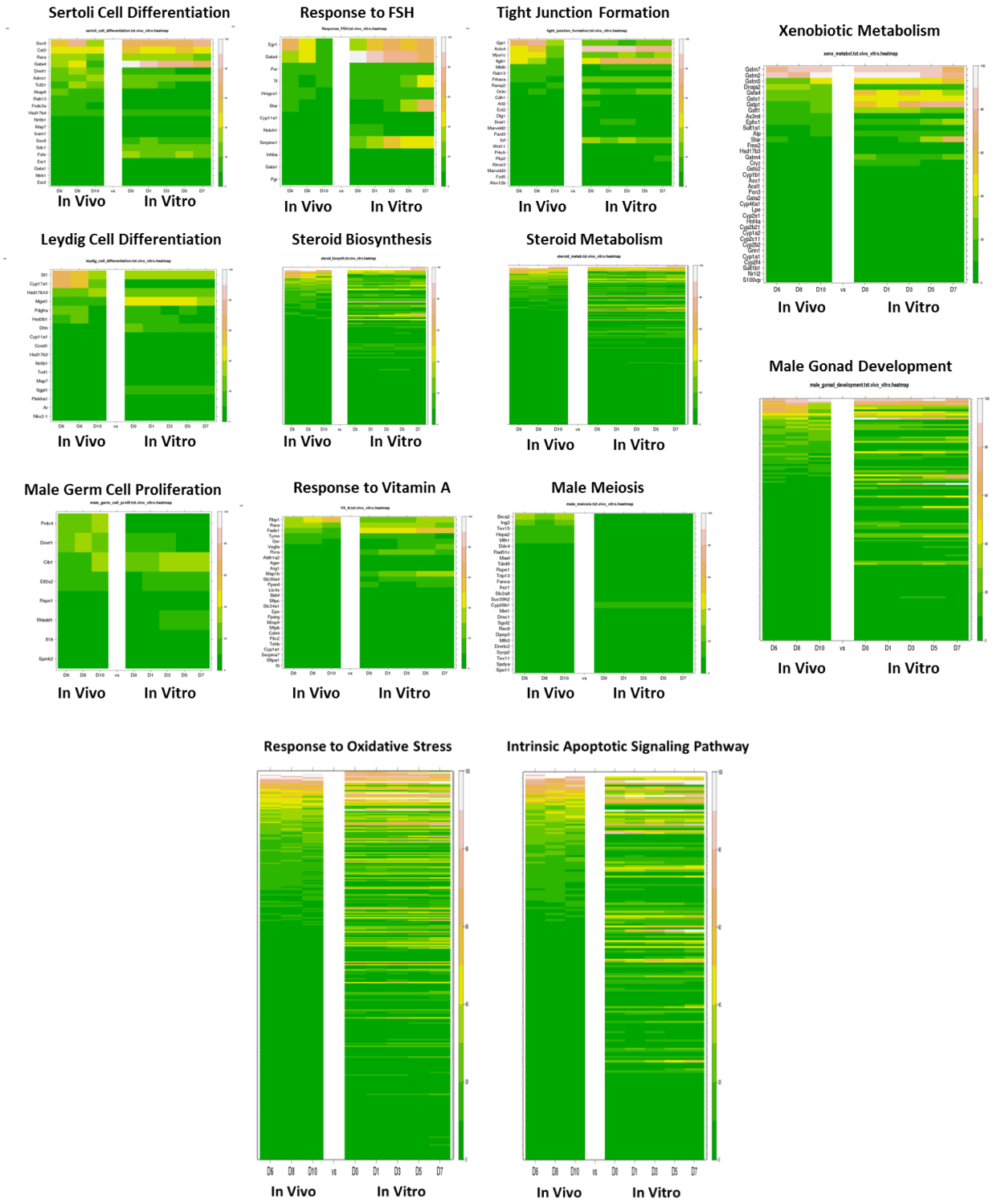

Figure 9. Pathways dynamics of targeted pathways of interest through time *in vivo* and *in vitro*. GO biological processes of relevance for testicular development were identified and relative gene expression intensity for all genes associated with each of these terms is compared between the *in vivo* and *in vitro* systems through time. Genes are clustered based on *in vivo* expression. Genes that were not present on both arrays were excluded.

Table 1. GO biological processes enriched among genes expressed in the top 95th percentile both *in vivo* and *in vitro* (Z>2, p<0.05)

Ontology-ID	Ontology Name	# Changed	# Measured	# in Ontology	% Changed	% Present	Z Score
GO:0008152	metabolic process	2882	4635	7187	62.18	64.49	23.79
GO:0009758	carbohydrate utilization	1037	1500	2585	69.13	58.03	17.17
GO:0071841	cellular component organization or biogenesis at cellular level	959	1440	2035	66.60	70.76	14.73
GO:0007587	sugar utilization	966	1501	2612	64.36	57.47	13.23
GO:0046907	intracellular transport	420	561	711	74.87	78.90	12.86
GO:0045184	establishment of protein localization	463	635	799	72.91	79.47	12.71
GO:0019222	regulation of metabolic process	1642	2860	3948	57.41	72.44	11.04
GO:0033554	cellular response to stress	366	523	695	69.98	75.25	10.11
GO:0022607	cellular component assembly	464	720	964	64.44	74.69	8.90
GO:0007049	cell cycle	160	204	256	78.43	79.69	8.67
GO:0048523	negative regulation of cellular process	983	1692	2146	58.10	78.84	8.62
GO:0051726	regulation of cell cycle	271	390	507	69.49	76.92	8.48
GO:0048522	positive regulation of cellular process	1111	1975	2473	56.25	79.86	7.65
GO:0022402	cell cycle process	219	315	431	69.52	73.09	7.61
GO:0010941	regulation of cell death	518	851	1033	60.87	82.38	7.57
GO:0043933	macromolecular complex subunit organization	345	540	717	63.89	75.31	7.38
GO:0006979	response to oxidative stress	154	212	247	72.64	85.83	7.14
GO:0051301	cell division	100	127	162	78.74	78.40	6.89
GO:0044085	cellular component biogenesis	51	54	103	94.44	52.43	6.79
GO:0061024	membrane organization	181	266	325	68.05	81.85	6.49
GO:0007017	microtubule-based process	131	186	284	70.43	65.49	6.07
GO:0001906	cell killing	99	133	174	74.44	76.44	6.05
GO:0006915	apoptosis	201	311	369	64.63	84.28	5.81
GO:0051236	establishment of RNA localization	46	52	75	88.46	69.33	5.80
GO:0050657	nucleic acid transport	46	52	75	88.46	69.33	5.80
GO:0051128	regulation of cellular component organization	451	774	983	58.27	78.74	5.70
GO:0009411	response to UV	53	63	77	84.13	81.82	5.69
GO:0007264	small GTPase mediated signal transduction	147	221	281	66.52	78.65	5.45
GO:0065009	regulation of molecular function	673	1208	1493	55.71	80.91	5.38
GO:0051641	cellular localization	107	153	195	69.93	78.46	5.37
GO:0006413	translational initiation	31	33	54	93.94	61.11	5.25
GO:0000910	cytokinesis	39	45	51	86.67	88.24	5.15
GO:0045454	cell redox homeostasis	43	52	69	82.69	75.36	4.96
GO:0009966	regulation of signal transduction	544	978	1235	55.62	79.19	4.74
GO:0080135	regulation of cellular response to stress	111	168	202	66.07	83.17	4.62

GO:0072331	signal transduction by p53 class mediator	30	35	46	85.71	76.09	4.43
GO:0009790	embryo development	159	260	327	61.15	79.51	4.17
GO:0006984	ER-nucleus signaling pathway	21	24	32	87.50	75.00	3.84
GO:0032869	cellular response to insulin stimulus	54	77	101	70.13	76.24	3.83
GO:0001101	response to acid	62	91	112	68.13	81.25	3.79
GO:0007179	transforming growth factor beta receptor signaling pathway	33	43	53	76.74	81.13	3.73
GO:0007243	intracellular protein kinase cascade	118	192	240	61.46	80.00	3.66
GO:0045767	regulation of anti-apoptosis	34	45	52	75.56	86.54	3.66
GO:0032392	DNA geometric change	15	16	21	93.75	76.19	3.64
GO:0032886	regulation of microtubule-based process	49	70	90	70.00	77.78	3.63
GO:0071478	cellular response to radiation	32	42	52	76.19	80.77	3.61
GO:0032465	regulation of cytokinesis	17	19	24	89.47	79.17	3.59
GO:0034330	cell junction organization	44	62	79	70.97	78.48	3.57
GO:0048008	platelet-derived growth factor receptor signaling pathway	18	21	26	85.71	80.77	3.43
GO:0046686	response to cadmium ion	27	35	41	77.14	85.37	3.41
GO:0007569	cell aging	30	40	49	75.00	81.63	3.38
GO:0016055	Wnt receptor signaling pathway	74	116	145	63.79	80.00	3.34
GO:0060612	adipose tissue development	13	14	21	92.86	66.67	3.33
GO:0051656	establishment of organelle localization	28	37	53	75.68	69.81	3.33
GO:0032507	maintenance of protein location in cell	28	37	60	75.68	61.67	3.33
GO:0007163	establishment or maintenance of cell polarity	31	42	57	73.81	73.68	3.31
GO:0030521	androgen receptor signaling pathway	15	17	21	88.24	80.95	3.29
GO:0007507	heart development	92	149	184	61.74	80.98	3.29
GO:0032386	regulation of intracellular transport	70	110	134	63.64	82.09	3.22
GO:0010212	response to ionizing radiation	58	89	121	65.17	73.55	3.18
GO:0033327	Leydig cell differentiation	12	13	16	92.31	81.25	3.17
GO:0071453	cellular response to oxygen levels	34	48	53	70.83	90.57	3.12
GO:0014910	regulation of smooth muscle cell migration	23	30	36	76.67	83.33	3.11
GO:0032469	endoplasmic reticulum calcium ion homeostasis	9	9	10	100.00	90.00	3.10
GO:0001843	neural tube closure	33	47	58	70.21	81.03	3.00
GO:0055072	iron ion homeostasis	30	42	67	71.43	62.69	3.00
GO:0046685	response to arsenic-containing substance	17	21	23	80.95	91.30	2.99
GO:0006986	response to unfolded protein	22	29	38	75.86	76.32	2.97
GO:0071417	cellular response to organic nitrogen	25	34	47	73.53	72.34	2.94
GO:0071445	cellular response to protein stimulus	36	53	69	67.92	76.81	2.86
GO:0006904	vesicle docking involved in exocytosis	16	20	22	80.00	90.91	2.83

GO:0007369	gastrulation	24	33	43	72.73	76.74	2.80
GO:0048608	reproductive structure development	66	107	133	61.68	80.45	2.77
GO:0032990	cell part morphogenesis	99	169	199	58.58	84.92	2.68
GO:0022415	viral reproductive process	20	27	38	74.07	71.05	2.68
GO:0014070	response to organic cyclic compound	162	289	321	56.06	90.03	2.65
GO:0042692	muscle cell differentiation	49	78	91	62.82	85.71	2.56
GO:0060249	anatomical structure homeostasis	60	98	119	61.22	82.35	2.56
GO:0071326	cellular response to monosaccharide stimulus	16	21	27	76.19	77.78	2.55
GO:0001889	liver development	50	80	102	62.50	78.43	2.54
GO:0032506	cytokinetic process	6	6	6	100.00	100.00	2.53
GO:0042386	hemocyte differentiation	436	829	1022	52.59	81.12	2.52
GO:0070542	response to fatty acid	22	31	37	70.97	83.78	2.52
GO:0048010	vascular endothelial growth factor receptor signaling pathway	12	15	17	80.00	88.24	2.45
GO:0010611	regulation of cardiac muscle hypertrophy	12	15	16	80.00	93.75	2.45
GO:0006825	copper ion transport	10	12	15	83.33	80.00	2.43
GO:0001841	neural tube formation	10	12	14	83.33	85.71	2.43
GO:0071496	cellular response to external stimulus	103	180	202	57.22	89.11	2.40
GO:0015988	energy coupled proton transport, against electrochemical gradient	18	25	38	72.00	65.79	2.37
GO:0007420	brain development	98	171	211	57.31	81.04	2.36
GO:0060762	regulation of branching involved in mammary gland duct morphogenesis	5	5	5	100.00	100.00	2.31
GO:0044342	type B pancreatic cell proliferation	5	5	5	100.00	100.00	2.31
GO:0021860	pyramidal neuron development	5	5	6	100.00	83.33	2.31
GO:0010761	fibroblast migration	5	5	7	100.00	71.43	2.31
GO:0051147	regulation of muscle cell differentiation	34	53	67	64.15	79.10	2.31
GO:0060325	face morphogenesis	16	22	28	72.73	78.57	2.29
GO:0019884	antigen processing and presentation of exogenous antigen	16	22	22	72.73	100.00	2.29
GO:0042493	response to drug	199	367	440	54.22	83.41	2.28
GO:0051881	regulation of mitochondrial membrane potential	11	14	14	78.57	100.00	2.26
GO:0030324	lung development	53	88	108	60.23	81.48	2.24
GO:0051181	cofactor transport	9	11	12	81.82	91.67	2.22
GO:0090342	regulation of cell aging	7	8	8	87.50	100.00	2.22
GO:0090075	relaxation of muscle	7	8	8	87.50	100.00	2.22
GO:0072401	signal transduction involved in DNA integrity checkpoint	7	8	12	87.50	66.67	2.22
GO:0032025	response to cobalt ion	7	8	9	87.50	88.89	2.22
GO:0021756	striatum development	7	8	10	87.50	80.00	2.22
GO:0015825	L-serine transport	7	8	8	87.50	100.00	2.22

GO:0001833	inner cell mass cell proliferation	7	8	10	87.50	80.00	2.22
GO:0045444	fat cell differentiation	41	67	78	61.19	85.90	2.11
GO:0030218	erythrocyte differentiation	22	33	41	66.67	80.49	2.11
GO:0061298	retina vasculature development in camera-type eye	4	4	4	100.00	100.00	2.07
GO:0015780	nucleotide-sugar transport	4	4	6	100.00	66.67	2.07
GO:0006403	RNA localization	4	4	5	100.00	80.00	2.07
GO:0030641	regulation of cellular pH	10	13	17	76.92	76.47	2.06
GO:0048009	insulin-like growth factor receptor signaling pathway	8	10	13	80.00	76.92	2.00

Table 2. GO biological processes enriched among genes significantly changed in a common direction both *in vivo* and *in vitro* (Z>2, p<0.05). GO terms grouped by general themes and ranked by Z-score within each theme.

Ontology-ID	Ontology Name	# Changed	# Measured	# in Ontology	% Changed	% Present	Z Score
Development and Morphogenesis							
GO:0048856	anatomical structure development	115	1521	1921	7.56	79.18	8.51
GO:0042482	positive regulation of odontogenesis	4	6	7	66.67	85.71	8.17
GO:0003156	regulation of organ formation	7	23	29	30.43	79.31	6.80
GO:0040007	growth	26	226	284	11.50	79.58	6.27
GO:0060740	prostate gland epithelium morphogenesis	6	24	24	25.00	100.00	5.53
GO:0060687	regulation of branching involved in prostate gland morphogenesis	3	7	7	42.86	100.00	5.49
GO:0031099	regeneration	15	121	141	12.40	85.82	5.09
GO:0007275	multicellular organismal development	32	391	479	8.18	81.63	4.77
GO:0061036	positive regulation of cartilage development	3	9	11	33.33	81.82	4.71
GO:0048634	regulation of muscle organ development	10	75	91	13.33	82.42	4.43
GO:0048070	regulation of developmental pigmentation	3	10	12	30.00	83.33	4.41
GO:0021602	cranial nerve morphogenesis	3	10	14	30.00	71.43	4.41
GO:0051960	regulation of nervous system development	28	349	435	8.02	80.23	4.34
GO:0021904	dorsal/ventral neural tube patterning	3	11	15	27.27	73.33	4.14
GO:0051093	negative regulation of developmental process	27	352	438	7.67	80.37	4.00
GO:0001701	in utero embryonic development	16	169	217	9.47	77.88	4.00
GO:0048638	regulation of developmental growth	10	84	99	11.90	84.85	4.00
GO:0007528	neuromuscular junction development	4	21	25	19.05	84.00	3.73
GO:0048645	organ formation	3	13	16	23.08	81.25	3.70
GO:0003179	heart valve morphogenesis	3	13	16	23.08	81.25	3.70
GO:0001974	blood vessel remodeling	4	24	30	16.67	80.00	3.37
GO:0009887	organ morphogenesis	23	322	413	7.14	77.97	3.31
GO:0009791	post-embryonic development	7	61	82	11.48	74.39	3.22
GO:0090103	cochlea morphogenesis	3	16	21	18.75	76.19	3.19
GO:0001525	angiogenesis	11	120	138	9.17	86.96	3.19
GO:0035137	hindlimb morphogenesis	4	29	41	13.79	70.73	2.88
GO:0048546	digestive tract morphogenesis	3	21	22	14.29	95.45	2.57
GO:0031069	hair follicle morphogenesis	3	22	24	13.64	91.67	2.47
GO:0016331	morphogenesis of embryonic epithelium	3	22	30	13.64	73.33	2.47
GO:0035113	embryonic appendage morphogenesis	6	63	85	9.52	74.12	2.45
GO:0009948	anterior/posterior axis specification	3	23	30	13.04	76.67	2.38
GO:0045766	positive regulation of angiogenesis	6	65	71	9.23	91.55	2.37
GO:0009952	anterior/posterior pattern formation	9	125	160	7.20	78.13	2.08
Reproductive process							
GO:0022602	ovulation cycle process	11	83	99	13.25	83.84	4.62
GO:0042698	ovulation cycle	3	11	13	27.27	84.62	4.14
GO:0007565	female pregnancy	8	69	72	11.59	95.83	3.48
GO:0007566	embryo implantation	4	25	30	16.00	83.33	3.26
GO:2000243	positive regulation of reproductive process	4	34	44	11.76	77.27	2.49
Tube Formation							
GO:0060601	lateral sprouting from an epithelium	5	8	9	62.50	88.89	8.81
GO:0072104	glomerular capillary formation	3	5	5	60.00	100.00	6.67
GO:0001763	morphogenesis of a branching structure	18	130	153	13.85	84.97	6.16

GO:0035148	tube formation	11	77	94	14.29	81.91	4.94
GO:0060562	epithelial tube morphogenesis	6	36	45	16.67	80.00	4.13
Cell Differentiation & Development							
GO:0048869	cellular developmental process	89	1270	1593	7.01	79.72	6.59
GO:0045595	regulation of cell differentiation	54	675	854	8.00	79.04	6.08
GO:0031175	neuron projection development	8	93	106	8.60	87.74	2.51
Cell Migration and Adhesion							
GO:0007156	homophilic cell adhesion	14	61	117	22.95	52.14	7.98
GO:0006935	chemotaxis	26	211	249	12.32	84.74	6.69
GO:0050920	regulation of chemotaxis	11	75	86	14.67	87.21	5.05
GO:0007162	negative regulation of cell adhesion	7	46	57	15.22	80.70	4.14
GO:0040013	negative regulation of locomotion	10	92	110	10.87	83.64	3.66
GO:0016477	cell migration	24	334	407	7.19	82.06	3.42
GO:0033628	regulation of cell adhesion mediated by integrin	3	22	26	13.64	84.62	2.47
GO:0030198	extracellular matrix organization	7	83	112	8.43	74.11	2.29
Cell Cycle							
GO:0072201	negative regulation of mesenchymal cell proliferation	3	4	4	75.00	100.00	7.55
GO:0050680	negative regulation of epithelial cell proliferation	12	63	71	19.05	88.73	6.47
GO:0007062	sister chromatid cohesion	4	11	18	36.36	61.11	5.74
GO:0048103	somatic stem cell division	4	13	18	30.77	72.22	5.17
GO:0001936	regulation of endothelial cell proliferation	9	54	64	16.67	84.38	5.06
GO:0051726	regulation of cell cycle	32	390	507	8.21	76.92	4.79
GO:0050673	epithelial cell proliferation	6	41	45	14.63	91.11	3.71
GO:0048145	regulation of fibroblast proliferation	7	56	62	12.50	90.32	3.50
GO:0000086	G2/M transition of mitotic cell cycle	4	25	36	16.00	69.44	3.26
GO:0000280	nuclear division	7	79	104	8.86	75.96	2.44
Hormones and Growth Factors							
GO:0040037	negative regulation of fibroblast growth factor receptor signaling pathway	4	8	9	50.00	88.89	6.94
GO:0032352	positive regulation of hormone metabolic process	4	12	15	33.33	80.00	5.44
GO:0006700	C21-steroid hormone biosynthetic process	4	12	14	33.33	85.71	5.44
GO:0090030	regulation of steroid hormone biosynthetic process	3	11	13	27.27	84.62	4.14
GO:0006695	cholesterol biosynthetic process	4	21	23	19.05	91.30	3.73
GO:0010893	positive regulation of steroid biosynthetic process	3	15	17	20.00	88.24	3.35
GO:0008209	androgen metabolic process	3	20	24	15.00	83.33	2.68
Signaling							
GO:0043408	regulation of MAPKKK cascade	26	231	272	11.26	84.93	6.14
GO:0061311	cell surface receptor linked signaling pathway involved in heart development	4	10	10	40.00	100.00	6.08
GO:0007167	enzyme linked receptor protein signaling pathway	25	260	316	9.62	82.28	5.11
GO:0060395	SMAD protein signal transduction	4	14	16	28.57	87.50	4.93
GO:0030510	regulation of BMP signaling pathway	7	39	51	17.95	76.47	4.72
GO:0007154	cell communication	31	387	462	8.01	83.77	4.56
GO:0090090	negative regulation of canonical Wnt receptor signaling pathway	8	55	64	14.55	85.94	4.27

GO:0035556	intracellular signal transduction	49	785	993	6.24	79.05	3.90
GO:0070303	negative regulation of stress-activated protein kinase signaling cascade	3	16	20	18.75	80.00	3.19
GO:0007224	smoothened signaling pathway	4	26	37	15.38	70.27	3.16
GO:0016055	Wnt receptor signaling pathway	10	116	145	8.62	80.00	2.82
GO:0007219	Notch signaling pathway	5	43	53	11.63	81.13	2.76
GO:0007212	dopamine receptor signaling pathway	3	20	25	15.00	80.00	2.68
GO:0008589	regulation of smoothened signaling pathway	4	34	40	11.76	85.00	2.49
Response to Stimulus							
GO:0048584	positive regulation of response to stimulus	52	658	794	7.90	82.87	5.87
GO:0016048	detection of temperature stimulus	3	7	10	42.86	70.00	5.49
GO:0010033	response to organic substance	79	1263	1506	6.25	83.86	5.07
GO:0009612	response to mechanical stimulus	16	140	157	11.43	89.17	4.87
GO:0009991	response to extracellular stimulus	28	380	432	7.37	87.96	3.85
GO:0042493	response to drug	27	367	440	7.36	83.41	3.77
GO:0009629	response to gravity	3	13	15	23.08	86.67	3.70
GO:0071496	cellular response to external stimulus	15	180	202	8.33	89.11	3.32
GO:0001101	response to acid	9	91	112	9.89	81.25	3.14
GO:0009611	response to wounding	22	326	370	6.75	88.11	2.95
GO:0009636	response to toxin	10	112	125	8.93	89.60	2.94
GO:0071241	cellular response to inorganic substance	6	70	81	8.57	86.42	2.16
GO:0010212	response to ionizing radiation	7	89	121	7.87	73.55	2.09
Cell Death							
GO:0043067	regulation of programmed cell death	55	823	1000	6.68	82.30	4.69
GO:0060548	negative regulation of cell death	34	449	533	7.57	84.24	4.43
Oxygen Regulation							
GO:0055093	response to hyperoxia	5	27	32	18.52	84.38	4.08
GO:0001666	response to hypoxia	16	226	254	7.08	88.98	2.72
GO:0006979	response to oxidative stress	14	212	247	6.60	85.83	2.26
Immune Response							
GO:0001960	negative regulation of cytokine-mediated signaling pathway	4	15	17	26.67	88.24	4.71
GO:0050663	cytokine secretion	3	11	17	27.27	64.71	4.14
GO:0002286	T cell activation involved in immune response	4	19	22	21.05	86.36	4.01
GO:0032677	regulation of interleukin-8 production	4	29	32	13.79	90.63	2.88
GO:0070664	negative regulation of leukocyte proliferation	5	45	49	11.11	91.84	2.64
GO:0050727	regulation of inflammatory response	9	119	132	7.56	90.15	2.24
GO:0001819	positive regulation of cytokine production	9	128	149	7.03	85.91	2.01
Metabolism							
GO:0006692	prostanoid metabolic process	4	16	20	25.00	80.00	4.52
GO:0009187	cyclic nucleotide metabolic process	7	42	50	16.67	84.00	4.46
GO:0032268	regulation of cellular protein metabolic process	46	751	924	6.13	81.28	3.63
Transport							
GO:0010959	regulation of metal ion transport	15	139	161	10.79	86.34	4.45
GO:0015758	glucose transport	5	24	30	20.83	80.00	4.45
GO:0006816	calcium ion transport	10	103	129	9.71	79.84	3.24
GO:0006813	potassium ion transport	9	121	150	7.44	80.67	2.19

General Biological Regulation							
GO:0048522	positive regulation of cellular process	120	1973	2473	6.08	79.78	6.11
GO:0051480	cytosolic calcium ion homeostasis	15	125	142	12.00	88.03	4.94
GO:0010518	positive regulation of phospholipase activity	8	50	55	16.00	90.91	4.62
GO:0009070	serine family amino acid biosynthetic process	3	10	14	30.00	71.43	4.41
GO:2000021	regulation of ion homeostasis	10	83	97	12.05	85.57	4.04
GO:0044062	regulation of excretion	3	18	19	16.67	94.74	2.92
GO:0051338	regulation of transferase activity	28	384	466	7.29	82.40	3.79
GO:0042325	regulation of phosphorylation	37	558	678	6.63	82.30	3.75
GO:0006468	protein phosphorylation	35	543	771	6.45	70.43	3.46
GO:0009758	carbohydrate utilization	78	1488	2585	5.24	57.56	3.36
GO:0030808	regulation of nucleotide biosynthetic process	9	96	112	9.38	85.71	2.96
GO:0052547	regulation of peptidase activity	14	184	225	7.61	81.78	2.83
GO:0008217	regulation of blood pressure	9	100	113	9.00	88.50	2.82
GO:0002027	regulation of heart rate	4	30	33	13.33	90.91	2.80
GO:0032845	negative regulation of homeostatic process	3	19	22	15.79	86.36	2.79
GO:0008299	isoprenoid biosynthetic process	3	21	28	14.29	75.00	2.57
GO:0001508	regulation of action potential	4	36	40	11.11	90.00	2.36
GO:0045017	glycerolipid biosynthetic process	6	66	79	9.09	83.54	2.33
GO:0009890	negative regulation of biosynthetic process	33	630	813	5.24	77.49	2.10
Cellular organization							
GO:0051128	regulation of cellular component organization	52	772	983	6.74	78.54	4.61
GO:0044089	positive regulation of cellular component biogenesis	3	15	18	20.00	83.33	3.35
GO:0000226	microtubule cytoskeleton organization	9	121	167	7.44	72.46	2.19
Uncategorized							
GO:0014829	vascular smooth muscle contraction	4	8	8	50.00	100.00	6.94
GO:0014820	tonic smooth muscle contraction	3	6	7	50.00	85.71	6.01
GO:0042487	regulation of odontogenesis of dentine-containing tooth	3	7	11	42.86	63.64	5.49
GO:0014742	positive regulation of muscle hypertrophy	3	7	8	42.86	87.50	5.49
GO:0050890	cognition	17	148	173	11.49	85.55	5.05
GO:0006937	regulation of muscle contraction	10	69	74	14.49	93.24	4.76
GO:0019229	regulation of vasoconstriction	7	42	46	16.67	91.30	4.46
GO:0017158	regulation of calcium ion-dependent exocytosis	5	24	27	20.83	88.89	4.45
GO:0002026	regulation of the force of heart contraction	4	17	20	23.53	85.00	4.33
GO:0002087	regulation of respiratory gaseous exchange by neurological system process	3	12	12	25.00	100.00	3.91
GO:0061041	regulation of wound healing	7	52	55	13.46	94.55	3.74
GO:0014821	phasic smooth muscle contraction	3	14	16	21.43	87.50	3.52
GO:0045778	positive regulation of ossification	5	33	41	15.15	80.49	3.49
GO:0003014	renal system process	5	39	41	12.82	95.12	3.02
GO:0018212	peptidyl-tyrosine modification	6	57	62	10.53	91.94	2.74
GO:0046717	acid secretion	3	20	22	15.00	90.91	2.68
GO:0001503	ossification	7	75	104	9.33	72.12	2.59
GO:0007568	aging	13	184	215	7.07	85.58	2.44

GO:0042311	vasodilation	3	24	24	12.50	100.00	2.29

SUPPLEMENTAL FIGURES

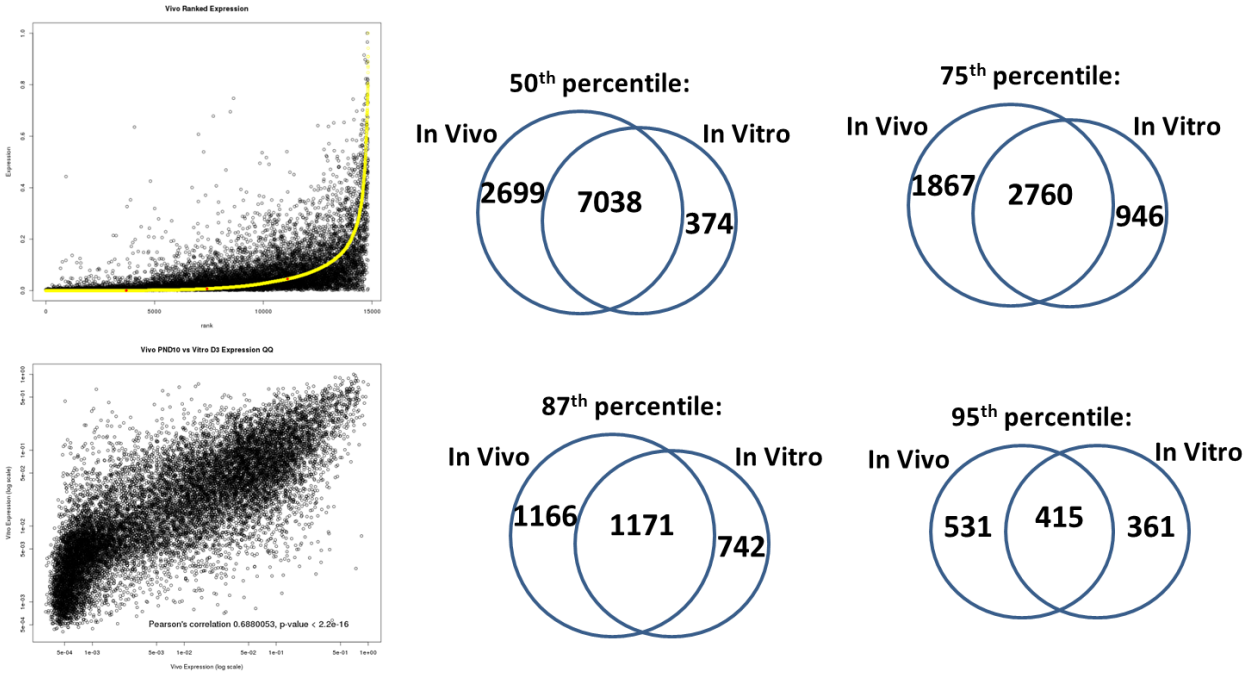

Figure S1. Comparison of gene expression on PND10 *in vivo* and experimental day 3 *in vitro*.

CHAPTER 4: Effect of dipentyl phthalate in 3-dimensional *in vitro* testis co-culture is attenuated by cyclooxygenase-2 inhibition

This chapter is in preparation for submission. The authors of the manuscript are:

Susanna Wegner, Xiaozhong Yu*, Hee Yeon Kim, Sean Harris, William C. Griffith, Sungwoo Hong, Elaine M. Faustman

Institute for Risk Analysis and Risk Communication, School of Public Health University of Washington

* Current Address: College of Public Health, University of Georgia

Abstract

Exposure to phthalate esters is associated with changes in steroidogenesis, leading to the hypothesis that this is a primary mechanism of phthalate reproductive toxicity. However, some phthalate-induced male reproductive toxicity has been demonstrated in the absence of changes to testosterone production, suggesting additional mechanisms of action. There is evidence that phthalate exposure increases expression of the inflammatory enzyme cyclooxygenase 2 (cox-2). Furthermore, inhibition of cox-2 enhances expression of the steroidogenic acute regulatory protein (StAR), which mediates the rate-limiting step in steroidogenesis. We hypothesize that phthalate-induced toxicity and testosterone perturbation are mediated in part by cox-2. We employed a 3D *in vitro* rat testis co-culture to explore the role of cox-2 in phthalate toxicity. Cells were treated with 100 μM dipentyl phthalate (DPP) with and without pre-treatment with the specific cox-2 inhibitor NS-398. Effects were evaluated after 8, 24, and 72 hrs. DPP exposure significantly increased cox-2 expression at 8 and 24 hrs ($p<0.01$) and resulted in significant, dose-dependent cytotoxicity. Pre-treatment with NS-398 significantly reduced the cytotoxicity of DPP at 8 and 24 hr ($p<0.01$). NS-398 also mitigated the effects of DPP on testosterone regulation. Total testosterone concentrations in cell culture media were significantly increased following 8 and 24 hr of DPP exposure ($p<0.001$) and NS-398 reduced this effect ($p<0.05$). Simultaneously, DPP significantly decreased StAR protein expression after 8 hrs ($p<0.01$) and this effect was

significantly attenuated by the presence of NS-398 ($p<0.01$). These results suggest that the DPP-induced changes in testosterone regulation observed in this experiment are mediated in part by an inflammatory response that is cox-2 dependent.

Introduction

Phthalates are a class of chemicals widely used as plastic softeners and stabilizers in a range of products including adhesives, lubricants and cosmetics. Because they are not bound covalently to these materials, phthalates are prone to leaching out of common consumer products, raising concern over ongoing human exposures. Monoester phthalate metabolites have been detected in maternal urine during pregnancy, amniotic fluid and breast milk, indicating that low levels of exposure can occur during critical periods of fetal development (Silva et al. 2004; Hauser and Calafat 2005; Fromme et al. 2011).

A subset of structurally similar phthalate esters are widely recognized as male reproductive toxicants. Male rats exposed to developmentally toxic phthalates *in utero* exhibit reduced testes size, undescended testes, decreased (feminized) anogenital distance, and decreased sperm count (Mylchreest et al. 1998; Gray et al. 2000). Related effects have been documented in humans as well. Male infants whose mothers had high levels of phthalate metabolites in their urine during pregnancy had significantly shortened anogenital distance (Swan et al. 2005; Swan 2008) and decreased masculine play behavior (Swan et al. 2010). In adult men, urinary concentrations of phthalate metabolites have been associated with a decline in sperm quality (Jurewicz et al. 2013). Dipentyl phthalate (DPP), a phthalate commonly used to soften PVC plastic, appears to have particularly potent effects on male reproductive development (Foster et al. 1980; Hannas et al. 2011).

Because fetal testosterone and insulin-like 3 peptide hormone are key regulators of male reproductive development, the decrease in these hormones observed in response to phthalate (David 2006; Howdeshell et al. 2008) is considered an important mechanism of male

reproductive toxicity of phthalates. Indeed, phthalate exposure has been shown to alter expression of a range of key steroidogenic factors, including transcription factors (e.g GATA4, C/EBPbeta), cholesterol transporters (e.g. the HDL receptor, steroidogenic acute regulatory protein) and enzymes involved in the conversion of cholesterol to testosterone (e.g. hydroxysteroid dehydrogenase) (Barlow et al. 2003; Lehmann et al. 2004; David 2006). Altered expression of the steroidogenic acute regulatory protein (StAR) is of particular interest because StAR mediates the transfer of cholesterol across the inner membrane of the mitochondria, the rate-limiting process in steroidogeneis, (David 2006; Clark and Cochrum 2007).

The mechanism of altered StAR expression and testosterone regulation in response to phthalate has not been fully elucidated. Characterization of upstream mechanisms that lead to reduced testosterone synthesis could offer a broader understanding of the full range of possible toxic responses to phthalate exposure. Some aspects of the toxic responses to phthalate cannot be attributed to altered hormone levels. Phthalates have been shown to alter germ cell development independent of effects on testosterone in mice, rats and human tissue (Gaido et al. 2007; Lambrot et al. 2009; Alam et al. 2010).

Several studies point to the inflammatory enzyme cyclooxygenase 2 (cox-2) as a negative regulator of StAR expression. The cyclooxygenases are a family of enzymes responsible for the conversion of fatty acids into prostaglandins and thromboxanes, mediators of inflammation and vasoconstriction. Cox inhibitors are a widely used class of anti-inflammatory drugs. In cultured mouse Leydig cells, specific inhibition of cox-2 has been shown to increase sensitivity to cAMP stimulation. This results in enhanced expression of both the StAR gene and StAR protein, promoting steroid production (Wang et al. 2003). Conversely, an age-related increase in cox-2 protein in Leydig cells has been associated with an inhibitory effect on StAR-mediated testosterone production (Wang et al. 2005). Furthermore, there is evidence that mono (2-ethylhexyl) phthalate exposure increases expression of cox-2 as well as mitochondrial expression of the redox protein peroxiredoxin 3 in spermatocytes (Onorato et al. 2008). However, the

increase in cox-2 following phthalate exposure has not yet been directly linked to subsequent changes in StAR expression or testosterone synthesis. We hypothesize that the change in StAR gene expression and testosterone production typically observed in response to phthalate exposure is mediated in part by cox-2.

In this study we employ our 3-dimensional *in vitro* testes-co-culture model (Yu et al. 2005; Yu et al. 2009) to evaluate the role of cox-2 in mediating DPP-induced testicular toxicity. Specifically, we compare the effects of DPP exposure on cox-2 protein expression, StAR protein expression and testosterone concentrations in the presence or absence of a specific cox-2 inhibitor.

Materials and Methods

Testis Cell Co-culture. Male Sprague-Dawley rat pups were obtained on postnatal day 4 (Harlan). On postnatal day 5, testis tissue was isolated and digested for cell culture as described previously (Yu et al. 2005; Wegner et al. 2013). Briefly, testes were removed and dissected to isolate seminiferous tubules, which were digested in a series of enzyme cocktails. Once dissociated, testis cells were suspended in serum-free Eagle's Minimal Essential Medium (Invitrogen) containing 0.1 mM nonessential amino acids, 1 mM sodium pyruvate, 3 mM sodium lactate, 1% ITS culture supplement (BD Biosciences) and plated in 35 mm culture dishes at a density of $1.6x10^6$ cells/plate. Ice-cold Matrigel (BD Biosciences) extracellular matrix overlay (30 μL, for a final concentration of 200 μg/ml) was immediately added to the center of each dish to provide a 3-dimensional scaffold.

Phthalate Treatment. 48 hours after plating, medium was removed and replaced with fresh medium containing 100 μM of the developmentally toxic phthalate DPP (Sigma Aldrich # 80154, 99% purity) or a DMSO (Sigma Aldrich) vehicle control. Pre-treatment with the cox-2 inhibitor NS-398 (EMD Chemicals Inc.) was done 30 minutes prior to treatment with DPP. Each treatment was repeated in a minimum of three plates for each experiment. Phthalate treatment concentration

was selected based on a previous assessment in our co-culture that found less than a 15% reduction in cell viability measured by neutral red uptake assay (Yu et al. 2009).

Microscopy. Following 8, 24 or 72 hours of treatment, each three-dimensional co-culture was visualized using an Olympus microscope with phase-contrast optics at 20X magnification. Images were captured and digitized with a Coolsnap camera (Roper Scientific, Inc.).

***Lactate Dehydrogenase Cytotoxicity Assay*.** Following 8, 24, or 72 hours of phthalate exposure, 50 μL media was collected from each culture plate for a lactate dehydrogenase (LDH) cytotoxicity assay (Promega Corporation), performed according to the kit protocol. Briefly, prior to harvesting cell lysates, 50 μL of media from each plate was added to a 96-well plate in triplicate. Samples were incubated with 50 μL substrate mix in the dark. After 30 minutes, reactions were stopped with stop solution and absorbance at 490 nm was read with a plate reader. OD values were normalized to blanks and presented relative to LDH positive controls (media from control plates killed by a freeze/thaw cycle). Data reflect at least 3 independent experiments. Statistical significance was determined by linear regression.

***Western Blotting*.** Following 8, 24, or 72 hours of treatment, cells were harvested in lysis buffer (Cell Signaling Technology) and protein was isolated by a series of freeze-thaw steps followed by centrifugation. Protein concentration was determined using a commercially available protein assay kit (Protein Assay kit, Bio-Rad Laboratories) and protein samples were diluted with sample buffer, reducing agent and buffer so that all samples contained equal protein concentrations. Samples were loaded in 4-12% Bis-Tris NuPage precast minigels (Invitrogen) and separated by running at 200V for approximately 45 minutes in running buffer containing 500 μL Antioxidant (Invitrogen). Protein was then transferred to polyvinylidene difluoride nylon membranes (Bio-Rad Laboratories) for immunoblotting. Efficiency of transfer was confirmed by commassie stain of the gel after the transfer was complete. Membranes were rinsed in tris-buffered saline (TBS) pH 7.6 then blocked with 5% nonfat dry milk in TBS with 0.1% Tween 20 (TTBS) for 1 hour. Membranes were rinsed with TTBS then incubated overnight with primary antibody and for 2

hours with secondary antibody conjugated to horseradish peroxidase. Primary antibodies included StAR (a generous gift from Dr. Douglas M Stocco, Texas Tech University), cox-2 (Cayman Chemical), actin (Sigma), anti-rabbit secondary antibody (Cell Signaling Technology Inc.), and anti-mouse secondary antibody (BD Pharminogen). After antibody incubations, membranes were washed 5 times for 5 minutes with TTBS and incubated with enhanced chemiluminescence detection reagent (GE Lifescience) and exposed to X-ray films. Western blots were analyzed by densitometry using ImageJ. The intensity of each band of interest was normalized to corresponding actin loading controls. Data presented here reflect at least 3 independent experiments. Statistical significance was determined by ANOVA using a mixed effects model and results are presented as the mean +/- standard error of the mean.

Testosterone Assay. Media was collected from cells under each treatment condition at 8, 24, and 72 hours following treatment. Testosterone concentrations in each medium sample were determined by an ELISA assay for total testosterone according to kit protocol (Neogen Corporation #402510). Testosterone concentrations measured in media were normalized to the protein content of corresponding cell lysate (determined as described above). Data on testosterone production are presented in terms of fold change in testosterone/protein relative to control. Data presented here reflect at least 3 independent experiments. Statistical significance was determined by linear regression using a mixed effects model.

Results

Morphology

Phase-contrast images illustrate the three-dimensional complexity provided by Matrigel overlay in these testicular co-cultures (Fig. 1). These images also provide initial qualitative evidence of the effects of phthalate treatment on the 3D co-cultures (indicated by the presence of condensed nuclei and some floating cells) and the prevention of these effects in cells pre-treated with NS-398, a specific cox-2 inhibitor.

Cytotoxicity

In order to evaluate the cytotoxic response to DPP in the presence or absence of NS-398 in the testicular co-culture we used a lactate dehydrogenase (LDH) release assay. We found that treatment with DPP resulted in significant cytotoxicity at all timepoints. Pre-treatment with NS-398 significantly decreased the cytotoxicity of DPP treatment at 8 and 24 hours (Fig. 2). By 72 hours, cox-2 inhibition was less effective in preventing cytotoxicity (data not shown). In order to ensure that NS-398, which has a slightly yellow color, did not interfere with the colorometric LDH assay reading, we ran an additional set of LDH assays using medium from a single untreated plate. We found no difference in LDH reading with and without the addition of NS-398 (data not shown).

Cox-2 Protein Expression

To further demonstrate that cox-2 is a plausible mediator of DPP-induced toxicity, we used Western blotting to measure the effect of DPP exposure on cox-2 protein expression. Cox-2 protein was significantly increased in response to 100 µM DPP following 8 and 24 hours of exposure (Fig. 3). Interestingly, inhibition of cox-2 ultimately led to a dramatic increase in cox-2 expression by 72 hours (data not shown), perhaps due to a feedback mechanism in response to the decrease in cox-2 activity.

Testosterone Production

In order to determine the role of cox-2 in mediating DPP induced changes in testosterone concentration, we used an ELISA assay to measure total testosterone in the culture media relative to total protein content in the cell lysate. There was a significant, dose-dependent increase in cell culture media testosterone concentrations following 8 and 24 hours of exposure to a cytotoxic

concentration of DPP (100 μM). Pre-treatment with NS-398 significantly attenuated the DPP-induced increase in testosterone concentrations after 24 hours ($p<0.05$) (Fig. 4).

StAR Protein Expression

We used western blotting to evaluate the effect of DPP exposure on expression of StAR protein, which mediates the rate limiting step in testosterone synthesis. In agreement with previous reports, we found that exposure to 100 μM DPP significantly decreased expression of StAR protein relative to β-Actin loading control after 8 hours of treatment (Fig. 5). In order to evaluate the role of cox-2 in this observed decrease in StAR expression, we tested the effect of cox-2 inhibition on the DPP-induced decrease in StAR expression. Pretreatment of co-cultures with NS-398 prevented the DPP-induced decrease in StAR protein at 8 hours (Fig. 5). By 72 hours of treatment, however, the preventive effect of NS-398 was gone.

Discussion

By attenuating the effects of DPP with cox-2 inhibitor pretreatment, we show that cox-2 activity is involved in mediating DPP toxicity. Inhibition of cox-2 prevents DPP-induced cytotoxicity and reduces the effect of DPP on media testosterone concentrations and StAR protein expression.

The increase in testosterone concentrations and simultaneous decrease in StAR protein expression observed following DPP treatment in our co-culture suggests a temporally dynamic response. While exposure to reproductively toxic phthalates is typically associated with a decrease in testosterone, we see an initial increase in testosterone concentrations in response to DPP at 8 and 24 hrs. The simultaneous downregulation of StAR protein at these timepoints may foreshadow an eventual decrease in testosterone concentrations. Our previous research has demonstrated a dramatic increase in StAR gene expression following 24 hours of phthalate exposure (Yu et al. 2009). These observations are consistent with previous reports that the

direction and magnitude of StAR gene expression responds to reproductively toxic phthalates in a time and dose-dependent manner (Lahousse et al. 2006).

It still remains to be seen how cox-2 influences StAR protein expression and testosterone concentrations in seemingly contradictory ways. Our current studies do not reveal whether DPP acts on StAR directly, or indirectly via effects on other aspects of testosterone production and metabolism.

Upregulation of cox-2 protein by DPP may be due to feedback in response to direct inhibition by phthalate. Indeed, several reproductively toxic phthalates have been shown to reduce prostaglandin synthesis following 24 hour exposures *in vitro*, suggesting a decrease in cyclooxygenase activity. Computer modeling simulations indicate that several phthalates can directly inhibit cyclooxygenase enzymes by direct binding (Kristensen et al. 2011). Because cox-2 is known to suppress testosterone, such inhibition of cox-2 by phthalate could explain the higher levels of testosterone measured in the cell culture media following DPP exposure. DPP induced inhibition of cox-2 may underlie the upregulation of cox-2 observed in this study.

Inflammatory signals like cox-2 can also be induced by cell death (Rock and Kono 2008). We were therefore unable to distinguish in our studies whether we were also seeing effects on cox2 via cell death.

The effect of phthalate on cox-2 expression has interesting implications. In addition to its effect on StAR expression, cox-2 contributes to prostaglandin and thromboxane synthesis and induces expression of other cytokines including IL1a and IL6 (Ishikawa et al. 2005). A phthalate-induced increase in cox-2 may therefore increase inflammatory secretions by Sertoli cells. Such paracrine signaling by Sertoli cells may be an important secondary mechanism of phthalate toxicity.

Further exploration of the upstream events that lead to altered StAR expression and subsequently altered testosterone concentrations may reveal common upstream mechanisms for other important pathways of phthalate toxicity. In particular, the role of inflammatory responses

in mediating phthalate toxicity warrants further investigation. There is a growing body of evidence to suggest that inflammation plays an important role in phthalate toxicity. For example, DPP has been linked to inflammatory response in adult male rat testes (Granholm et al. 1992) and MEHP exposure in immature rats has been shown to lead to an increase in recruitment of immune cells into the testis, followed by an increase in germ cell apoptosis (Murphy et al. 2014). Furthermore, NHANES data shows a correlation between phthalate metabolite levels and markers of inflammation and oxidative stress in humans (Ferguson et al. 2011) and epidemiological evidence suggests that phthalate exposure increases the risk of asthma and allergies (Bornehag and Nanberg 2010; Kimber and Dearman 2010). A clearer understanding of the underlying mechanism of the inflammation mediated effects of phthalates will inform risk assessment and facilitate construction of adverse outcome pathways for male reproductive toxicity.

Future studies should address the mechanism of phthalate influence on cox-2 activity. Cox-2 in Sertoli cells has previously been shown to be induced by the cytokine interleukin-1beta (IL1B) via JNK signaling (Ishikawa et al. 2005). This evidence warrants further exploration of these regulatory pathways in response to phthalate exposure. Further research should also explore the cell-type specific mechanisms of phthalate toxicity. These results also need to be replicated with other phthalates to determine whether this inflammatory mechanism is consistent across reproductively toxic phthalates or unique to DPP.

Better understanding of the mechanisms of phthalate toxicity will contribute to more informed risk assessment of this ubiquitously used class of chemicals.

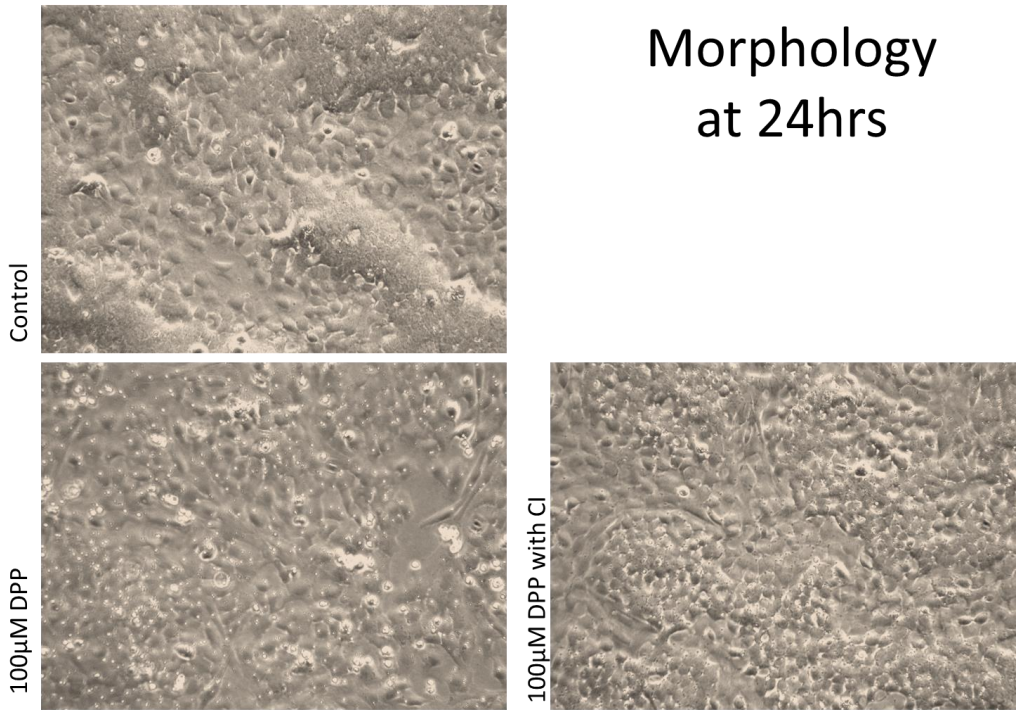

Figure 1. Morphological changes in response to DPP exposure with and without Cox2 inhibitor. A) Representative morphology of control plates 24 hr post treatment (72 hr post plating). Cultures contain germ cells, Sertoli cells, Leydig cells in three-dimensional Matrigel matrix B) Representative morphology of 24 hr 100 µM DPP exposed plates. Note the increase in dense nuclei, indicative of apoptotic cells. C) Representative morphology of 24 hr 100 µM DPP exposed plates with NS-398 cox2 inhibitor pre-treatment

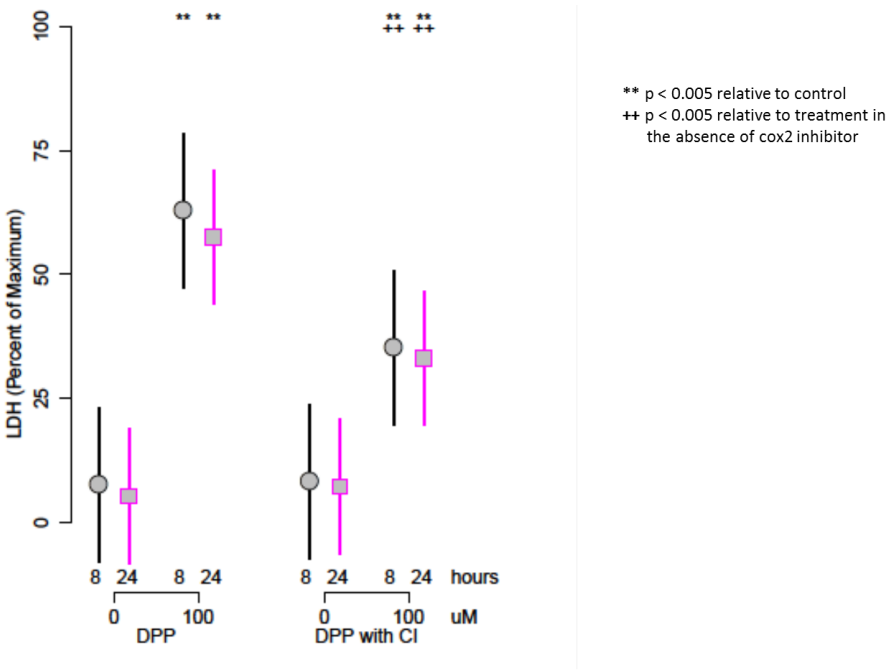

Figure 2. Effect of Cox2 Inhibition on DPP Phthalate-Induced Cytotoxicity. After 8 or 24 hrs of treatment with 100 µM DPP with or without COX2 inhibitor, medium was harvested and assayed for lactate dehydrogenase (LDH) as an indicator of cytotoxicity. 100 µM DPP dramatically increases cytotoxicity relative to controls. After 8 and 24 hrs of exposure, pre-treatment with NS-398 cox inhibitor (CI) significantly reduces cytotoxicity ($p<0.05$). Each data point represents results from at least 3 independent experiments. Error bars indicate standard error of the mean.

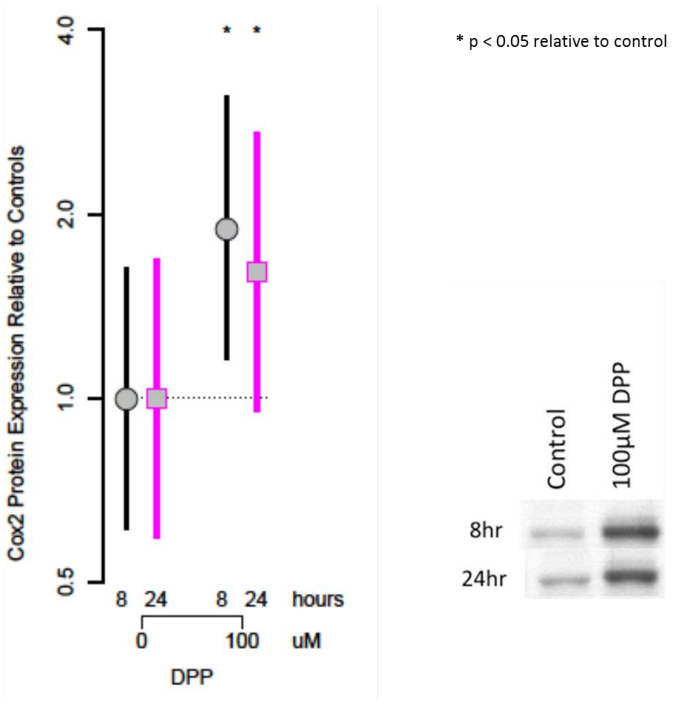

Figure 3. Effect of COX2 inhibition on DPP-induced changes in Cox2 protein expression. After 8 or 24 hrs of treatment with 100µM DPP with or without Cox2 inhibitor, protein was harvested, run on western blot, and probed with an antibody to Cox2 protein. Cox2 protein expression was significantly increased in response to DPP phthalate after 8 ($p<0.009$) and 24 hrs ($p=0.000167$). Cox inhibition significantly increases Cox2 protein expression by 72 hrs ($p=0.00057$). Each datapoint represents Western results from at least 3 independent experiments. Error bars indicate standard error of the mean.

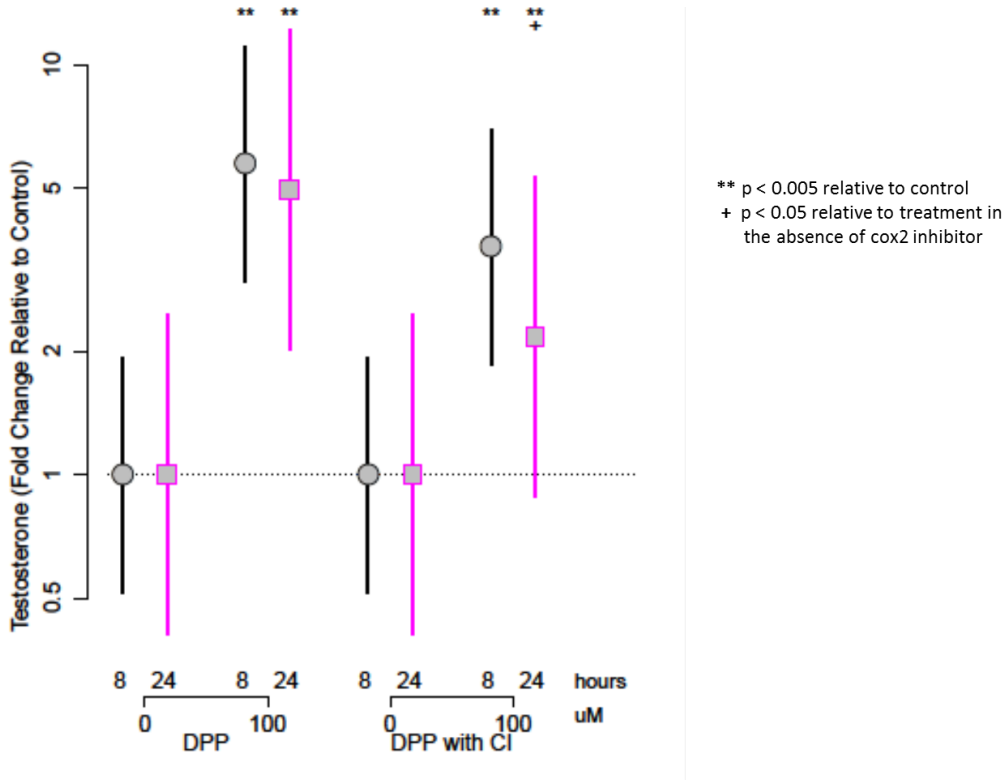

Figure 4. Effect of DPP on Testosterone Production. After 8 or 24 hrs of treatments with 100µM DPP with or without Cox2 inhibitor, media was collected and assayed for testosterone concentration by ELISA assay. Testosterone concentrations were normalized to protein content and are presented here in terms of fold change relative to the control. Each datapoint represents Western results from at least 3 independent experiments. Error bars indicate standard error of the mean.

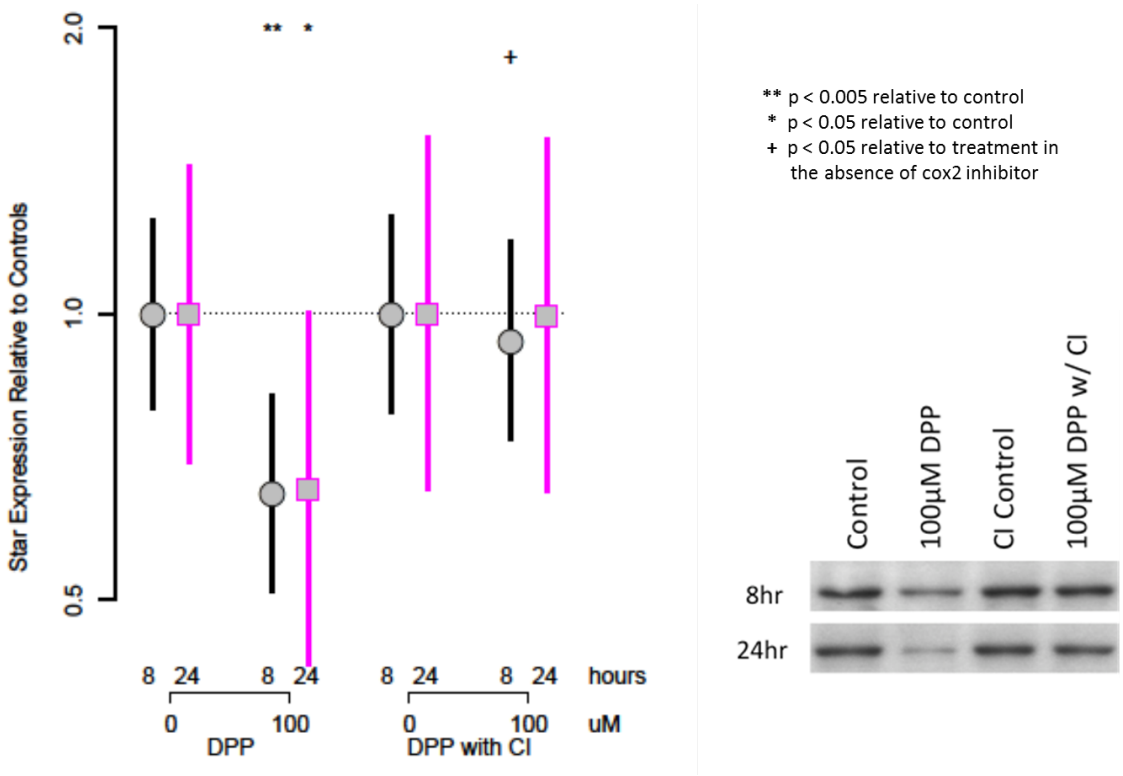

Figure 5. Effect of COX2 inhibition on DPP-induced changes in StAR protein expression. After 8 or 24 hrs of treatment with 100µM DPP with or without Cox2 inhibitor, protein was harvested, run on western blot, and probed with an antibody to StAR protein. At 8 hrs, StAR protein expression was significantly decreased in response to DPP phthalate (p=0.0025). Pre-treatment with Cox2 inhibitor (CI) prevented this effect (p=0.019). Each datapoint represents western results from at least 3 independent experiments. Error bars indicate standard error.

CHAPTER 5: Anchoring a dynamic *in vitro* model of human neuronal differentiation to key processes of early brain development *in vivo*

This chapter is in preparation for submission. The authors of the manuscript are:

Susanna Wegner, Ian B Stanaway, Hee Yeon, Julie Park, , Bill Griffith, Sungwoo Hong, Elaine M. Faustman

Institute for Risk Analysis and Risk Communication, University of Washington School of Public Health

Abstract

In vitro models of neuronal differentiation are emerging as an important tool for high throughput and high content screening in neurodevelopmental toxicology. However, interpreting results of *in vitro* neuronal differentiation assays for hazard characterization requires a clear understanding of how these models reflect vulnerable developmental processes *in vivo*. We have previously used a commercially available neural progenitor cell line to explore the mechanisms of developmental neurotoxicants. To assess the relevance of this model for *in vivo* development, we cultured hNPCs up to 21 days in differentiation conditions and used Western blotting and immunofluorescence to measure changes in protein expression though time. Global gene expression dynamics were measured using Affymetrix Human gene 2.0 ST microarrays. Over time in differentiation conditions, hNPCs aqcuired morphological characteristics of mature neuronal networks and increased expression of neuronal differentiation markers, including beta tubulin III, MAP2, and synaptophysin. Significantly changed genes were organized into 2 groups using k-means clustering. Pathway analysis reveals that GO terms enriched among genes decreased over time are largely associated with proliferation, and stem cell maintenance. GO terms enriched among genes with significantly increasing expression over time are dominated by

key developmental processes, including neuronal differentiation, migration, and synaptogenesis. Enrichment of several GO terms associated with forebrain development indicates that these culture conditions promote differentiation towards a forebrain identity. We compared *in vitro* pathway dynamics with pathway dynamics apparent in publicly available data from developing human brain tissue. Key processes important for the identification of Adverse Outcome Pathways (AOPs) of proliferation, differentiation, and functional maturation matched *in vivo* patterns. Given the heightened sensitivity of the brain to toxicant perturbation during critical windows of development, it is important that we understand which sensitive developmental pathways are captured *in vitro* and which are not so that *in vitro* assays can be interpreted appropriately.

Introduction

Developmental neurotoxicity and public health trends

Disruption of the precisely timed regulation of critical processes in brain development can result in lifelong neuropathologies (Rodier 1995; Rice and Barone 2000). There is increasing evidence that environmental exposures to a diverse set of chemicals can result in cognitive deficits and contribute to neurodevelopmental disorders such as autism, attention deficit disorder, cerebral palsy and mental retardation (Grandjean and Landrigan 2006; Landrigan 2010; Grandjean and Landrigan 2014). Indeed, the severe, well-characterized neurodevelopmental effects of gestational exposures to methylmercury (Grandjean and Herz 2011) and alcohol (de Sanctis et al. 2011) that have minimal lasting effect on maternal health, demonstrate the relative sensitivity of the developing brain.

Effects of toxicant exposures on brain development and function are dependent on developmental context. The brain regions that are actively developing at the time of an environmental exposure tend to be most susceptible to perturbation (Rice and Barone 2000). At the cellular level, the proliferation and differentiation status of cells can influence their susceptibility (Lim et al. 2009; Debeb et al. 2010; Theunissen et al. 2010). Furthermore, toxicant exposure can alter the process of differentiation itself, redirecting differentiating cells towards inappropriate neuronal subtypes. For example, methylmercury targets genes involved in promotion and regulation of differentiation (Robinson et al. 2010), and several other toxicants have been shown to influence the regional identity adopted by differentiating neurons (Zimmer et al. 2011). This evidence, along with the critical developmental windows of susceptibility observed in human populations, demonstrates that the developmental processes occurring at the time of exposure influence the type and severity of the effect. Given the vulnerability of the developing brain, it is important to develop a toxicity testing paradigm that reflects a range of developmental processes and incorporates these into prediction of adverse neurodevelopmental endpoints.

Need for in vitro models of developmental processes

Despite the clear public health need to prevent hazardous exposures during sensitive stages of development, the vast majority of chemicals in commerce remain untested for developmental neurotoxicity (Judson et al. 2009; Crofton et al. 2012). Given the large number of chemicals that still need to be evaluated for potential hazard, the expensive and time consuming animal models that have long been the gold standard of developmental toxicology are insufficient for addressing this data gap. Emerging high throughput and high content *in vitro* models offer promising alternatives. Such models can be used to quantify pathway perturbation *in vitro* to predict adverse effects on pathways that could adversely impact development in a range of developmental contexts (NRC 2007; Judson et al. 2010; Judson et al. 2011).

Anchoring neuronal differentiation in vitro to in vivo development

There has already been great progress in the development and optimization of *in vitro* models of neuronal differentiation and brain development. A diverse set of primary and organotypic co-cultures are able to capture interactions between differentiating neurons, glial cells, and other cell types, development of functionally competent neurons and the formation of complex structures (Ponce et al. 1994; Sidhu et al. 2006; Guizzetti et al. 2008; Bal-Price et al. 2010; Roque et al. 2014).

Stem cell differentiation models are also rapidly emerging as a valuable tool in developmental neurotoxicology. In early brain development, pluripotent stem cells are differentiated to multipotent neural progenitor cells (NPCs) which can then differentiate into neurons, oligodendrocytes, and/or astrocytes (Gaspard and Vanderhaeghen 2010). Proliferating NPCs can be maintained indefinitely *in vitro* and introduction of controlled differentiation conditions yields a range of specific neuronal subtypes (Conti and Cattaneo 2010).

The most sophisticated stem cell-based models are able to recapitulate specific brain structures *in vitro*. For example several emerging stem cell models methods successfully capture the complex ‘inside-out’ nature of cortical development, with neurons migrating outward upon

differentiation and establishing clear cortical layers (Eiraku et al. 2008; Gaspard et al. 2008; Mariani et al. 2012) and even producing cerebral "organoids" that recapitulate aspects of cortical development *in vitro* (Lancaster et al. 2013). Such models offer exciting opportunities to capture a wide range of processes in differentiation of regional identities and diverse neural subtypes. For applications in toxicology, the complexity of a model system has to be balanced with consistency and reproducibility for high throughput and high content screening. For this reason, these more complex models need to be supplemented with more easily reproducible and scalable models, such as those afoorded through differentiation of commercially available neural progenitor cell lines.

Stem cell-based models have already been widely applied for neurodevelopmental toxicity testing, to evaluate toxicant perturbation of differentiation status, regional identity, neurite outgrowth, migration, synaptogenesis, and gene expression (Breier et al. 2008; Radio and Mundy 2008; Buzanska et al. 2010; Garavaglia et al. 2010; Harrill et al. 2010; Fritsche et al. 2011; Zimmer et al. 2011; Theunissen et al. 2012; Hayess et al. 2013; Hogberg et al. 2013; Krug et al. 2013). Translation of the results of these models for risk assessment will require a clear delineation of how precisely the developmental processes captured in each model reflect *in vivo* developmental processes.

Meanwhile, tremendous progress has recently been made in high resolution characterization of gene expression throughout human brain development. Publicly available transcriptomic data are available for specific brain structures as they form and mature through time (Kang et al. 2011; Miller et al. 2014). These rich *in vivo* datasets allow us to anchor *in vitro* models to *in vivo* biology and understand how *in vitro* models succeed or fail to capture processes susceptible to toxicant perturbation. In the research presented here, we anchor the neurodevelopmental processes we capture *in vitro* to *in vivo* processes apparent in these publicly available datasets.

Specifically, in this work, we characterize pathway dynamics throughout neuronal differentiation of a commercially available human neural progenitor cell (hNPC) line that provides a particularly promising, scalable and reproducible model for high throughput and high content neurodevelopmental toxicity screening. This hNPC cell line, derived from NIH approved H9 embryonic stem cells (Thomson et al. 1998; Shin et al. 2006) is inherently proliferative and doesn't require feeder cells. Under proliferation conditions, cultures are >90% positive for the neural progenitor marker Nestin and <5% positive for the pluripotency marker Oct-4 (Shin et al. 2006). Upon withdrawal of fibroblast growth factor and addition of neurotrophic factors, these hNPC cultures undergo a dramatic morphological and functional transition to become mature, excitable neurons engaged in complex neuronal networks (Young et al. 2011). This cell line has already been employed in the development of high throughput toxicological screening methods (Breier et al. 2008; Radio and Mundy 2008).

In order to understand the relevance of this commercially available model to *in vivo* developmental processes, we evaluated global gene expression patterns through differentiation *in vitro* using a pathway based approach. We compared pathway dynamics of differentiating neural progenitor cells over time to key pathways dominating early neocortical brain development *in vivo* in a publicly available dataset (Kang et al. 2011). The *in vivo* period we examined corresponds to the phase during which the neocortex is thought to be most actively developing (Rice and Barone 2000). In particular, we compared *in vivo* and *in vitro* gene expression relating to processes known to be crucial for brain development, including proliferation, migration, differentiation, synaptogenesis, cell signaling and neurotransmission (Rice and Barone 2000). The resulting analysis helps to more clearly define the appropriate applications of this model as a tool for developmental neurotoxicity testing.

Methods

Cell Preparation. Commercially available human neural progenitor cells were obtained (ArunA Biomedical) and expanded up to 8-10 passages in ENStem-A neural expansion medium (Millipore). For longterm differentiation experiments, passage 8-10 cells were plated at a density of (200,000/ml) in 35mm dishes coated in Matrigel (BD Biosciences) diluted 1:200 in PBS. Cells were allowed to attach and proliferate for 24 hours, then medium was replaced with Hyclone neuronal differentiation medium (Thermo Scientific) in the absence of growth factor to initiate differentiation. Cells were maintained in differentiation conditions for up to 21 days, with half of the medium refreshed every two days.

Live/Dead Cell Imaging. In order to characterize morphology and cell viability through time in culture, differentiating cultures were incubated 15 minutes 37° C with Calcien AM, propidium iodide, and Hoechst 33342, to specifically stain live cells, dead cells, and nuclei, respectively. Cells were visualized with a fluorescent microscope at 20x magnification. Images were processed and color channels were combined using ImageJ software.

Western Blotting. Western blotting was used to quantify changes in expression of key protein markers of differentiation status and function, over time. Protein samples were harvested in cell lysis buffer (Cell Signaling) at 0, 24 hr, 72 hr, 5, 7, 10, 14, and 21 days following initiation of differentiation conditions. Protein was isolated by sonication followed by centrifugation and the protein concentration of each sample was quantified by protein assay (BioRad) according to kit protocol. Western samples were prepared by appropriately diluting samples to equal protein concentrations and addition of sample loading buffer, and reducing agent (Life Technologies). Protein samples were boiled then loaded at least 10 ug/well in a 4-12% bis-tris gel and Western gels were run at 200V. Protein was transferred to poly-vinyl difluoride membrane in chilled transfer buffer (Biorad) using a transfer apparatus at 100V for 100 minutes. Following transfer, membranes were washed in Tris-buffered Saline (TBS) and blocked in 5% milk in TBS with Tween (TTBS) for one hour. Membranes were washed 3 times for 5 minutes in TTBS and incubated at 4º C overnight with primary antibodies diluted in 5% BSA. Primary antibodies

include beta-tubulin, MAP-2, Nestin, alpha synuclein, PCNA, and secondary antibodies include goat anti mouse (BD Biosciences) and anti rabbit (BD Biosciences). Membranes were washed in TTBS 3 times for 5 minutes and incubated for two hours at room temperature with secondary antibody diluted in 5% Milk in TTBS. Following secondary antibody incubation, membranes were then washed for an additional 5 times in TTBS for 5 minutes then incubated with ECL buffer (GE). Film was exposed to ECL-reactive membranes and developed. Intensity of western bands was quantified with ImageJ software.

Immunofluorescence. Plates were fixed in 4% paraformaldehyde 30 minutes at 0, 24 hr, 72 hr, 5, 7, 10, 14, and 21 days following initiation of differentiation and stored in PBS at 4º C. Once all timepoints were collected, plates were washed 3 times in PBS and incubated with blocking buffer (5% Goat serum in PBS with Tween) to permeablize cell membranes for 1 hour then incubated overnight with primary antibodies diluted in antibody dilution buffer (5% BSA in PBS with Tween). Plates were washed 3 times with PBS then incubated for 2 hours in Alexa-flour tagged secondary antibodies in antibody dilution buffer. Plates were then washed 3 times for 5 minutes in PBS with Hoechst in the final wash to counterstain nuclei. Labeled cells were visualized under a fluorescent microscope at 20-40x magnification and images were processed and compiled using ImageJ software.

Microarray Processing. RNA from differentiating hNPC plates was harvested in Trizol 0, 24 hr, 72 hr, 7, 14, and 21 days following initiation of differentiation. RNA was then isolated using an RNA isolation kit (Ambion/mirVAna) according to kit protocol and samples were further purified with a cleanup kit (Qiagen) according to kit protocol. Purified RNA samples were then hybridized to Affymetrix Human 2.0 microarrays to measure global gene expression in each sample. Expression data reflects replicate samples from 3 independent cell preparations.

Quantification of Pathway Dynamics In vitro. Data was normalized and annotated using the Bioconductor Limma package for R software. Genes significantly changed through time were identified as those with a greater than 2 fold change from D0 at any subsequent timepoint.

Significantly changed genes were then grouped according to general expression dynamics through time using *K*-means clustering (Soukas et al. 2000). DAVID Gene ontology software (Huang et al. 2009) was used to identify GO biological processes enriched among each cluster of significantly changed genes. Analysis was performed with a count threshold of 3 genes and an ease of 0.1. A Benjamini adjusted p-value cutoff of $p<0.05$ was applied to adjust for multiple comparisons in evaluating the significance of enriched GO terms. Terms significantly enriched among each of the clusters were then grouped by general theme to identify broad trends in temporal pathway dynamics.

Comparison of Gene Expression In vivo and In vitro. We used an *in vivo* dataset of gene expression through time across brain regions (Kang et al. 2011). This dataset includes global gene expression in brain tissue samples across a range of specific brain regions from 4 individuals at postcoital weeks 5.7, 6, 8, and 9 (Table 1). These were grouped into 2 periods. Period 1 (the embryonic period) included weeks 5.7 and 6; period 2 (the early fetal period) included weeks 8 and 9. Because our *in vitro* differentiation protocol is expected to produce cortical neurons, we focused our *in vivo* comparison on neocortical brain regions, which are expected to be actively developing during the *in vivo* period examined (Rice and Barone 2000).

In order to compare expression patterns *in vivo* and *in vitro*, we first compared the correlation between relative expression intensity for individual genes *in vivo* and *in vitro*. Because gene expression *in vivo* is not uniform across neocortical brain regions and over time, individual comparisons were made between each *in vitro* timepoint and specific *in vivo* brain regions from specific individuals. Pearson's correlation coefficients were calculated to evaluate the similarity in expression patterns between *in vivo* and *in vitro* samples. We then compared the overlap in genes expressed in the top 50^{th} and 95^{th} percentiles of expression both *in vitro* and *in vivo*, in both period 1 and period 2 *in vivo* samples.

Comparison of genes significantly changed through time in vivo and in vitro. Genes with a fold change in expression >2 in specific neocortical region *in vivo* between individual samples in

period 1 and period 2 were considered significantly changed between those samples. We compared the list of significantly changed genes in each of the regional *in vivo* comparisons across time with the list of all genes changed significantly (fold change >2) at any timepoint *in vitro*. We then identified the set of genes changed commonly *in vivo* and *in vitro* or uniquely only *in vivo* or only *in vitro* across a substantial portion of neocortical brain regions. This was accomplished by generating histograms of the frequency with which each gene was among those commonly or uniquely changed through time across all of the sample-to-sample comparisons. Lists of genes commonly or uniquely changed through time were generated by selecting cutoffs for the number of comparisons a gene had to be consistently present in (Figure 7). Cutoffs selected were 30 (shared genes), 55 (genes changed *in vitro* only), and 25 (genes changed *in vivo* only). DAVID was used to identify GO biological processes enriched among genes commonly enriched both *in vivo* and *in vitro* or among genes uniquely changing only *in vivo* or only *in vitro*. Pathway analysis was performed with a count threshold of 3 genes and an ease of 0.1. GO terms were considered significantly enriched if they had a Benajimi adjusted p–value <0.05.

Comparison of Gene Expression in Targeted Pathways of Interest. *In vivo* and *in vitro* gene expression was compared among genes associated with a set of pathways identified *a priori* as particularly important during early brain development. Gene lists were generated using the Gene Ontology database by including all genes associated with a given GO term of interest. We generated heatmaps depicting gene expression through time in each of these pathways *in vivo* and *in vitro* in order to compare consistency of these key pathways across the two systems. *In vivo* gene expression in each sample was averaged across all neocortical tissues and *in vitro* expression at each timepoint was averaged across replicates. Expression intensity was normalized to maximum expression on each microarray. Genes were clustered according to *in vivo* expression patterns.

Results

Morphological Changes and Longterm Viability

Over time in differentiation conditions, neural progenitor cultures increasingly displayed characteristics of differentiated neural networks. Fluorescent images illustrate formation of three-dimensional neural networks and extension of neurite outgrowths. Live-Dead cells staining through time indicates that some cell death occurred through this process, but that a strong population of viable cells was consistently maintained, particularly within the growing neural clusters (Figure 1).

Protein Expression

Progression of cells through neuronal differentiation was further illustrated by changing protein expression over time in culture. Western blots demonstrate that expression of neuronal differentiation markers such as beta-tubulin III and MAPII increased significantly through time (Figure 2). We also observed a significant increase in alpha-synuclein, indicating an increase in the formation of functional synapses necessary for functional neural networks.

The neural progenitor cell marker nestin also increases over time, indicating a growing population of cells that continues to maintain multipotency even as differentiation progresses (Figure 2). Continual PCNA expression through time further indicates the presence of proliferative cells for at least 21 days following initiation of differentiation. Simultaneously, total protein content increased through time, likely due to a combination of continued cell proliferation and increasing mass of each differentiating and maturing neuron as it accumulates additional complex structures (Figure 3).

Immunofluorescent imaging of beta-tubulin further demonstrates the progression of differentiation in culture. The images offer a qualitative confirmation of the increase in beta-tubulin III expression and demonstrate dramatic morphological development, with the extension of neurite outgrowths and formation of increasingly large, dense neural networks over time in differentiating conditions (Figure 4).

Global gene expression and pathway dynamics in vitro

To identify key developmental pathways captured in this *in vitro* culture, global gene expression was measured by microarray 0, 1, 3, 7, 14, 21 days after initiation of differentiation conditions. We identified 2953 genes significantly changed over time in culture. *K*-means clustering identified 3 major clusters among this set of significantly changed genes based on expression dynamics through time (Figure 5). For each of these clusters, DAVID software was used to identify GO biological processes significantly enriched (Benjamini adjusted $p<0.05$) among each of these clusters.

Genes in Cluster 1 typically had low expression on day 3 and peak in expression around day 14 in culture. Among genes in Cluster 1, we found significant enrichment for GO terms associated with neuron differentiation and development, synapse function and neurotransmission, cell adhesion and migration, and signal transduction (including BMP, Wnt, and receptor tyrosine kinase pathways). Genes in Cluster 2 typically peaked in expression around day 7, decreasing by days 14 and 21. Among these genes, significantly enriched GO terms were primarily associated with cell cycling. There was also enrichment for a range of GO terms related to developmental processes, including a term specific to forebrain development. Genes in Cluster 3 generally decreased in expression by day 7 or 14. GO terms significantly enriched among these genes were associated with general developmental processes, cell adhesion and migration, and signal transduction pathways (including Rho and MAP kinase pathways).

Comparison of expressed genes in vivo and in vitro

In order to compare *in vivo* and *in vitro* expression dynamics, we first compared relative expression intensity of all genes. We found strong correlations between relative gene expression intensity in *in vivo* and *in vivo* samples across all regions and timepoints. For example, relative expression intensity for genes on *in vitro* day 0 is highly correlated with expression intensity in

the developing temporal cortex *in vitro*, both at week 5.7 (Pearson correlation = 0.71) and at week 9 (Pearson correlation = 0.73) (Figure 6). This overall correlation in relative gene expression intensity is maintained through day 14 *in vitro*. Pearson correlations between *in vitro* samples at all timepoints and *in vivo* samples across all neocortical regions at all *in vivo* timepoints range between 0.58 to 0.73. The substantial correlation across all samples at all timepoints indicates a general consistency in gene expression across all neocortical brain tissue at this early stage of development and in our *in vitro* model.

Comparison of significantly changed genes in vivo and in vitro

We next compared genes that were significantly changed through time across multiple neocortical regions *in vivo* and *in vitro* (Figure 7). We identified 297 genes that were significantly changed through time both in neocortical tissue *in vivo* and in differentiating hNPCs *in vitro*. Dominant themes apparent among GO terms enriched among genes changed through time both *in vivo* and *in vitro* include neuron differentiation and development, general developmental processes, specific brain development processes, cell adhesion and migration, and signal transduction (Table 5).

There were also 354 genes uniquely changed *in vitro* and 354 other genes uniquely changed through time in neocortical tissue. Among GO terms significantly enriched among genes uniquely changing *in vivo*, many of the same themes emerge, indicating that several genes important to these processes are not captured *in vitro*. We also see enrichment for many more GO terms associated with neurotransmission, indicating that the *in vivo* brain samples progress further in development of functionally competent synapse formation (Table 6). GO terms significantly enriched among genes uniquely changed *in vitro* include several associated with cell stress signaling, including the NF-kappaB cascade, response to cytokine stimulus, and response to organic substance (Table 7).

Comparison of gene expression in targeted pathways

We explored expression dynamics of several key pathways identified *a priori* as pathways of particular interest for brain development. These include several generic developmental pathways as well as terms associated with specific neuronal subtypes and functions and regional identities. These comparisons help to identify broad trends in pathways that are consistently reflected *in vitro* and genes among these pathways that may have more divergent patterns of expression. For many of these targeted pathways the most highly expressed genes *in vivo* are also among the most highly expressed *in vitro* (Figure 8). For example, there is strong agreement between *in vivo* and *in vitro* gene expression among genes associated with synaptic transmission of GABA. Genes associated with the GO terms "neuron fate commitment", "neuron maturation" and "forebrain neuron migration" display similar relative expression intensities *in vivo* and *in vitro*, though *in vitro* expression of the most highly expressed genes is not as dramatically upregulated through time as it is *in vivo*. There are notable exceptions to the overall agreement within these pathways. For example, FOXG1 and GNAQ, the most highly expressed genes associated with "forebrain neuron development" *in vivo*, are not expressed highly *in vitro*. These comparisons define similarities and differences between *in vivo* and *in vitro* overall dynamics for pathways and specific genes of interest for brain development.

Discussion

By anchoring *in vitro* gene expression dynamics to *in vivo* dynamics, this analysis begins to define the appropriate applications of this *in vitro* model of neuronal differentiation for developmental neurotoxicology. The neuronal differentiation model evaluated here captures several essential processes of early brain development *in vivo*, including neuronal differentiation and development, neuronal migration, synapse formation, and neurotransmission.

What stages and regions are best represented in this model

Basic characterization of viability, protein expression and morphology indicates that hNPCs in differentiation conditions produce mature neurons that form dense neuronal networks while maintaining a population of progenitor cells. Increasing protein expression of neuronal markers beta –tubulin III and MAP2 through time in differentiating conditions indicates that cultures are actively differentiating to become neurons. Expression of the synaptic protein alpha synuclein likely indicates the formation of synapses in culture. Meanwhile, increasing expression of the neural progenitor marker Nestin and consistent expression of the proliferation marker PCNA indicate a growing population of progenitor cells is present despite the emergence of differentiated neurons. Morphological images demonstrate the formation of dense neural networks that require neuronal migration to form.

These observations are supported by gene expression through time as well. Among genes significantly changed through time in culture, significantly enriched GO terms were primarily associated with neuron differentiation, cell migration and localization, neurotransmission, cell proliferation, and conserved signal transduction pathways. In addition to these general neuronal differentiation and developmental signals, enriched GO terms point to specific regionalization and neuronal-subtype specification. For example, enrichment for forebrain development indicates that this *in vitro* culture is differentiating towards a forebrain identity. This is consistent with the predicted outcome of neuronal differentiation in the absence of morphogenic signals (Gaspard and Vanderhaeghen 2010).

Comparisons with gene expression *in vivo* demonstrate that relative gene expression intensity in the *in vitro* model is highly concordant with gene expression in developing forebrain tissue. There is also substantial overlap between the genes significantly changed through time in this dynamic phase of differentiation and development *in vivo* and *in vitro*. Pathway enrichment analysis confirms that the commonly changing genes are enriched for GO terms associated with neuron differentiation and development, migration, neurotransmission and signal transduction.

Furthermore, comparisons of gene expression in specific targeted pathways of interest demonstrates strong similarities in overall gene expression trends across several specific processes, including forebrain-specific morphogenesis and migration, excitatory synapse activity, and synaptic transmission of GABA. The ability of this *in vitro* system to reflect such important developmental processes reflecting the context of a specific developmental stage and regional identity makes it a promising model for developmental neurotoxicity testing that can capture both general and context-specific developmental processes.

Opportunities for enhancing the in vitro model

Comparisons between *in vivo* and *in vitro* systems also define areas where the *in vitro* model does not yet entirely reflect *in vivo* conditions. Among genes uniquely changed through time *in vivo* there was a much more dramatic enrichment of GO terms associated with synapse organization and neurotransmission, suggesting the *in vitro* model does not achieve the same level of synaptic activity *in vitro*. Among genes significantly changed only *in vitro* we observed enrichment for GO terms associated with stress signaling, indicating a higher baseline level of stress in the *in vitro* model. Further optimization of culture methods by an increase in cell culture density, addition of 3 dimensional scaffolding, or supplementation with morphogenic cues could reduce these differences. Ultimately optimization of the culture to reflect the complexity of *in vivo* development must be balanced with the need to maintain a system that is sufficiently consistent and reproducible for toxicity testing.

Relevance for developmental neurotoxicity

Neurotoxicity can be highly context-specific, varying across differentiation status, developmental stages, and brain region (Rice and Barone 2000; Kirkeby et al. 2012). The regional specificity of differentiating neurons in the *in vitro* differentiation system described here system makes it an ideal model for the specific developmental context of early forebrain

development. Protein expression, morphology, and gene expression data indicate that this model captures neuronal differentiation, migration, and synapse formation in a population of neurons adopting a forebrain identity, with gene expression patterns largely consistent with those observed in developing neocortical tissue *in vivo*. Clearly, context-specific effects measured in this model in response to toxicants cannot be extrapolated to inform toxicity in other neurodevelopmental contexts. Alternate *in vitro* models anchored to other specific developmental contexts *in vivo* would be required to predict perturbation of processes specific to other regional identities or developmental stages.

In addition to context-specific processes, this model also captures several generic developmental pathways important throughout development. For example, pathway analysis revealed activity in signal transduction pathways and general differentiation and morphogenesis processes that are ubiquitous in development. Detection of perturbation of generic developmental pathways in this model may be able to predict perturbation in a broader set of developmental contexts.

Anchoring dynamic *in vitro* models to *in vivo* developmental contexts is an important first step in defining appropriate applications for these models in neurotoxicity testing. Incorporating *in vitro* models like this one into developmental neurotoxicity screening and risk assessment will require further characterization to define *in vitro* kinetics and dosimetry and relate *in vitro* concentrations to relevant human exposure scenarios (Wetmore et al. 2012). Furthermore, it will require creation of a framework to interpret how perturbation of developmental pathway dynamics or functional endpoints *in vitro* translates to adverse outcomes *in vivo*. Ultimately, *in vitro* systems like this could be used to anchor toxicogenomic signals to pathways previously linked to behavioral effects (Bushnell et al. 2010) and other adverse outcomes.

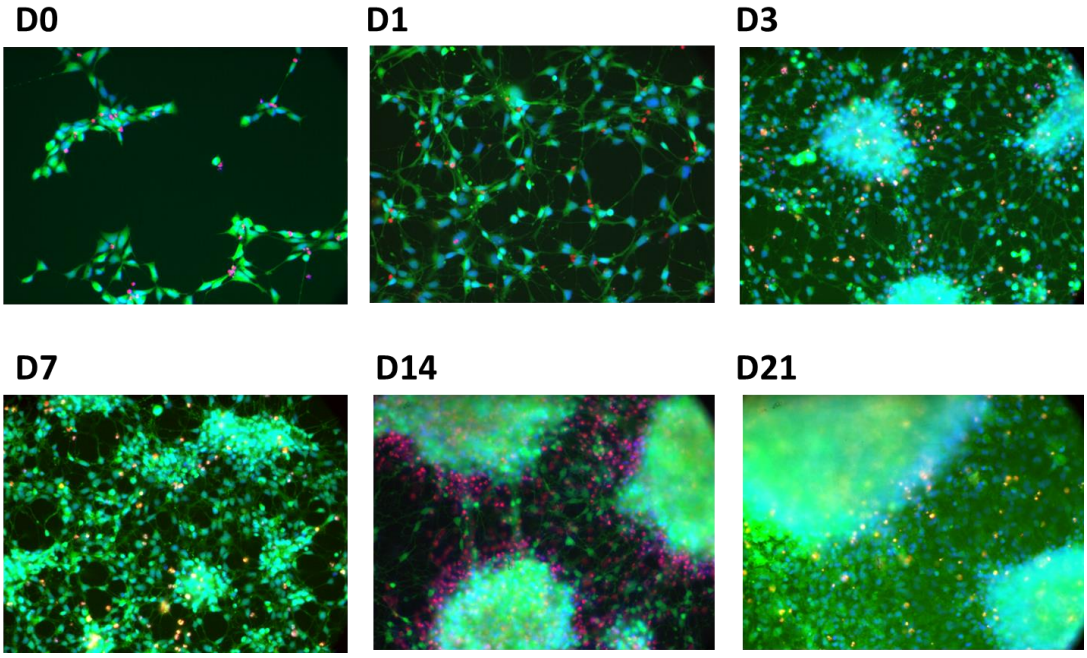

Figure 1. Longterm viability and morphology of differentiating hNPCs. Qualitative evaluation of cell viability was performed with live/dead cell imaging 0, 1, 3, 7, 14, and 21 days following initiation of differentiation. Cells were incubated for 15 minutes at 37˚ C with Calcien AM, propidium iodide, and Hoechst 33342 dyes to stain live cells (green), dead cells (red), and total nuclei (blue), respectively. Cells were visualized with a fluorescent microscope at 20x magnification.

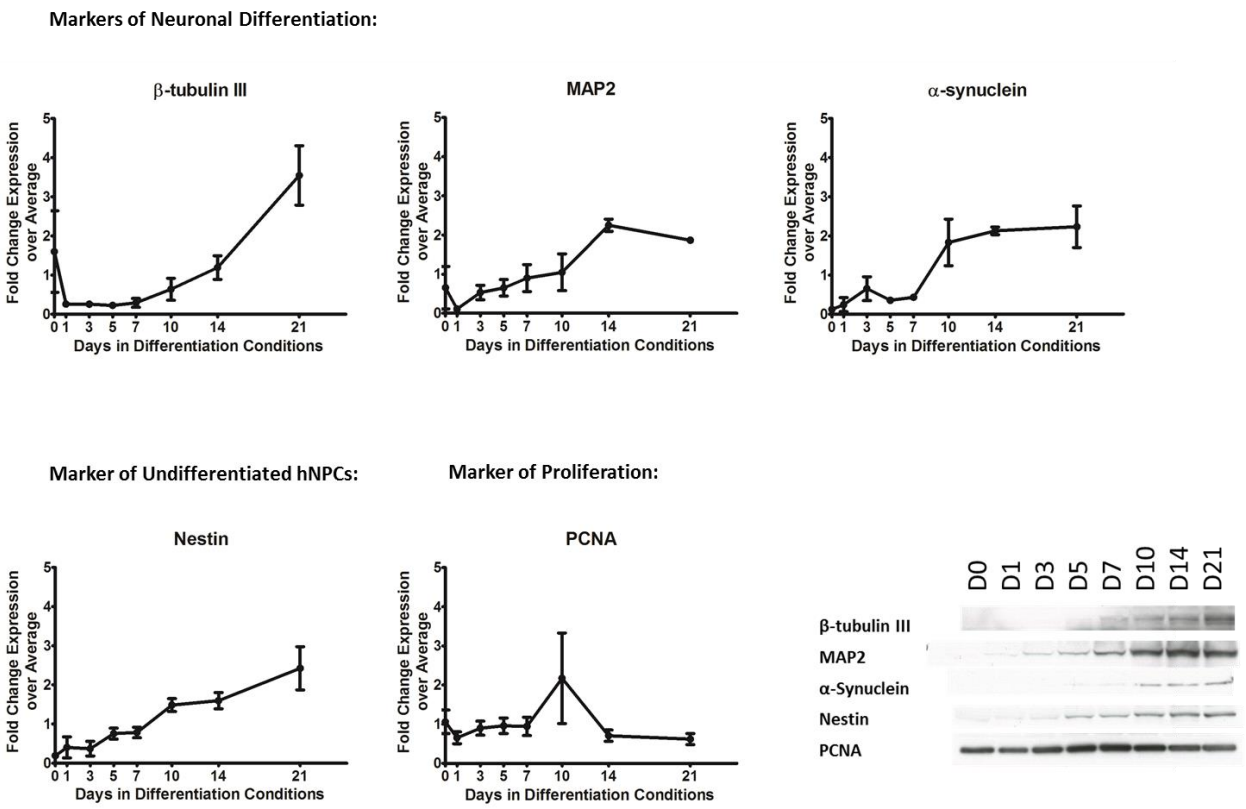

Figure 2. Protein expression in differentiating hNPC cultures through time. Protein was harvested from differentiating hNPCs and expression of specific markers was evaluated by western blotting. Data is presented as fold change expression intensity at each timepoint over expression average across time and reflects results of three independent experiments. Error bars indicate standard error. β-tubulin III, MAP2, α-synuclein, and nestin expression all increase significantly over time (one-way ANOVA $p<0.5$).

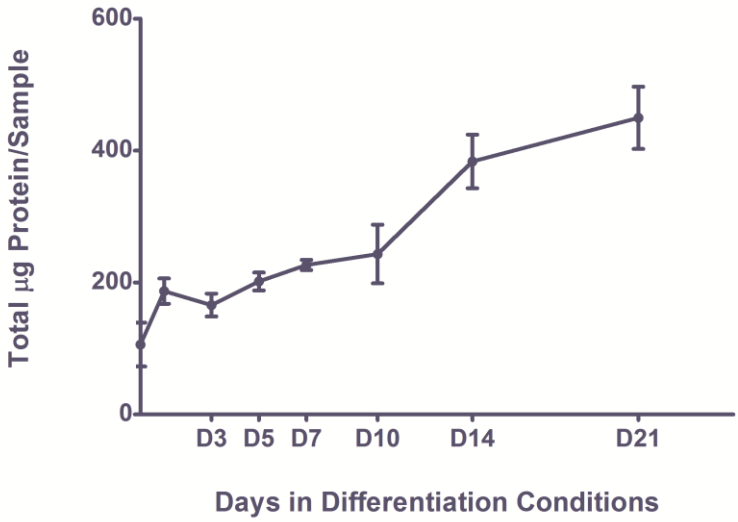

Figure 3. Accumulation of protein content through time in differentiating hNPCs. Protein was harvested from differentiating hNPCs through time and quantified by protein assay. Data represents 3 independent experiments. Error bars indicate standard error of the mean. Protein content increases significantly across time ($p<0.05$).

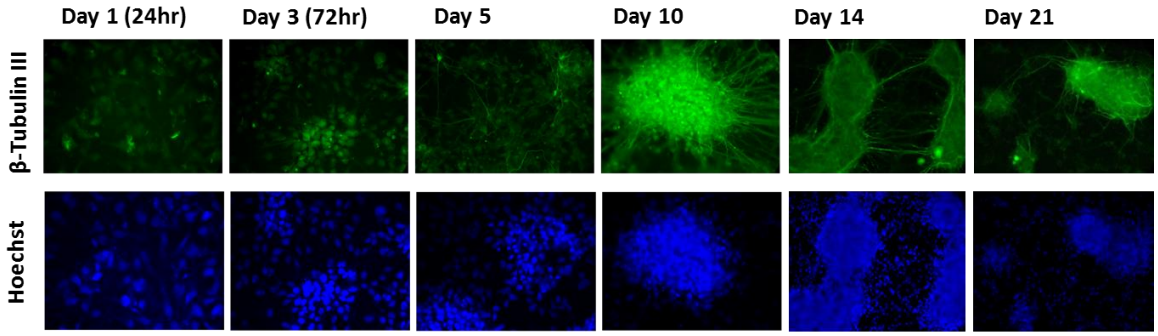

Figure 4. Morphological development of differentiating hNPCs. Differentiating hNPCs were fixed and β-tubulin III expression was visualized with a fluorescent tag (green). Nuclei are countered stained with Hoechst 33342 (blue).

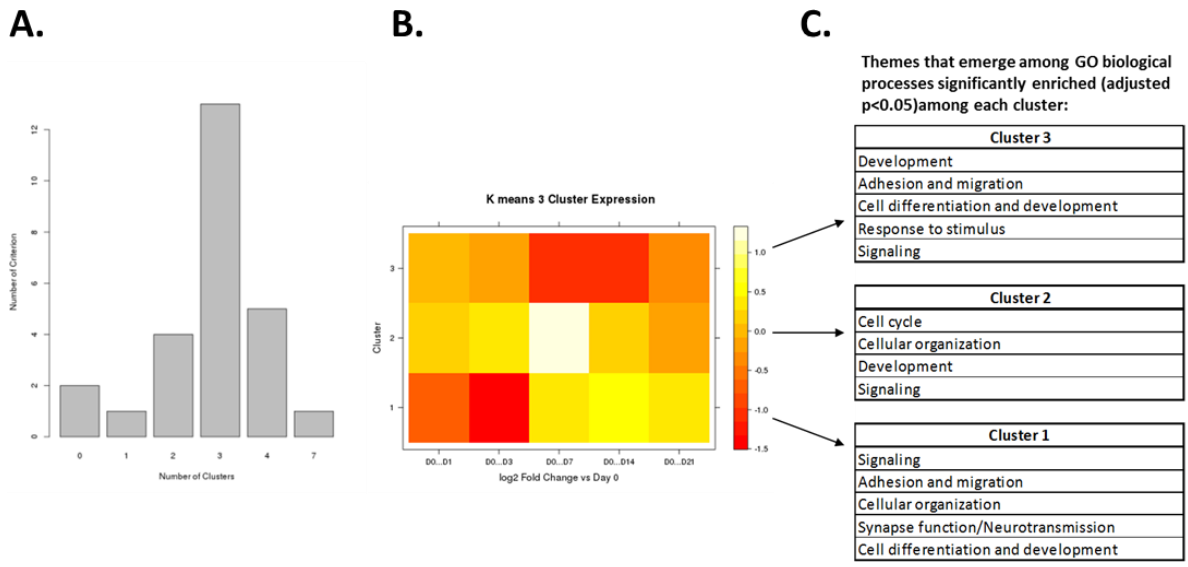

Figure 5. Gene expression and pathway dynamics of genes significantly changed over time in differentiating hNPCs. Unsupervised *K*-Means clustering identified 3 dominant patterns of expression among genes significantly changed through time in differentiating hNPCs (A). A heatmap summarizes temporal gene expression trends among each of the three clusters (B). GO biological processes significantly enriched (Benjamini adjusted $p<0.05$) among each of these clusters were identified by pathway enrichment analysis. Dominant themes among these enriched GO terms are presented here (Full lists of enriched GO terms are presented in Tables 2-4).

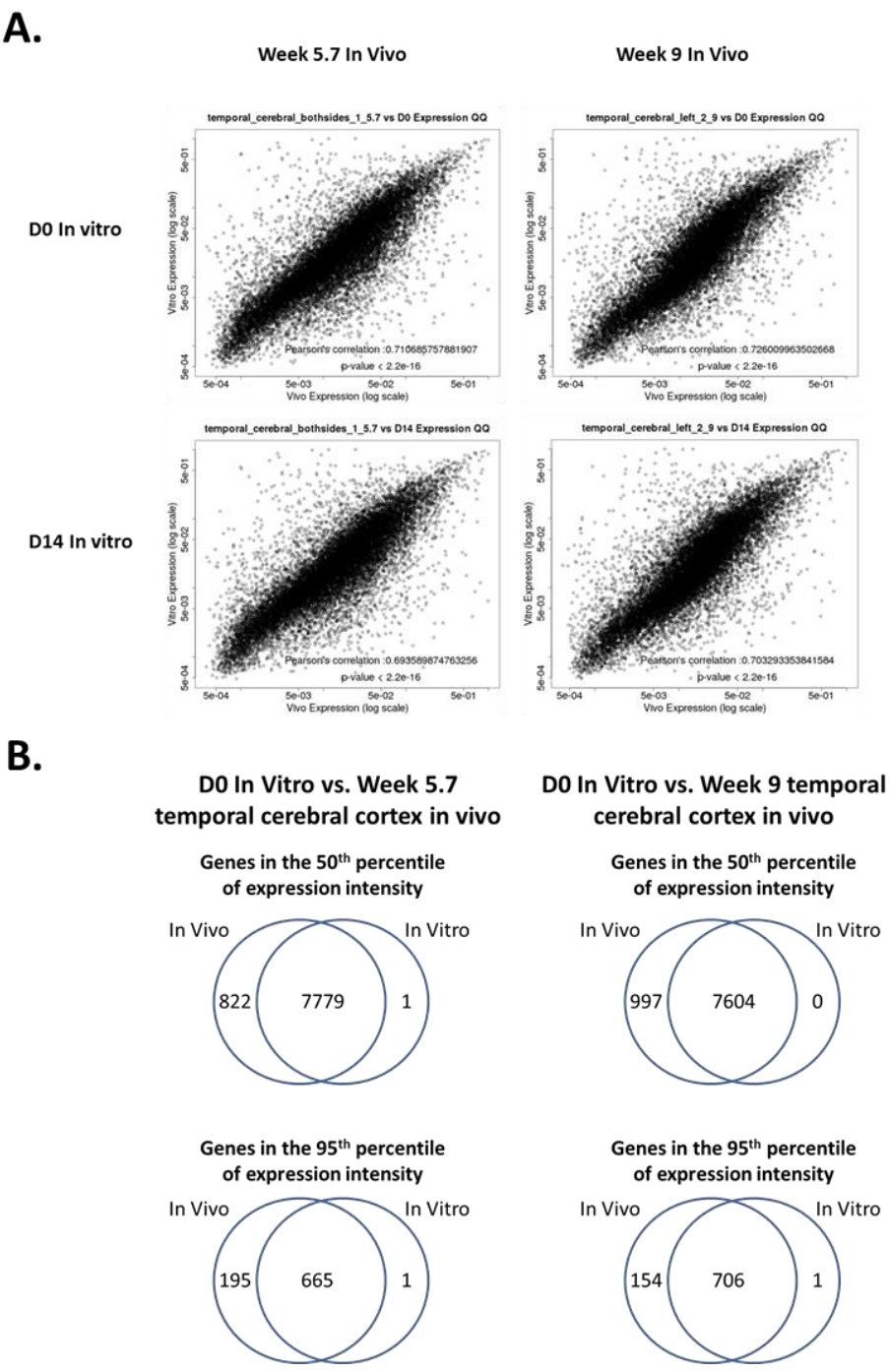

Figure 6. Correlation between relative gene expression intensity *in vivo* and *in vitro*. Relative gene expression intensity in undifferentiated hNPCs (D0) and differentiating hNPCs (D14) was compared to expression in a range of neocortical regions in embryonic (week 5.7) and early fetal (week 9) samples. Pearson's correlation coefficients range from 0.58-0.73. Comparisons between *in vitro* hNPCs and developing temporal cerebral cortex are shown here as an example (A). Genes expressed in the top 50th and 95th percentiles of relative expression intensity were compared *in vivo* and *in vitro*. Venn diagrams show numbers of genes commonly or uniquely present among these most highly expressed genes *in vivo* and *in vitro* (B).

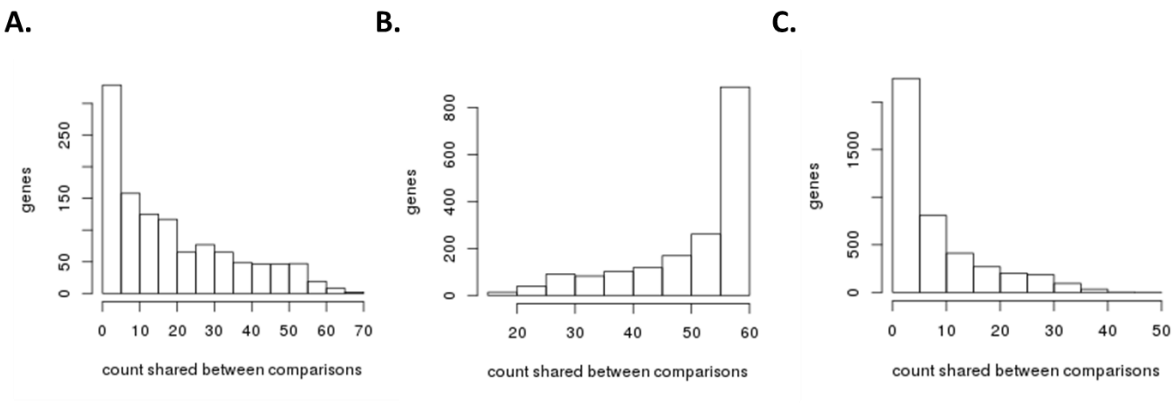

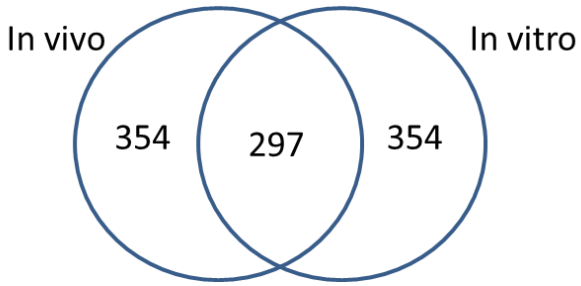

Figure 7. Generation of lists of significantly changed genes shared or unique between *in vitro* and *in vivo* across neocortical regions. In order to identify genes that were commonly or uniquely changed *in vivo* and *in vitro*, lists of genes with Fold change>2 *in vitro* were compared to lists of genes fold changed in each region between samples in period 1 and samples in period 2. This comparison resulted in 70 *in vitro* to *in vivo* comparisons. In order to identify genes that were commonly shared or commonly unique to one system across a substantial number of comparisons, histograms were used to plot the frequency that genes were shared between *in vivo* and *in vitro* (A) unique to *in vitro* (B) or unique to *in vivo* (C). Genes lists were generated by selecting cutoffs for the number of comparisons a gene had to be consistently present in. Cutoffs selected were 30 (A), 55(B), and 25 (C).

Synaptic transmission of glutamate

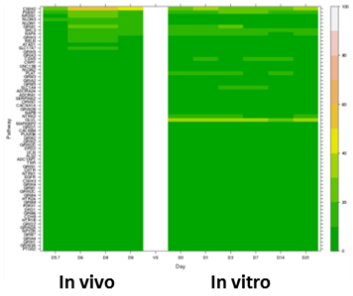

Synaptic transmission of GABA

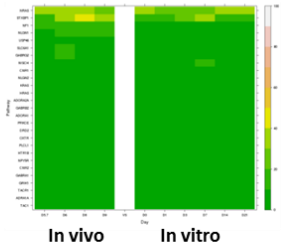

Excitatory Synapse

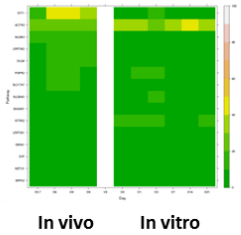

Response to thyroid

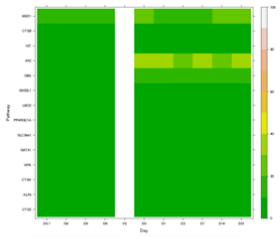

Response to testosterone

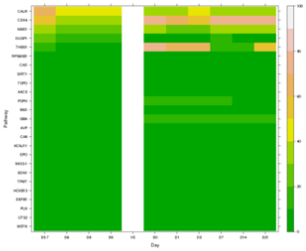

Response to estrogen

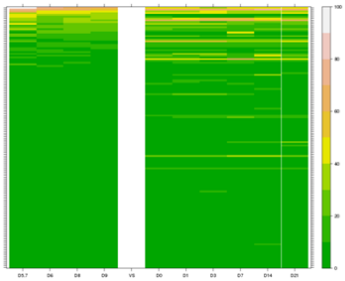

Neuron fate commitment

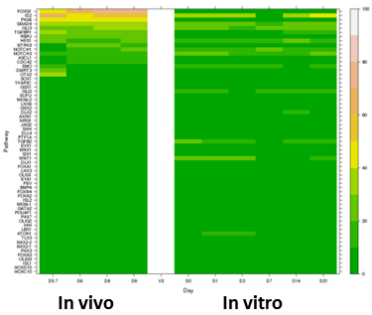

Neuron maturation

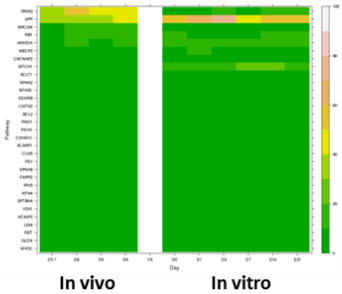

NPC proliferation

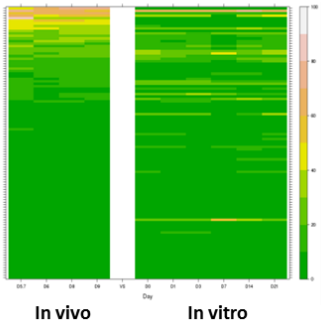

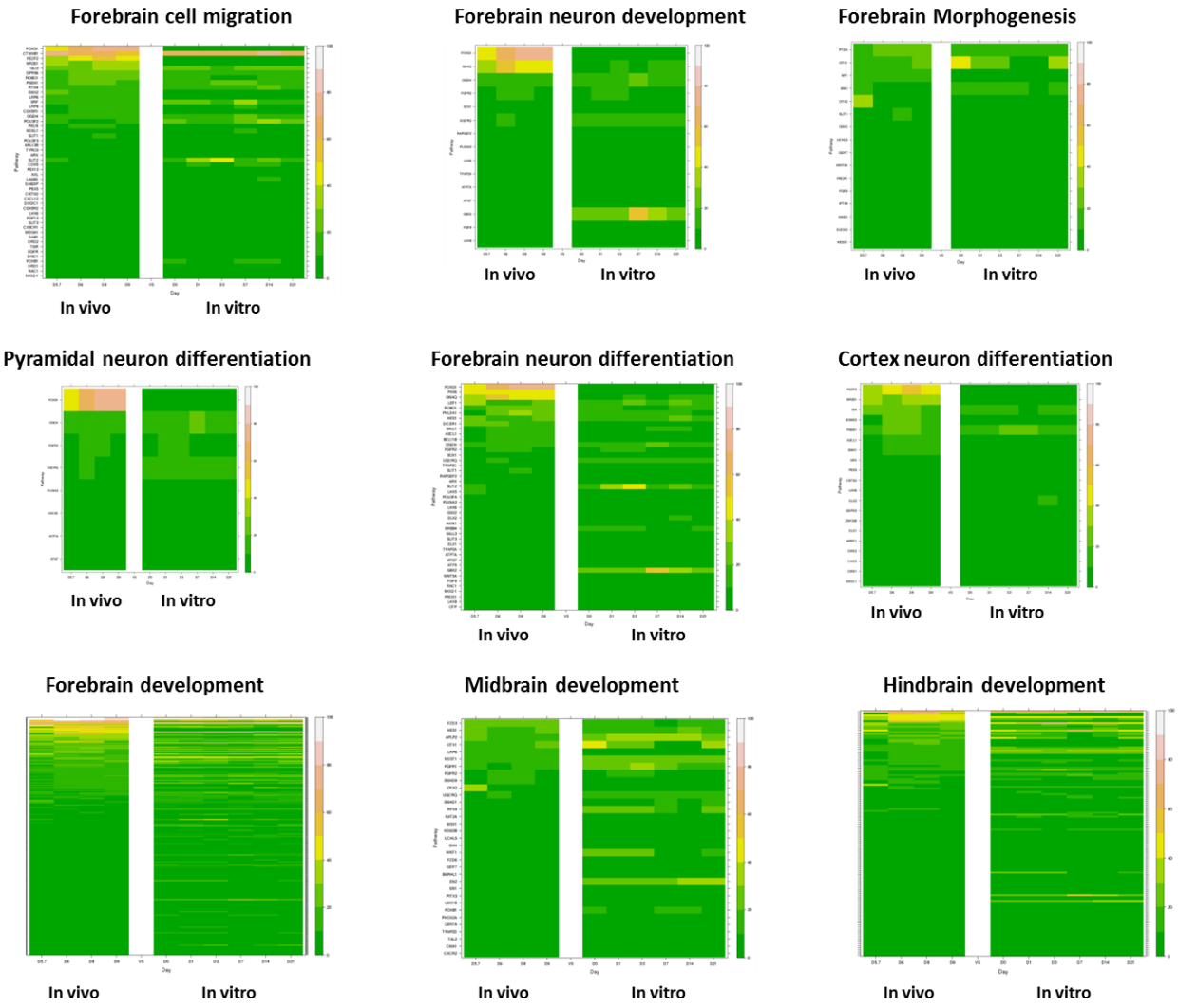

Figure 8. Pathway dynamics of targeted pathways of interest through time *in vivo* and *in vitro*. GO biological process of particular importance to neuronal differentiation and forebrain development were identified and human-specific lists of genes associated with these terms were obtained from the Gene Ontology database. Heatmaps depict relative expression intensity of genes associated with these terms *in vivo* and *in vitro* through time. *In vivo* expression is averaged across all neocortical tissue at each timepoint (weeks 5.7, 6, 8, and 9). Genes are clustered according to *in vivo* expression patterns. Expression intensity is normalized to the maximum expression on each array. Dark green represents low expression and white indicates the highest level of expression.

Table 1. Summary of *In vivo* neocortical tissue samples.

	Period 1		Period 2	
	HSB104 PCW 5.7	HSB185 PCW 6	HSB112 PCW 8	HSB148 PCW 9
FC, frontal cerebral wall	FC LR	FC L; FC R		
OFC, orbital prefrontal cortex			OFC L; OFC R	OFC L; OFC R
DFC, dorsolateral prefrontal cortex			DFC L; DFC R	DFC L; DFC R
VFC, ventrolateral prefrontal cortex			VFC L; VFC R	
MFC, medial prefrontal cortex			MFC L; MFC R	MFC L; MFC R
MSC, motor sensory cortex			MSC L; MSC R	MSC L; MSC R
PC, parietal cerebral wall	PC LR	PC L	PC L; PC R	PC L; PC R
TC, temporal Cerebral wall	TC LR	TC L; TC R		TC L; TC R
OC, occipital cerebral wall	OC LR		OC L; OC R	OC L; OC R

L=left hemisphere; right= right hemisphere; LR= both hemispheres pooled
PCW= postcoital week.
Fold change in gene expression was determined by comparing expression in each region between samples in period 1 and samples in period 2.

Table 2. GO terms enriched among Cluster 1 of genes significantly changed *in vitro*

Cluster 1				
Term	**Count**	**%**	**P-Value**	**Benjamini**
Signaling				
enzyme linked receptor protein signaling pathway	25	5.9	7.30E-07	1.50E-03
cell surface receptor linked signal transduction	70	16.5	9.60E-06	3.20E-03
BMP signaling pathway	8	1.9	4.90E-05	9.00E-03
Wnt receptor signaling pathway	12	2.8	1.90E-04	2.00E-02
transmembrane receptor protein serine/threonine kinase signaling pathway	10	2.4	4.90E-04	4.20E-02
transmembrane receptor protein tyrosine kinase signaling pathway	15	3.5	5.10E-04	4.30E-02
Adhesion and migration				
cell adhesion	37	8.7	2.60E-06	2.60E-03
biological adhesion	37	8.7	2.60E-06	1.70E-03
cell-matrix adhesion	12	2.8	4.40E-06	2.30E-03
cell motion	28	6.6	8.30E-06	3.40E-03
cell-substrate adhesion	12	2.8	1.10E-05	3.30E-03
cell migration	20	4.7	1.40E-05	3.60E-03
cell motility	21	4.9	1.90E-05	4.30E-03
localization of cell	21	4.9	1.90E-05	4.30E-03
Cellular Organization				
cellular component morphogenesis	23	5.4	8.50E-05	1.40E-02
cell morphogenesis	21	4.9	1.50E-04	1.80E-02
cell projection organization	20	4.7	6.20E-04	4.50E-02
Synapse function/Neurotransmission				
transmission of nerve impulse	21	4.9	1.20E-04	1.80E-02
synaptic transmission	19	4.5	1.30E-04	1.90E-02
neurotransmitter transport	9	2.1	5.20E-04	4.20E-02
Neuron Differentiation and development				
neuron differentiation	24	5.6	1.30E-04	1.80E-02
cell morphogenesis involved in neuron differentiation	15	3.5	2.50E-04	2.60E-02
axonogenesis	14	3.3	4.00E-04	3.60E-02
neuron migration	8	1.9	5.40E-04	4.10E-02
neuron development	19	4.5	6.20E-04	4.40E-02
Uncategorized				
skeletal system development	21	4.9	3.20E-05	6.60E-03
behavior	25	5.9	1.40E-04	1.80E-02
response to organic substance	33	7.8	1.60E-04	1.80E-02
cell morphogenesis involved in differentiation	16	3.8	3.90E-04	3.70E-02

Table 3. GO terms enriched among Cluster 2 of genes significantly changed *in vitro*

Cluster 2				
Term	**Count**	**%**	**P-Value**	**Benjamini**
Cell cycle				
M phase	71	7.7	9.80E-25	2.80E-21
M phase of mitotic cell cycle	58	6.3	2.20E-24	3.10E-21
nuclear division	57	6.1	5.40E-24	5.10E-21
mitosis	57	6.1	5.40E-24	5.10E-21
cell cycle phase	79	8.5	6.70E-24	4.70E-21
organelle fission	58	6.3	7.10E-24	4.00E-21
cell cycle	113	12.2	7.70E-24	3.60E-21
cell division	62	6.7	5.30E-21	2.10E-18
cell cycle process	89	9.6	5.30E-21	1.90E-18
mitotic cell cycle	70	7.6	5.60E-21	1.80E-18
chromosome segregation	28	3	2.40E-15	6.60E-13
chromosome organization	65	7	5.30E-12	1.40E-09
mitotic sister chromatid segregation	16	1.7	1.00E-10	2.40E-08
sister chromatid segregation	16	1.7	1.60E-10	3.60E-08
DNA replication	31	3.3	5.20E-08	7.80E-06
spindle organization	14	1.5	3.00E-07	4.20E-05
mitotic spindle organization	7	0.8	6.60E-05	5.90E-03
regulation of cell cycle process	18	1.9	8.50E-05	6.90E-03
M phase of meiotic cell cycle	16	1.7	1.60E-04	1.20E-02
meiosis	16	1.7	1.60E-04	1.20E-02
meiotic cell cycle	16	1.7	2.00E-04	1.50E-02
regulation of cell cycle	34	3.7	2.80E-04	1.90E-02
mitotic chromosome condensation	6	0.6	3.50E-04	2.10E-02
regulation of mitosis	11	1.2	5.70E-04	3.10E-02
regulation of nuclear division	11	1.2	5.70E-04	3.10E-02
regulation of mitotic metaphase/anaphase transition	7	0.8	7.20E-04	3.80E-02
chromosome localization	6	0.6	7.40E-04	3.80E-02
cell cycle checkpoint	14	1.5	8.60E-04	4.20E-02
Cellular Organization				
cytoskeleton organization	54	5.8	7.40E-09	1.30E-06
microtubule cytoskeleton organization	28	3	9.20E-09	1.50E-06
DNA packaging	21	2.3	2.50E-06	3.10E-04
macromolecular complex subunit organization	63	6.8	4.40E-05	4.30E-03
cellular macromolecular complex subunit organization	38	4.1	5.40E-05	5.10E-03
regulation of organelle organization	27	2.9	6.70E-05	5.70E-03
organelle localization	16	1.7	7.80E-05	6.50E-03
establishment of organelle localization	13	1.4	2.10E-04	1.50E-02
Development				
pattern specification process	38	4.1	5.20E-08	8.20E-06
regionalization	30	3.2	4.00E-07	5.50E-05
anterior/posterior pattern formation	22	2.4	1.20E-05	1.30E-03

heart development	27	2.9	5.70E-05	5.20E-03
segmentation	10	1.1	7.40E-04	3.80E-02
forebrain development	19	2	9.70E-04	4.50E-02
Signaling				
enzyme linked receptor protein signaling pathway	36	3.9	1.10E-04	8.60E-03
BMP signaling pathway	10	1.1	3.80E-04	2.20E-02
Metabolism				
DNA metabolic process	63	6.8	2.70E-10	5.40E-08
phosphorus metabolic process	76	8.2	4.00E-04	2.30E-02
phosphate metabolic process	76	8.2	4.00E-04	2.30E-02
Uncategorized				
microtubule-based process	39	4.2	3.60E-09	6.90E-07
cellular response to stress	58	6.3	1.30E-06	1.70E-04
protein amino acid phosphorylation	63	6.8	6.50E-06	7.70E-04
response to DNA damage stimulus	41	4.4	1.20E-05	1.30E-03
DNA repair	33	3.6	3.50E-05	3.60E-03
phosphorylation	69	7.4	4.40E-05	4.40E-03
chromosome condensation	8	0.9	2.20E-04	1.50E-02
protein-DNA complex assembly	15	1.6	2.50E-04	1.70E-02
negative regulation of organelle organization	14	1.5	3.10E-04	2.00E-02
nucleosome organization	15	1.6	3.20E-04	2.00E-02
chromatin assembly or disassembly	18	1.9	3.20E-04	2.00E-02
macromolecular complex assembly	56	6	4.70E-04	2.70E-02
negative regulation of macromolecule biosynthetic process	48	5.2	5.30E-04	3.00E-02
cellular macromolecular complex assembly	32	3.5	6.20E-04	3.30E-02
establishment of chromosome localization	6	0.6	7.40E-04	3.80E-02
regulation of cell adhesion	18	1.9	7.90E-04	3.90E-02
transmembrane receptor protein serine/threonine kinase signaling pathway	15	1.6	9.10E-04	4.40E-02
negative regulation of cellular biosynthetic process	48	5.2	9.10E-04	4.30E-02
regulation of mitotic cell cycle	19	2	9.70E-04	4.50E-02
regulation of locomotion	22	2.4	1.10E-03	4.90E-02

Table 4. GO terms enriched among Cluster 3 of genes significantly changed *in vitro*

Cluster 3				
Term	**Count**	**%**	**P-Value**	**Benjamini**
Development				
blood vessel development	24	6.4	3.50E-09	7.40E-06
vasculature development	24	6.4	5.60E-09	5.90E-06
blood vessel morphogenesis	21	5.6	3.20E-08	2.30E-05
angiogenesis	16	4.3	7.50E-07	1.60E-04
tube development	15	4	3.20E-04	2.30E-02
hemopoietic or lymphoid organ development	16	4.3	5.50E-04	3.20E-02
immune system development	16	4.3	1.00E-03	4.10E-02
Adhesion and migration				
regulation of cell adhesion	17	4.5	4.40E-08	1.80E-05
biological adhesion	40	10.7	5.40E-08	1.90E-05
cell motion	31	8.3	1.50E-07	4.40E-05
cell adhesion	39	10.4	1.60E-07	3.70E-05
positive regulation of cell motion	11	2.9	5.10E-05	6.60E-03
positive regulation of locomotion	11	2.9	5.10E-05	6.60E-03
regulation of cell migration	14	3.7	7.90E-05	8.70E-03
regulation of locomotion	15	4	7.60E-05	8.80E-03
regulation of cell motion	15	4	8.00E-05	8.40E-03
cell migration	18	4.8	1.10E-04	1.10E-02
localization of cell	19	5.1	1.30E-04	1.20E-02
cell motility	19	5.1	1.30E-04	1.20E-02
positive regulation of cell migration	10	2.7	1.30E-04	1.10E-02
cell adhesion mediated by integrin	4	1.1	3.30E-04	2.30E-02
regulation of cell-cell adhesion	5	1.3	1.20E-03	4.50E-02
Differentiation and development				
neuron differentiation	25	6.7	3.00E-05	4.20E-03
neuron projection development	16	4.3	4.70E-04	3.00E-02
neuron projection morphogenesis	14	3.7	7.60E-04	3.60E-02
negative regulation of cell differentiation	14	3.7	8.70E-04	3.90E-02
cell fate commitment	11	2.9	8.90E-04	3.90E-02
neuron development	18	4.8	1.20E-03	4.50E-02
Response to stimulus				
response to wounding	33	8.8	1.50E-07	4.00E-05
response to organic substance	32	8.6	2.10E-04	1.70E-02
response to inorganic substance	14	3.7	5.30E-04	3.20E-02
response to endogenous stimulus	21	5.6	5.40E-04	3.20E-02
response to hypoxia	11	2.9	6.70E-04	3.40E-02
regulation of response to external stimulus	15	4	9.20E-06	1.80E-03
response to hormone stimulus	20	5.3	4.10E-04	2.80E-02
response to steroid hormone stimulus	13	3.5	9.80E-04	4.20E-02
response to progesterone stimulus	5	1.3	7.90E-04	3.70E-02
response to oxygen levels	11	2.9	9.90E-04	4.20E-02

Signaling				
intracellular signaling cascade	46	12.3	5.10E-04	3.20E-02
positive regulation of signal transduction	17	4.5	7.20E-04	3.60E-02
positive regulation of cell communication	18	4.8	8.40E-04	3.90E-02
negative regulation of MAP kinase activity	6	1.6	1.00E-03	4.10E-02
Rho protein signal transduction	6	1.6	1.30E-03	4.80E-02
Uncateogrized				
wound healing	20	5.3	3.30E-08	1.70E-05
regulation of cell proliferation	37	9.9	1.70E-05	3.00E-03
hemostasis	12	3.2	2.20E-05	3.50E-03
aging	12	3.2	2.60E-05	3.90E-03
coagulation	11	2.9	7.20E-05	8.80E-03
blood coagulation	11	2.9	7.20E-05	8.80E-03
regeneration	9	2.4	1.20E-04	1.10E-02
leukocyte differentiation	12	3.2	1.30E-04	1.10E-02
vasculogenesis	7	1.9	2.30E-04	1.80E-02
regulation of body fluid levels	12	3.2	2.50E-04	1.80E-02
negative regulation of protein kinase activity	9	2.4	5.80E-04	3.30E-02
hemopoiesis	15	4	6.40E-04	3.50E-02
positive regulation of positive chemotaxis	5	1.3	6.50E-04	3.40E-02
regulation of positive chemotaxis	5	1.3	6.50E-04	3.40E-02
negative regulation of kinase activity	9	2.4	7.30E-04	3.60E-02
negative regulation of transferase activity	9	2.4	1.10E-03	4.40E-02

Table 5. GO terms enriched among genes significantly changed both *in vivo* and *in vitro*

GO Terms enriched among genes FC>2 BOTH *in vivo* and *in vitro*				
Term	**Count**	**%**	**P-Value**	**Benjamini adjusted p-value**
Neuron differentiation and development				
neuron differentiation	33	11.1	2.50E-11	4.50E-08
neuron development	28	9.4	1.50E-10	6.60E-08
cell morphogenesis involved in neuron differentiation	22	7.4	2.70E-10	9.70E-08
neuron projection morphogenesis	22	7.4	3.80E-10	1.20E-07
axonogenesis	21	7.1	4.20E-10	1.10E-07
neuron projection development	23	7.7	2.00E-09	3.20E-07
axon guidance	14	4.7	7.90E-08	9.60E-06
central nervous system projection neuron axonogenesis	4	1.3	1.20E-03	5.00E-02
Ggeneral cell differentiation and development				
cell projection morphogenesis	23	7.7	8.60E-10	1.70E-07
cell morphogenesis involved in differentiation	22	7.4	4.60E-09	6.90E-07
cellular component morphogenesis	27	9.1	2.00E-08	2.80E-06
cell morphogenesis	25	8.4	4.20E-08	5.50E-06
cell fate commitment	11	3.7	2.50E-04	1.40E-02
Cellular organization				
cell projection organization	28	9.4	9.10E-10	1.70E-07
cell part morphogenesis	23	7.7	2.00E-09	3.20E-07
extracellular structure organization	15	5.1	1.90E-06	1.80E-04
regulation of cell projection organization	8	2.7	1.30E-03	5.00E-02
Development				
skeletal system development	21	7.1	1.80E-06	1.90E-04
pattern specification process	18	6.1	9.20E-06	8.30E-04
blood vessel development	15	5.1	1.80E-04	1.20E-02
tube development	14	4.7	2.20E-04	1.40E-02
vasculature development	15	5.1	2.30E-04	1.40E-02
blood vessel morphogenesis	13	4.4	5.40E-04	2.90E-02
heart development	13	4.4	6.40E-04	3.20E-02
regionalization	12	4	1.10E-03	4.70E-02
Brain development				
synapse organization	7	2.4	8.70E-04	4.10E-02
regulation of neurogenesis	11	3.7	1.00E-03	4.60E-02
Signaling				
enzyme linked receptor protein signaling pathway	24	8.1	8.60E-08	9.70E-06
cell surface receptor linked signal transduction	60	20.2	1.30E-05	1.10E-03
transmembrane receptor protein tyrosine kinase signaling pathway	16	5.4	1.70E-05	1.40E-03
cell-cell signaling	25	8.4	3.00E-04	1.70E-02
Wnt receptor signaling pathway	10	3.4	7.90E-04	3.80E-02
positive regulation of cell communication	16	5.4	1.20E-03	5.00E-02
BMP signaling pathway	6	2	1.20E-03	5.00E-02
Cell adhesion and migration				
cell adhesion	42	14.1	3.60E-11	3.20E-08
biological adhesion	42	14.1	3.70E-11	2.20E-08

cell motion	32	10.8	8.50E-10	1.90E-07
positive regulation of cell adhesion	10	3.4	1.40E-06	1.50E-04
cell migration	18	6.1	1.40E-05	1.20E-03
neuron migration	9	3	2.10E-05	1.60E-03
cell motility	18	6.1	5.50E-05	4.00E-03
localization of cell	18	6.1	5.50E-05	4.00E-03
positive regulation of cell-substrate adhesion	6	2	1.40E-04	9.80E-03
regulation of cell adhesion	11	3.7	2.20E-04	1.40E-02
cell-cell adhesion	15	5.1	6.00E-04	3.10E-02
Uncategorized				
positive regulation of multicellular organismal process	14	4.7	6.00E-04	3.10E-02
ossification	9	3	1.30E-03	5.00E-02

Table 6. GO terms enriched among genes significantly changed only *in vivo*

GO Terms enriched among genes FC>2 ONLY *in vivo*				
Term	**Count**	**%**	**P-Value**	**Benjamini Adjusted P-Value**
Neuron differentiation and development				
neuron differentiation	38	10.8	8.50E-14	4.80E-11
cell morphogenesis involved in neuron differentiation	26	7.4	5.80E-13	2.00E-10
axonogenesis	25	7.1	7.40E-13	2.10E-10
neuron projection morphogenesis	25	7.1	6.40E-12	1.50E-09
neuron development	30	8.5	3.70E-11	7.90E-09
neuron projection development	26	7.4	5.40E-11	1.00E-08
axon guidance	12	3.4	9.30E-06	7.80E-04
regulation of neuron differentiation	11	3.1	3.30E-04	1.50E-02
Neurotransmission				
synaptic transmission	32	9.1	4.00E-14	6.80E-11
transmission of nerve impulse	34	9.7	9.70E-14	4.10E-11
neurotransmitter transport	10	2.8	4.00E-05	2.90E-03
regulation of neurotransmitter levels	9	2.6	5.30E-05	3.50E-03
synapse organization	8	2.3	2.00E-04	1.10E-02
regulation of synaptic transmission	11	3.1	4.00E-04	1.70E-02
synaptic vesicle transport	6	1.7	4.60E-04	1.90E-02
neuron recognition	5	1.4	7.10E-04	2.60E-02
regulation of transmission of nerve impulse	11	3.1	7.30E-04	2.60E-02
glutamate signaling pathway	5	1.4	1.40E-03	4.40E-02
Brain development				
forebrain development	16	4.6	3.70E-07	3.90E-05
neurological system process	46	13.1	3.10E-05	2.40E-03
regulation of nervous system development	14	4	1.30E-04	7.60E-03
regulation of neurological system process	11	3.1	1.00E-03	3.40E-02
hindbrain morphogenesis	5	1.4	1.00E-03	3.40E-02
Cell differentiation and development				
cell morphogenesis involved in differentiation	29	8.3	6.30E-14	5.40E-11
cell projection morphogenesis	25	7.1	1.20E-10	1.90E-08
cell part morphogenesis	25	7.1	3.10E-10	4.30E-08
cell morphogenesis	29	8.3	5.80E-10	7.50E-08
Cellular organization				
cell projection organization	28	8	5.40E-09	6.50E-07
cellular component morphogenesis	29	8.3	6.60E-09	7.50E-07
Signaling				
cell-cell signaling	40	11.4	6.20E-11	1.10E-08
Transport				
ion transport	38	10.8	5.50E-07	5.40E-05
Cell adhesion and migration				
cell adhesion	35	10	1.40E-06	1.30E-04
biological adhesion	35	10	1.40E-06	1.30E-04
cell motion	26	7.4	9.80E-06	7.90E-04
cell-cell adhesion	16	4.6	4.40E-04	1.80E-02
Development				

ear morphogenesis	9	2.6	4.80E-05	3.40E-03
embryonic morphogenesis	18	5.1	1.50E-04	8.60E-03
limb morphogenesis	10	2.8	1.60E-04	8.90E-03
appendage morphogenesis	10	2.8	1.60E-04	8.90E-03
appendage development	10	2.8	2.10E-04	1.10E-02
limb development	10	2.8	2.10E-04	1.10E-02
pattern specification process	16	4.6	3.10E-04	1.50E-02
embryonic limb morphogenesis	9	2.6	3.40E-04	1.50E-02
embryonic appendage morphogenesis	9	2.6	3.40E-04	1.50E-02
skeletal system morphogenesis	10	2.8	4.00E-04	1.70E-02
regionalization	13	3.7	6.00E-04	2.30E-02
ear development	9	2.6	6.20E-04	2.30E-02
sensory organ development	14	4	7.00E-04	2.60E-02
inner ear morphogenesis	7	2	8.40E-04	2.90E-02
dorsal/ventral pattern formation	7	2	1.20E-03	3.90E-02
embryonic organ morphogenesis	10	2.8	1.40E-03	4.40E-02
Uncategorized				
regulation of system process	19	5.4	4.90E-05	3.30E-03
response to inorganic substance	15	4.3	6.40E-05	4.00E-03
metal ion transport	23	6.6	1.60E-04	8.80E-03
response to metal ion	11	3.1	2.60E-04	1.30E-02
behavior	22	6.3	4.80E-04	1.90E-02
response to organic nitrogen	7	2	1.60E-03	4.80E-02
extracellular structure organization	11	3.1	1.60E-03	4.80E-02
cation transport	23	6.6	1.70E-03	4.90E-02
learning or memory	9	2.6	1.70E-03	4.90E-02

Table 7. GO terms enriched among genes significantly changed only *in vitro*

GO Terms enriched among genes FC>2 ONLY *in vitro*				
Term	**Count**	**%**	**P-Value**	**Benjamini Adjusted P-Value**
Stress response/ stress signaling				
response to organic substance	26	7.4	1.80E-03	3.50E-01
positive regulation of I-kappaB kinase/NF-kappaB cascade	8	2.3	2.10E-03	3.70E-01
regulation of I-kappaB kinase/NF-kappaB cascade	8	2.3	3.60E-03	3.80E-01
response to cytokine stimulus	7	2	3.30E-03	4.00E-01
response to glucocorticoid stimulus	7	2	3.10E-03	4.00E-01
response to corticosteroid stimulus	7	2	4.80E-03	4.50E-01
Signaling				
positive regulation of protein kinase cascade	12	3.4	2.70E-04	4.10E-01
positive regulation of signal transduction	16	4.6	3.80E-04	2.20E-01
positive regulation of cell communication	17	4.9	4.00E-04	1.80E-01
Cell adhesion and migration				
regulation of cell migration	12	3.4	3.00E-04	2.50E-01
regulation of locomotion	12	3.4	8.70E-04	2.90E-01
regulation of cell motion	12	3.4	9.00E-04	2.60E-01
positive regulation of cell migration	8	2.3	1.30E-03	3.00E-01
positive regulation of cell motion	8	2.3	2.20E-03	3.50E-01
positive regulation of locomotion	8	2.3	2.20E-03	3.50E-01
Uncategorized				
regulation of protein kinase cascade	13	3.7	2.20E-03	3.30E-01
negative regulation of transport	9	2.6	3.50E-03	3.90E-01

CHAPTER 6: Significance and future research questions

In vitro models are emerging as a necessary tool to screen the large number of chemicals already in commerce for potential developmental toxicity. In order to interpret results from these *in vitro* assays appropriately, there is a pressing need to clearly define what sensitive developmental stages and processes are captured in each of these models and which are not.

We have established and characterized long term dynamics of two *in vitro* models that reflect key developmental processes in two organ systems. I employed a quantitative pathway analysis to characterize pathway dynamics in *in vitro* models through time, first demonstrating the power of this approach in defining normal *in vivo* development throughout the sensitive process of male reproductive development, then applying this approach to evaluate *in vitro* models and characterize normal gene expression through time *in vitro*. Each model was evaluated according to a common set of criteria, including morphological features, protein expression, functional endpoints, gene expression and the presence of specific toxicant targets *in vitro*. We found that both *in vitro* models capture important, context-specific developmental pathways that may be sensitive to toxicant perturbation.

The *in vitro* testicular co-culture serves as a model for a sensitive phase of testicular development during which multiple cell types are partially differentiated and becoming functionally competent. Basic characterization of the *in vitro* testis model demonstrates that the culture contains Sertoli, Leydig, and spermatogonial cells, produces testosterone and develops morphological characteristics important for testicular development and function. Pathway enrichment analysis confirms that the model closely mirrors gene expression patterns apparent for many pathways in corresponding *in vivo* samples. These include pathways related to testicular cell differentiation, tight junction formation, testosterone production, immune processes, and metabolism.

The hNPC differentiation culture captures differentiation processes that occur throughout brain development across different brain regions. Basic characterization of the model demonstrates that hNPCs increasingly express markers of mature neurons, develop morphological characteristics of mature neurons, and form dense neuronal networks through time in differentiating conditions. Pathway analysis demonstrates that the model captures neuronal differentiation towards a forebrain identity and generation of a range of specific neuronal subtypes, expressing glutamatergic and GABAergic receptors.

By defining normal pathway dynamics through time we create a framework for measuring toxicant perturbation of developmental pathways both *in vivo* and *in vitro*.

Future Work to optimize and utilize these *In vitro* models

Future work in these systems could further enhance the ability of the model to capture *in vivo* processes. For example, transferring these cultures to a microfluidic system with the capacity to regulate chemical signals more precisely would allow us to supplement cultures with hormonal cues or growth factors that would typically be circulating *in vivo*.

In the testis co-culture, the presence of multiple cell types poses a special challenge. Similarly, in the neuronal differentiation culture, pathway analysis indicates the emergence of multiple neuronal subtypes as neurons differentiate. Optimizing assays for more cell-type specific endpoints would allow us a clearer understanding of specific cell targets and mechanism of action.

Applications for developmental toxicology screening

The baseline assessments completed here will inform future applications of these culture systems for toxicogenomic analysis as well as endpoint assays that reflect developmental signaling pathway perturbation or cell type-specific functions. This type of toxicity screening

could capture perturbation of both general developmental signaling pathways and context-specific endpoints.

The *in vitro* models explored here must be used in concert with a panel of assays aimed at capturing the full range of developmental stages across tissue types/regions. There is still much work to be done to identify and optimize additional *in vitro* models to evaluate developmental processes that are not yet captured *in vitro* and close the remaining gaps in what existing models can tell us and developmental endpoints we need to be able to evaluate.

Translating *in vitro* toxicology for risk assessment

The developmental toxicology community is increasingly embracing screening tools based on quantification of pathway perturbation *in vitro*. By carefully characterizing the pathways that are captured in the models we work with, this work begins to define the domain of applicability for each of these models. Furthermore, this type of analysis provides a framework for quantification of perturbation of pathway dynamics *in vitro* that can be interpreted with a clearer understanding of how *in vitro* responses are related to *in vivo* development. There are plenty of opportunities in the existing developmental biology and toxicogenomic literature to anchor additional *in vitro* models to an *in vivo* developmental context.

Before toxicity data from *in vitro* models can be fully incorporated into risk assessment, cultures need to be further characterized to determine the extent to which toxicants are metabolized in culture, and how toxicants partition in media and cells once added to culture. This type of characterization will facilitate translation between *in vitro* toxicant concentrations and relevant human exposure scenarios (Wetmore et al. 2012).

Ultimately this type of early *in vitro* pathway based screening tool could be incorporated into product and drug design at the outset so that consumer products and industrial processes are safer by design. Anticipating toxicants with the potential to perturb development and epigenetic

programming that influences health throughout life should be seen as an essential step in protecting public health and preventing diseases.

References

Adiga., S., V. Jayaraman., et al. (2008). "Declining semen quality among south Indian infertile men: A retrospective study." Journal of human reproductive sciences **1**(1): 15-18.

Adler, S., D. Basketter, et al. (2011). "Alternative (non-animal) methods for cosmetics testing: current status and future prospects-2010." Archives of toxicology **85**(5): 367-485.

Al-Shahrour, F., R. Diaz-Uriarte, et al. (2004). "FatiGO: a web tool for finding significant associations of Gene Ontology terms with groups of genes." Bioinformatics **20**(4): 578-580.

Alam, M. S., S. Ohsako, et al. (2010). "Induction of spermatogenic cell apoptosis in prepubertal rat testes irrespective of testicular steroidogenesis: a possible estrogenic effect of di(n-butyl) phthalate." Reproduction **139**(2): 427-437.

Andersen, A. G., T. K. Jensen, et al. (2000). "High frequency of sub-optimal semen quality in an unselected population of young men." Hum Reprod **15**(2): 366-372.

Andersen, M. E., H. J. Clewell, 3rd, et al. (2008). "Genomic signatures and dose-dependent transitions in nasal epithelial responses to inhaled formaldehyde in the rat." Toxicological sciences : an official journal of the Society of Toxicology **105**(2): 368-383.

Ankley, G. T., R. S. Bennett, et al. (2010). "Adverse outcome pathways: a conceptual framework to support ecotoxicology research and risk assessment." Environ Toxicol Chem **29**(3): 730-741.

Armit, C. (2007). "Developmental biology and databases: how to archive, find and query gene expression patterns using the world wide web." Organogenesis **3**(2): 70-73.

Baarends, W. M., R. van der Laan, et al. (2000). "Specific aspects of the ubiquitin system in spermatogenesis." J Endocrinol Invest **23**(9): 597-604.

Bal-Price, A. K., H. T. Hogberg, et al. (2010). "In vitro developmental neurotoxicity (DNT) testing: relevant models and endpoints." Neurotoxicology **31**(5): 545-554.

Barker, D. J. (2004). "The developmental origins of adult disease." Journal of the American College of Nutrition **23**(6 Suppl): 588S-595S.

Barker, D. J. (2007). "The origins of the developmental origins theory." Journal of internal medicine **261**(5): 412-417.

Barlow, N. J., S. L. Phillips, et al. (2003). "Quantitative changes in gene expression in fetal rat testes following exposure to di(n-butyl) phthalate." Toxicol Sci **73**(2): 431-441.

Barouki, R., P. D. Gluckman, et al. (2012). "Developmental origins of non-communicable disease: implications for research and public health." Environ Health **11**: 42.

Barsoum, I. B. and H. H. Yao (2010). "Fetal Leydig cells: progenitor cell maintenance and differentiation." J Androl **31**(1): 11-15.

Beissbarth, T. and T. P. Speed (2004). "GOstat: find statistically overrepresented Gene Ontologies within a group of genes." Bioinformatics **20**(9): 1464-1465.

Belliveau, M. E. (2011). "The drive for a safer chemicals policy in the United States." New Solut **21**(3): 359-386.

Berruti, G. (1998). "Signaling events during male germ cell differentiation: bases and perspectives." Front Biosci **3**: D1097-1108.

Bornehag, C. G. and E. Nanberg (2010). "Phthalate exposure and asthma in children." Int J Androl **33**(2): 333-345.
Bouma, G. J., Q. J. Hudson, et al. (2010). "New candidate genes identified for controlling mouse gonadal sex determination and the early stages of granulosa and Sertoli cell differentiation." Biol Reprod **82**(2): 380-389.
Bowles, J. and P. Koopman (2007). "Retinoic acid, meiosis and germ cell fate in mammals." Development **134**(19): 3401-3411.
Bowles, J. and P. Koopman (2010). "Sex determination in mammalian germ cells: extrinsic versus intrinsic factors." Reproduction **139**(6): 943-958.
Boyd, N. L., S. K. Dhara, et al. (2007). "BMP4 promotes formation of primitive vascular networks in human embryonic stem cell-derived embryoid bodies." Experimental biology and medicine **232**(6): 833-843.
Breier, J. M., N. M. Radio, et al. (2008). "Development of a high-throughput screening assay for chemical effects on proliferation and viability of immortalized human neural progenitor cells." Toxicological sciences : an official journal of the Society of Toxicology **105**(1): 119-133.
Brennan, J. and B. Capel (2004). "One tissue, two fates: molecular genetic events that underlie testis versus ovary development." Nat Rev Genet **5**(7): 509-521.
Buck Louis, G. M., R. Sundaram, et al. (2014). "Urinary bisphenol A, phthalates, and couple fecundity: the Longitudinal Investigation of Fertility and the Environment (LIFE) Study." Fertil Steril **101**(5): 1359-1366.
Bugiak, B. J. and L. P. Weber (2010). "Phenotypic anchoring of gene expression after developmental exposure to aryl hydrocarbon receptor ligands in zebrafish." Aquatic toxicology **99**(3): 423-437.
Bushnell, P. J., R. J. Kavlock, et al. (2010). "Behavioral toxicology in the 21st century: challenges and opportunities for behavioral scientists. Summary of a symposium presented at the annual meeting of the neurobehavioral teratology society, June, 2009." Neurotoxicol Teratol **32**(3): 313-328.
Buzanska, L., M. Zychowicz, et al. (2010). "Neural stem cells from human cord blood on bioengineered surfaces--novel approach to multiparameter bio-tests." Toxicology **270**(1): 35-42.
Carlsen, E., A. Giwercman, et al. (1992). "Evidence for decreasing quality of semen during past 50 years." BMJ **305**(6854): 609-613.
Chapin, R. E., K. Boekelheide, et al. (2013). "Assuring safety without animal testing: the case for the human testis in vitro." Reprod Toxicol **39**: 63-68.
Chia, V. M., S. M. Quraishi, et al. (2010). "International trends in the incidence of testicular cancer, 1973-2002." Cancer epidemiology, biomarkers & prevention : a publication of the American Association for Cancer Research, cosponsored by the American Society of Preventive Oncology **19**(5): 1151-1159.
Cho, E. and W. J. Li (2007). "Human stem cells, chromatin, and tissue engineering: boosting relevancy in developmental toxicity testing." Birth defects research. Part C, Embryo today : reviews **81**(1): 20-40.
Clark, B. J. and R. K. Cochrum (2007). "The steroidogenic acute regulatory protein as a target of endocrine disruption in male reproduction." Drug Metab Rev **39**(2-3): 353-370.

Clemente, E. J., R. A. Furlong, et al. (2006). "Gene expression study in the juvenile mouse testis: identification of stage-specific molecular pathways during spermatogenesis." Mamm Genome **17**(9): 956-975.
Conti, L. and E. Cattaneo (2010). "Neural stem cell systems: physiological players or in vitro entities?" Nat Rev Neurosci **11**(3): 176-187.
Creasy, D. M. and P. M. D. Foster (1984). "The Morphological Development of Glycol Ether-Induced Testicular Atrophy in the Rat." Experimental and Molecular Pathology **40**(2): 169-176.
Crofton, K. M., W. R. Mundy, et al. (2012). "Developmental neurotoxicity testing: a path forward." Congenit Anom (Kyoto) **52**(3): 140-146.
Cunnigham, M. L. (2006). "Putting the fun into functional toxicogenomics." Toxicol Sci **92**(2): 347-348.
Dahlquist, K. D., N. Salomonis, et al. (2002). "GenMAPP, a new tool for viewing and analyzing microarray data on biological pathways." Nat Genet **31**(1): 19-20.
Daston, G. P. (2008). "Gene expression, dose-response, and phenotypic anchoring: applications for toxicogenomics in risk assessment." Toxicological sciences : an official journal of the Society of Toxicology **105**(2): 233-234.
David, R. M. (2006). "Proposed mode of action for in utero effects of some phthalate esters on the developing male reproductive tract." Toxicol Pathol **34**(3): 209-219.
de Sanctis, L., L. Memo, et al. (2011). "Fetal alcohol syndrome: new perspectives for an ancient and underestimated problem." The journal of maternal-fetal & neonatal medicine : the official journal of the European Association of Perinatal Medicine, the Federation of Asia and Oceania Perinatal Societies, the International Society of Perinatal Obstetricians **24 Suppl 1**: 34-37.
de Sanctis, L., L. Memo, et al. (2011). "Fetal alcohol syndrome: new perspectives for an ancient and underestimated problem." J Matern Fetal Neonatal Med **24 Suppl 1**: 34-37.
Debeb, B. G., W. Xu, et al. (2010). "Differential radiosensitizing effect of valproic acid in differentiation versus self-renewal promoting culture conditions." International journal of radiation oncology, biology, physics **76**(3): 889-895.
DeFalco, T., I. Bhattacharya, et al. (2014). "Yolk-sac-derived macrophages regulate fetal testis vascularization and morphogenesis." Proc Natl Acad Sci U S A **111**(23): E2384-2393.
Dennery, P. A. (2007). "Effects of oxidative stress on embryonic development." Birth Defects Res C Embryo Today **81**(3): 155-162.
Dennis, G., Jr., B. T. Sherman, et al. (2003). "DAVID: Database for Annotation, Visualization, and Integrated Discovery." Genome Biol **4**(5): P3.
Dere, E., D. R. Boverhof, et al. (2006). "In vivo-in vitro toxicogenomic comparison of TCDD-elicited gene expression in Hepa1c1c7 mouse hepatoma cells and C57BL/6 hepatic tissue." BMC Genomics **7**: 80.
Dillman, J. F., 3rd, C. S. Phillips, et al. (2005). "Genomic analysis of rodent pulmonary tissue following bis-(2-chloroethyl) sulfide exposure." Chem Res Toxicol **18**(1): 28-34.
Doktorova, T. Y., H. Ellinger-Ziegelbauer, et al. (2012). "Comparison of genotoxicant-modified transcriptomic responses in conventional and epigenetically stabilized

primary rat hepatocytes with in vivo rat liver data." Archives of toxicology **86**(11): 1703-1715.
Doniger, S. W., N. Salomonis, et al. (2003). "MAPPFinder: using Gene Ontology and GenMAPP to create a global gene-expression profile from microarray data." Genome Biol **4**(1): R7.
Eiraku, M., K. Watanabe, et al. (2008). "Self-organized formation of polarized cortical tissues from ESCs and its active manipulation by extrinsic signals." Cell Stem Cell **3**(5): 519-532.
Escalier, D. (2001). "Impact of genetic engineering on the understanding of spermatogenesis." Human reproduction update **7**(2): 191-210.
EU (2006). "Regulation (EC) No 1907/2006 concerning the Registration, Evaluation, Authorisation and Restriction
of Chemicals (REACH), establishing a European Chemicals Agency, …", . Official Journal of the European Union, L 396:1-849
Fabro, S., R. L. Smith, et al. (1967). "Toxicity and teratogenicity of optical isomers of thalidomide." Nature **215**(5098): 296.
Ferguson, K. K., R. Loch-Caruso, et al. (2011). "Urinary phthalate metabolites in relation to biomarkers of inflammation and oxidative stress: NHANES 1999-2006." Environ Res **111**(5): 718-726.
Fiorini, C., A. Tilloy-Ellul, et al. (2004). "Sertoli cell junctional proteins as early targets for different classes of reproductive toxicants." Reprod Toxicol **18**(3): 413-421.
Flint, O. P. (1983). "A micromass culture method for rat embryonic neural cells." Journal of cell science **61**: 247-262.
Flint, O. P., T. C. Orton, et al. (1984). "Differentation of rat embryo cells in culture: response following acute maternal exposure to teratogens and non-teratogens." Journal of applied toxicology : JAT **4**(2): 109-116.
Foster, P. M., L. V. Thomas, et al. (1980). "Study of the testicular effects and changes in zinc excretion produced by some n-alkyl phthalates in the rat." Toxicol Appl Pharmacol **54**(3): 392-398.
Fritsche, E., K. Gassmann, et al. (2011). "Neurospheres as a model for developmental neurotoxicity testing." Methods in molecular biology **758**: 99-114.
Fritsche, E., K. Gassmann, et al. (2011). "Neurospheres as a model for developmental neurotoxicity testing." Methods Mol Biol **758**: 99-114.
Fromme, H., L. Gruber, et al. (2011). "Phthalates and their metabolites in breast milk--results from the Bavarian Monitoring of Breast Milk (BAMBI)." Environ Int **37**(4): 715-722.
Gaido, K. W., J. B. Hensley, et al. (2007). "Fetal mouse phthalate exposure shows that Gonocyte multinucleation is not associated with decreased testicular testosterone." Toxicol Sci **97**(2): 491-503.
Garavaglia, A., A. Moiana, et al. (2010). "Adaptation of NS cells growth and differentiation to high-throughput screening-compatible plates." BMC Neurosci **11**: 7.
Gaspard, N., T. Bouschet, et al. (2008). "An intrinsic mechanism of corticogenesis from embryonic stem cells." Nature **455**(7211): 351-357.
Gaspard, N. and P. Vanderhaeghen (2010). "Mechanisms of neural specification from embryonic stem cells." Curr Opin Neurobiol **20**(1): 37-43.

Gerhart, J. (1999). "1998 Warkany lecture: signaling pathways in development." Teratology **60**(4): 226-239.
Goldman, L. R. and S. Koduru (2000). "Chemicals in the environment and developmental toxicity to children: a public health and policy perspective." Environmental health perspectives **108 Suppl 3**: 443-448.
Grandjean, P. and K. T. Herz (2011). "Methylmercury and brain development: imprecision and underestimation of developmental neurotoxicity in humans." Mt Sinai J Med **78**(1): 107-118.
Grandjean, P. and K. T. Herz (2011). "Methylmercury and brain development: imprecision and underestimation of developmental neurotoxicity in humans." The Mount Sinai journal of medicine, New York **78**(1): 107-118.
Grandjean, P. and P. J. Landrigan (2006). "Developmental neurotoxicity of industrial chemicals." Lancet **368**(9553): 2167-2178.
Grandjean, P. and P. J. Landrigan (2014). "Neurobehavioural effects of developmental toxicity." Lancet Neurol **13**(3): 330-338.
Granholm, T., D. M. Creasy, et al. (1992). "Di-n-pentyl phthalate-induced inflammatory changes in the rat testis are accompanied by local production of a novel lymphocyte activating factor." J Reprod Immunol **21**(1): 1-14.
Gray, L. E., Jr., J. Ostby, et al. (2000). "Perinatal exposure to the phthalates DEHP, BBP, and DINP, but not DEP, DMP, or DOTP, alters sexual differentiation of the male rat." Toxicol Sci **58**(2): 350-365.
Gregotti, C. F., Z. Kirby, et al. (1994). "Effects of styrene oxide on differentiation and viability of rodent embryo cultures." Toxicology and applied pharmacology **128**(1): 25-35.
Groudine, M. and K. F. Conkin (1985). "Chromatin structure and de novo methylation of sperm DNA: implications for activation of the paternal genome." Science **228**(4703): 1061-1068.
Guizzetti, M., N. H. Moore, et al. (2008). "Modulation of neuritogenesis by astrocyte muscarinic receptors." J Biol Chem **283**(46): 31884-31897.
Habert, R., V. Muczynski, et al. (2014). "Concerns about the widespread use of rodent models for human risk assessments of endocrine disruptors." Reproduction **147**(4): R119-129.
Hannas, B. R., J. Furr, et al. (2011). "Dipentyl phthalate dosing during sexual differentiation disrupts fetal testis function and postnatal development of the male Sprague-Dawley rat with greater relative potency than other phthalates." Toxicol Sci **120**(1): 184-193.
Harrill, J. A., T. M. Freudenrich, et al. (2010). "Quantitative assessment of neurite outgrowth in human embryonic stem cell-derived hN2 cells using automated high-content image analysis." Neurotoxicology **31**(3): 277-290.
Hartung, T. (2010). "Evidence-based toxicology - the toolbox of validation for the 21st century?" ALTEX **27**(4): 253-263.
Hartung, T., B. J. Blaauboer, et al. (2011). "An expert consortium review of the EC-commissioned report "alternative (Non-Animal) methods for cosmetics testing: current status and future prospects - 2010"." ALTEX **28**(3): 183-209.
Hauser, R. and A. M. Calafat (2005). "Phthalates and human health." Occup Environ Med **62**(11): 806-818.

Hauser, R., J. D. Meeker, et al. (2006). "Altered semen quality in relation to urinary concentrations of phthalate monoester and oxidative metabolites." Epidemiology **17**(6): 682-691.
Hayess, K., C. Riebeling, et al. (2013). "The DNT-EST: a predictive embryonic stem cell-based assay for developmental neurotoxicity testing in vitro." Toxicology **314**(1): 135-147.
Hermo, L., R. M. Pelletier, et al. (2010). "Surfing the wave, cycle, life history, and genes/proteins expressed by testicular germ cells. Part 1: background to spermatogenesis, spermatogonia, and spermatocytes." Microsc Res Tech **73**(4): 241-278.
Hermo, L., R. M. Pelletier, et al. (2010). "Surfing the wave, cycle, life history, and genes/proteins expressed by testicular germ cells. Part 5: intercellular junctions and contacts between germs cells and Sertoli cells and their regulatory interactions, testicular cholesterol, and genes/proteins associated with more than one germ cell generation." Microsc Res Tech **73**(4): 409-494.
Hogarth, C. A. and M. D. Griswold (2010). "The key role of vitamin A in spermatogenesis." J Clin Invest **120**(4): 956-962.
Hogberg, H. T., J. Bressler, et al. (2013). "Toward a 3D model of human brain development for studying gene/environment interactions." Stem Cell Res Ther **4 Suppl 1**: S4.
Houmard, B., C. Small, et al. (2009). "Global gene expression in the human fetal testis and ovary." Biol Reprod **81**(2): 438-443.
Howdeshell, K. L., C. V. Rider, et al. (2008). "Mechanisms of action of phthalate esters, individually and in combination, to induce abnormal reproductive development in male laboratory rats." Environ Res **108**(2): 168-176.
Huang, D. W., B. T. Sherman, et al. (2009). "Systematic and integrative analysis of large gene lists using DAVID bioinformatics resources." Nature Protocols **4**(1): 44-57.
Ishikawa, T., K. Hwang, et al. (2005). "Sertoli cell expression of steroidogenic acute regulatory protein-related lipid transfer 1 and 5 domain-containing proteins and sterol regulatory element binding protein-1 are interleukin-1beta regulated by activation of c-Jun N-terminal kinase and cyclooxygenase-2 and cytokine induction." Endocrinology **146**(12): 5100-5111.
Jenkins, T. G. and D. T. Carrell (2012). "The sperm epigenome and potential implications for the developing embryo." Reproduction **143**(6): 727-734.
Jensen, T. K., E. Carlsen, et al. (2002). "Poor semen quality may contribute to recent decline in fertility rates." Hum Reprod **17**(6): 1437-1440.
Judson, R., A. Richard, et al. (2009). "The toxicity data landscape for environmental chemicals." Environmental health perspectives **117**(5): 685-695.
Judson, R., A. Richard, et al. (2009). "The toxicity data landscape for environmental chemicals." Environ Health Perspect **117**(5): 685-695.
Judson, R. S., K. A. Houck, et al. (2010). "In vitro screening of environmental chemicals for targeted testing prioritization: the ToxCast project." Environmental health perspectives **118**(4): 485-492.
Judson, R. S., R. J. Kavlock, et al. (2011). "Estimating toxicity-related biological pathway altering doses for high-throughput chemical risk assessment." Chemical research in toxicology **24**(4): 451-462.

Judson, R. S., R. J. Kavlock, et al. (2011). "Estimating toxicity-related biological pathway altering doses for high-throughput chemical risk assessment." Chem Res Toxicol **24**(4): 451-462.
Jurewicz, J., W. Hanke, et al. (2009). "Environmental factors and semen quality." International journal of occupational medicine and environmental health **22**(4): 305-329.
Jurewicz, J., M. Radwan, et al. (2013). "Human urinary phthalate metabolites level and main semen parameters, sperm chromatin structure, sperm aneuploidy and reproductive hormones." Reprod Toxicol **42**: 232-241.
Kang, H. J., Y. I. Kawasawa, et al. (2011). "Spatio-temporal transcriptome of the human brain." Nature **478**(7370): 483-489.
Kimber, I. and R. J. Dearman (2010). "An assessment of the ability of phthalates to influence immune and allergic responses." Toxicology **271**(3): 73-82.
Kirkeby, A., S. Grealish, et al. (2012). "Generation of regionally specified neural progenitors and functional neurons from human embryonic stem cells under defined conditions." Cell Rep **1**(6): 703-714.
Knudsen, T. B., R. J. Kavlock, et al. (2011). "Developmental toxicity testing for safety assessment: new approaches and technologies." Birth defects research. Part B, Developmental and reproductive toxicology **92**(5): 413-420.
Krewski, D., M. Westphal, et al. (2011). "New directions in toxicity testing." Annu Rev Public Health **32**: 161-178.
Kristensen, D. M., M. L. Skalkam, et al. (2011). "Many putative endocrine disruptors inhibit prostaglandin synthesis." Environ Health Perspect **119**(4): 534-541.
Krug, A. K., R. Kolde, et al. (2013). "Human embryonic stem cell-derived test systems for developmental neurotoxicity: a transcriptomics approach." Arch Toxicol **87**(1): 123-143.
Kuranaga, E. (2012). "Beyond apoptosis: caspase regulatory mechanisms and functions in vivo." Genes Cells **17**(2): 83-97.
Lahousse, S. A., D. G. Wallace, et al. (2006). "Testicular gene expression profiling following prepubertal rat mono-(2-ethylhexyl) phthalate exposure suggests a common initial genetic response at fetal and prepubertal ages." Toxicol Sci **93**(2): 369-381.
Laiho, A., N. Kotaja, et al. (2013). "Transcriptome profiling of the murine testis during the first wave of spermatogenesis." PLoS One **8**(4): e61558.
Lambrot, R., V. Muczynski, et al. (2009). "Phthalates impair germ cell development in the human fetal testis in vitro without change in testosterone production." Environ Health Perspect **117**(1): 32-37.
Lancaster, M. A., M. Renner, et al. (2013). "Cerebral organoids model human brain development and microcephaly." Nature **501**(7467): 373-379.
Landrigan, P. J. (2010). "What causes autism? Exploring the environmental contribution." Current opinion in pediatrics **22**(2): 219-225.
Landrigan, P. J., L. Lambertini, et al. (2012). "A research strategy to discover the environmental causes of autism and neurodevelopmental disabilities." Environmental health perspectives **120**(7): a258-260.

Lee, V. W., D. M. de Kretser, et al. (1975). "Variations in serum FSH, LH and testosterone levels in male rats from birth to sexual maturity." J Reprod Fertil **42**(1): 121-126.
Lehmann, K. P., S. Phillips, et al. (2004). "Dose-dependent alterations in gene expression and testosterone synthesis in the fetal testes of male rats exposed to di (n-butyl) phthalate." Toxicol Sci **81**(1): 60-68.
Lejeune, H., P. Sanchez, et al. (1998). "Enhancement of long-term testosterone secretion and steroidogenic enzyme expression in human Leydig cells by co-culture with human Sertoli cell-enriched preparations." Int J Androl **21**(3): 129-140.
Li, F., Q. Huang, et al. (2010). "Apoptotic cells activate the "phoenix rising" pathway to promote wound healing and tissue regeneration." Sci Signal **3**(110): ra13.
Lim, C. K., S. K. Kim, et al. (2009). "Differential cytotoxic effects of mono-(2-ethylhexyl) phthalate on blastomere-derived embryonic stem cells and differentiating neurons." Toxicology **264**(3): 145-154.
Liu, T. D., B. Y. Yu, et al. (2012). "Gene expression profiling of rat testis development during the early post-natal stages." Reprod Domest Anim **47**(5): 724-731.
Malkov, M., Y. Fisher, et al. (1998). "Developmental schedule of the postnatal rat testis determined by flow cytometry." Biol Reprod **59**(1): 84-92.
Mariani, J., M. V. Simonini, et al. (2012). "Modeling human cortical development in vitro using induced pluripotent stem cells." Proc Natl Acad Sci U S A **109**(31): 12770-12775.
Marjani, S. L., D. Le Bourhis, et al. (2009). "Embryonic gene expression profiling using microarray analysis." Reproduction, fertility, and development **21**(1): 22-30.
Mathur, P. P. and S. C. D'Cruz (2011). "The effect of environmental contaminants on testicular function." Asian journal of andrology **13**(4): 585-591.
Mendis-Handagama, S. M. and H. B. Ariyaratne (2001). "Differentiation of the adult Leydig cell population in the postnatal testis." Biol Reprod **65**(3): 660-671.
Miller, J. A., S. L. Ding, et al. (2014). "Transcriptional landscape of the prenatal human brain." Nature **508**(7495): 199-206.
Murphy, C. J., A. R. Stermer, et al. (2014). "Age- and Species-Dependent Infiltration of Macrophages into the Testis of Rats and Mice Exposed to Mono-(2-Ethylhexyl) Phthalate (MEHP)." Biol Reprod.
Mylchreest, E., R. C. Cattley, et al. (1998). "Male reproductive tract malformations in rats following gestational and lactational exposure to Di(n-butyl) phthalate: an antiandrogenic mechanism?" Toxicol Sci **43**(1): 47-60.
NRC (2000). Scientific Frontiers in Developmental Toxicology and Risk Assessment, The National Academies Press.
NRC (2007). Toxicity Testing in the 21st Century: A Vision and a Strategy, The National Academies Press.
O'Shaughnessy, P. J. and P. A. Fowler (2011). "Endocrinology of the mammalian fetal testis." Reproduction **141**(1): 37-46.
Oatley, J. M. and R. L. Brinster (2012). "The germline stem cell niche unit in mammalian testes." Physiol Rev **92**(2): 577-595.
Onorato, T. M., P. W. Brown, et al. (2008). "Mono-(2-ethylhexyl) phthalate increases spermatocyte mitochondrial peroxiredoxin 3 and cyclooxygenase 2." J Androl **29**(3): 293-303.

Pal, R., M. K. Mamidi, et al. (2011). "Human embryonic stem cell proliferation and differentiation as parameters to evaluate developmental toxicity." Journal of cellular physiology **226**(6): 1583-1595.

Parks, L. G., J. S. Ostby, et al. (2000). "The plasticizer diethylhexyl phthalate induces malformations by decreasing fetal testosterone synthesis during sexual differentiation in the male rat." Toxicol Sci **58**(2): 339-349.

Parks Saldutti, L., B. K. Beyer, et al. (2013). "In vitro testicular toxicity models: opportunities for advancement via biomedical engineering techniques." ALTEX **30**(3): 353-377.

Pierret, C., J. A. Morrison, et al. (2010). "Developmental cues and persistent neurogenic potential within an in vitro neural niche." BMC developmental biology **10**: 5.

Piprek, R. P. (2010). "Molecular and cellular machinery of gonadal differentiation in mammals." Int J Dev Biol **54**(5): 779-786.

Ponce, R. A., T. J. Kavanagh, et al. (1994). "Effects of methyl mercury on the cell cycle of primary rat CNS cells in vitro." Toxicology and applied pharmacology **127**(1): 83-90.

Povey, A. C. and S. J. Stocks (2010). "Epidemiology and trends in male subfertility." Human fertility **13**(4): 182-188.

Radio, N. M. and W. R. Mundy (2008). "Developmental neurotoxicity testing in vitro: models for assessing chemical effects on neurite outgrowth." Neurotoxicology **29**(3): 361-376.

Reif, D. M., M. T. Martin, et al. (2010). "Endocrine profiling and prioritization of environmental chemicals using ToxCast data." Environmental health perspectives **118**(12): 1714-1720.

Rice, D. and S. Barone, Jr. (2000). "Critical periods of vulnerability for the developing nervous system: evidence from humans and animal models." Environ Health Perspect **108 Suppl 3**: 511-533.

Rice, D. and S. Barone, Jr. (2000). "Critical periods of vulnerability for the developing nervous system: evidence from humans and animal models." Environmental health perspectives **108 Suppl 3**: 511-533.

Robinson, J. F., Z. Guerrette, et al. (2010). "A systems-based approach to investigate dose- and time-dependent methylmercury-induced gene expression response in C57BL/6 mouse embryos undergoing neurulation." Birth defects research. Part B, Developmental and reproductive toxicology **89**(3): 188-200.

Robinson, J. F., Z. Guerrette, et al. (2010). "A systems-based approach to investigate dose- and time-dependent methylmercury-induced gene expression response in C57BL/6 mouse embryos undergoing neurulation." Birth Defects Res B Dev Reprod Toxicol **89**(3): 188-200.

Robinson, J. F., P. T. Theunissen, et al. (2011). "Comparison of MeHg-induced toxicogenomic responses across in vivo and in vitro models used in developmental toxicology." Reproductive toxicology **32**(2): 180-188.

Robinson, J. F., A. Verhoef, et al. (2012). "A comparison of gene expression responses in rat whole embryo culture and in vivo: time-dependent retinoic acid-induced teratogenic response." Toxicol Sci **126**(1): 242-254.

Robinson, J. F., A. Verhoef, et al. (2012). "Transcriptomic analysis of neurulation and early organogenesis in rat embryos: an in vivo and ex vivo comparison." Toxicol Sci **126**(1): 255-266.
Rock, K. L. and H. Kono (2008). "The inflammatory response to cell death." Annu Rev Pathol **3**: 99-126.
Rodier, P. M. (1995). "Developing brain as a target of toxicity." Environ Health Perspect **103 Suppl 6**: 73-76.
Rolland, M., J. Le Moal, et al. (2013). "Decline in semen concentration and morphology in a sample of 26,609 men close to general population between 1989 and 2005 in France." Hum Reprod **28**(2): 462-470.
Roque, P. J., M. Guizzetti, et al. (2014). "Synaptic structure quantification in cultured neurons." Curr Protoc Toxicol **60**: 12 22 11-12 22 32.
Rusyn, I. and G. P. Daston (2010). "Computational toxicology: realizing the promise of the toxicity testing in the 21st century." Environmental health perspectives **118**(8): 1047-1050.
Sanderson, J. T. (2006). "The steroid hormone biosynthesis pathway as a target for endocrine-disrupting chemicals." Toxicol Sci **94**(1): 3-21.
Schmid, W. (1961). "The Differential Susceptibility of Sperm and Spermatids to Ionizing Radiations." American Naturalist **95**(881): 103-111.
Seiler, A., A. Visan, et al. (2004). "Improvement of an in vitro stem cell assay for developmental toxicity: the use of molecular endpoints in the embryonic stem cell test." Reproductive toxicology **18**(2): 231-240.
Sharpe, R. M., C. McKinnell, et al. (2003). "Proliferation and functional maturation of Sertoli cells, and their relevance to disorders of testis function in adulthood." Reproduction **125**(6): 769-784.
Sharpe, R. M. and N. E. Skakkebaek (2008). "Testicular dysgenesis syndrome: mechanistic insights and potential new downstream effects." Fertil Steril **89**(2 Suppl): e33-38.
Shima, J. E., D. J. McLean, et al. (2004). "The murine testicular transcriptome: characterizing gene expression in the testis during the progression of spermatogenesis." Biol Reprod **71**(1): 319-330.
Shin, S., M. Mitalipova, et al. (2006). "Long-term proliferation of human embryonic stem cell-derived neuroepithelial cells using defined adherent culture conditions." Stem cells **24**(1): 125-138.
Shine, R., J. Peek, et al. (2008). "Declining sperm quality in New Zealand over 20 years." The New Zealand medical journal **121**(1287): 50-56.
Sidhu, J. S., R. A. Ponce, et al. (2006). "Cell cycle inhibition by sodium arsenite in primary embryonic rat midbrain neuroepithelial cells." Toxicological sciences : an official journal of the Society of Toxicology **89**(2): 475-484.
Silva, M. J., J. A. Reidy, et al. (2004). "Detection of phthalate metabolites in human amniotic fluid." Bull Environ Contam Toxicol **72**(6): 1226-1231.
Sipes, N. S., M. T. Martin, et al. (2013). "Profiling 976 ToxCast chemicals across 331 enzymatic and receptor signaling assays." Chem Res Toxicol **26**(6): 878-895.
Skakkebaek, N. E., E. Rajpert-De Meyts, et al. (2001). "Testicular dysgenesis syndrome: an increasingly common developmental disorder with environmental aspects." Hum Reprod **16**(5): 972-978.

Small, C. L., J. E. Shima, et al. (2005). "Profiling gene expression during the differentiation and development of the murine embryonic gonad." Biol Reprod **72**(2): 492-501.
Snyder, E. M., C. L. Small, et al. (2009). "Regulation of gene expression by estrogen and testosterone in the proximal mouse reproductive tract." Biology of reproduction **81**(4): 707-716.
Soukas, A., P. Cohen, et al. (2000). "Leptin-specific patterns of gene expression in white adipose tissue." Genes Dev **14**(8): 963-980.
States, J. C., A. Barchowsky, et al. (2011). "Arsenic toxicology: translating between experimental models and human pathology." Environmental health perspectives **119**(10): 1356-1363.
Stephens, M. L., M. Andersen, et al. (2013). "Evidence-based toxicology for the 21st century: opportunities and challenges." ALTEX **30**(1): 74-103.
Stummann, T. C. and S. Bremer (2008). "The possible impact of human embryonic stem cells on safety pharmacological and toxicological assessments in drug discovery and drug development." Current stem cell research & therapy **3**(2): 118-131.
Stummann, T. C., L. Hareng, et al. (2009). "Hazard assessment of methylmercury toxicity to neuronal induction in embryogenesis using human embryonic stem cells." Toxicology **257**(3): 117-126.
Swan, S. H. (2008). "Environmental phthalate exposure in relation to reproductive outcomes and other health endpoints in humans." Environ Res **108**(2): 177-184.
Swan, S. H., E. P. Elkin, et al. (1997). "Have sperm densities declined? A reanalysis of global trend data." Environmental health perspectives **105**(11): 1228-1232.
Swan, S. H., E. P. Elkin, et al. (2000). "The question of declining sperm density revisited: an analysis of 101 studies published 1934-1996." Environmental health perspectives **108**(10): 961-966.
Swan, S. H., R. L. Kruse, et al. (2003). "Semen quality in relation to biomarkers of pesticide exposure." Environmental health perspectives **111**(12): 1478-1484.
Swan, S. H., F. Liu, et al. (2010). "Prenatal phthalate exposure and reduced masculine play in boys." Int J Androl **33**(2): 259-269.
Swan, S. H., K. M. Main, et al. (2005). "Decrease in anogenital distance among male infants with prenatal phthalate exposure." Environ Health Perspect **113**(8): 1056-1061.
Swan, S. H., K. M. Main, et al. (2005). "Decrease in anogenital distance among male infants with prenatal phthalate exposure." Environmental health perspectives **113**(8): 1056-1061.
Tamm, C., J. Duckworth, et al. (2006). "High susceptibility of neural stem cells to methylmercury toxicity: effects on cell survival and neuronal differentiation." J Neurochem **97**(1): 69-78.
Theunissen, P. T., J. L. Pennings, et al. (2011). "Time-response evaluation by transcriptomics of methylmercury effects on neural differentiation of murine embryonic stem cells." Toxicological sciences : an official journal of the Society of Toxicology **122**(2): 437-447.
Theunissen, P. T., J. F. Robinson, et al. (2012). "Transcriptomic concentration-response evaluation of valproic acid, cyproconazole, and hexaconazole in the neural

embryonic stem cell test (ESTn)." Toxicological sciences : an official journal of the Society of Toxicology **125**(2): 430-438.
Theunissen, P. T., J. F. Robinson, et al. (2012). "Compound-specific effects of diverse neurodevelopmental toxicants on global gene expression in the neural embryonic stem cell test (ESTn)." Toxicology and applied pharmacology **262**(3): 330-340.
Theunissen, P. T., S. H. Schulpen, et al. (2010). "An abbreviated protocol for multilineage neural differentiation of murine embryonic stem cells and its perturbation by methyl mercury." Reprod Toxicol **29**(4): 383-392.
Thomas, R. S., H. J. Clewell, 3rd, et al. (2011). "Application of transcriptional benchmark dose values in quantitative cancer and noncancer risk assessment." Toxicological sciences : an official journal of the Society of Toxicology **120**(1): 194-205.
Thomson, J. A., J. Itskovitz-Eldor, et al. (1998). "Embryonic stem cell lines derived from human blastocysts." Science **282**(5391): 1145-1147.
Tilton, F. and R. L. Tanguay (2008). "Exposure to sodium metam during zebrafish somitogenesis results in early transcriptional indicators of the ensuing neuronal and muscular dysfunction." Toxicological sciences : an official journal of the Society of Toxicology **106**(1): 103-112.
van Dartel, D. A. and A. H. Piersma (2011). "The embryonic stem cell test combined with toxicogenomics as an alternative testing model for the assessment of developmental toxicity." Reproductive toxicology **32**(2): 235-244.
Verhoeven, G. and J. Cailleau (1990). "Influence of coculture with Sertoli cells on steroidogenesis in immature rat Leydig cells." Mol Cell Endocrinol **71**(3): 239-251.
Verhoeven, G., A. Willems, et al. (2010). "Androgens and spermatogenesis: lessons from transgenic mouse models." Philos Trans R Soc Lond B Biol Sci **365**(1546): 1537-1556.
Wang, X., M. T. Dyson, et al. (2003). "Inhibition of cyclooxygenase-2 activity enhances steroidogenesis and steroidogenic acute regulatory gene expression in MA-10 mouse Leydig cells." Endocrinology **144**(8): 3368-3375.
Wang, X., C. L. Shen, et al. (2005). "Cyclooxygenase-2 regulation of the age-related decline in testosterone biosynthesis." Endocrinology **146**(10): 4202-4208.
Wegner, S., S. Hong, et al. (2013). "Preparation of rodent testis co-cultures." Curr Protoc Toxicol **Chapter 16**: Unit 16 10.
Wells, P. G., G. P. McCallum, et al. (2009). "Oxidative stress in developmental origins of disease: teratogenesis, neurodevelopmental deficits, and cancer." Toxicological sciences : an official journal of the Society of Toxicology **108**(1): 4-18.
Western, P. (2009). "Foetal germ cells: striking the balance between pluripotency and differentiation." Int J Dev Biol **53**(2-3): 393-409.
Wetmore, B. A., J. F. Wambaugh, et al. (2012). "Integration of dosimetry, exposure, and high-throughput screening data in chemical toxicity assessment." Toxicological sciences : an official journal of the Society of Toxicology **125**(1): 157-174.
Whittaker, S. G. and E. M. Faustman (1992). "Effects of benzimidazole analogs on cultures of differentiating rodent embryonic cells." Toxicology and applied pharmacology **113**(1): 144-151.

Young, A., D. W. Machacek, et al. (2011). "Ion channels and ionotropic receptors in human embryonic stem cell derived neural progenitors." Neuroscience **192**: 793-805.

Yu, X., W. C. Griffith, et al. (2006). "A system-based approach to interpret dose- and time-dependent microarray data: quantitative integration of gene ontology analysis for risk assessment." Toxicol Sci **92**(2): 560-577.

Yu, X., S. Hong, et al. (2009). "Improving in vitro Sertoli cell/gonocyte co-culture model for assessing male reproductive toxicity: Lessons learned from comparisons of cytotoxicity versus genomic responses to phthalates." Toxicology and applied pharmacology **239**(3): 325-336.

Yu, X., S. Hong, et al. (2009). "Improving in vitro Sertoli cell/gonocyte co-culture model for assessing male reproductive toxicity: Lessons learned from comparisons of cytotoxicity versus genomic responses to phthalates." Toxicol Appl Pharmacol **239**(3): 325-336.

Yu, X., J. S. Sidhu, et al. (2005). "Essential role of extracellular matrix (ECM) overlay in establishing the functional integrity of primary neonatal rat Sertoli cell/gonocyte co-cultures: an improved in vitro model for assessment of male reproductive toxicity." Toxicol Sci **84**(2): 378-393.

Yu, X., J. S. Sidhu, et al. (2005). "Essential role of extracellular matrix (ECM) overlay in establishing the functional integrity of primary neonatal rat Sertoli cell/gonocyte co-cultures: an improved in vitro model for assessment of male reproductive toxicity." Toxicological sciences : an official journal of the Society of Toxicology **84**(2): 378-393.

Zhao, G. Q. and D. L. Garbers (2002). "Male germ cell specification and differentiation." Dev Cell **2**(5): 537-547.

Zimmer, B., P. B. Kuegler, et al. (2011). "Coordinated waves of gene expression during neuronal differentiation of embryonic stem cells as basis for novel approaches to developmental neurotoxicity testing." Cell Death Differ **18**(3): 383-395.

Zimmer, B., P. B. Kuegler, et al. (2011). "Coordinated waves of gene expression during neuronal differentiation of embryonic stem cells as basis for novel approaches to developmental neurotoxicity testing." Cell death and differentiation **18**(3): 383-395.

zur Nieden, N. I., G. Kempka, et al. (2004). "Molecular multiple endpoint embryonic stem cell test--a possible approach to test for the teratogenic potential of compounds." Toxicology and applied pharmacology **194**(3): 257-269.